Graz University of Technology

Institute for Computer Graphics and Vision

Dissertation

Improved Methods for the Application of Brain Signals to Communication and Diagnosis

---

Peter Brunner

Graz, Austria, September 2013

Thesis supervisors

Prof. Dr. Horst Bischof

Prof. Dr. Gerwin Schalk

To my parents for their love and support.

Most of the fundamental ideas of science are essentially simple, and may, as a rule, be expressed in a language comprehensible to everyone.

Albert Einstein

Abstract

The last two decades have seen the advent of applications that use brain signals for communication and diagnosis. Such applications include brain-computer interfaces (BCIs) that support communication for people affected by severe neuromuscular disorders and mapping of eloquent cortex prior to resective brain surgery. A BCI measures brain signals to provide a non-muscular communication channel to those that lost muscular control in the progress of neuromuscular disorders and can no longer use conventional assistive devices. Mapping of eloquent cortex is often performed prior to surgical resection of abnormal brain tissue. Surgical planning of the resection procedure depends substantially on the delineation of abnormal tissue, and on the creation of a functional map of eloquent cortex in the area close to that abnormal tissue.

While these applications could replace or enhance established clinical procedures, their utility remains impeded by low communication performance and by the dependence on experts and post-hoc analysis. These impediments mainly result from limitations in current sensory technology, signal processing, machine learning and interface design.

This dissertation set out to address these problems by developing methods that improve the utility of applications that use brain signals for communication and diagnosis. The results show that signals recorded from the surface of the brain could support communication performance that is 3-4 times higher than what had previously been reported, and that eloquent cortex can be mapped without previously required experts and post-hoc analysis.

In summary, the results presented in this dissertation encompass two advances that are critical to the utility of applications that use brain signals for communication and diagnosis.

Keywords: electroencephalography (EEG), electrocorticography (ECoG), brain-computer interface (BCI), assistive devices, P300, event-related potential (ERP), visual evoked potential (VEP), event-related synchronization (ERS), event-related desynchronization (ERD), epilepsy, neurosurgery, functional brain mapping

Kurzfassung

Die letzten zwei Jahrzehnte haben Anwendungen hervorgebracht, welche Gehirnsignale für Kommunikation und Diagnose verwenden. Solche Anwendungen umfassen Gehirn-Computer Schnittstellen (engl. brain-computer interfaces (BCIs)) zur Kommunikation mit Schwerbehinderten und die Kartierung kortikaler Gehirnfunktionen. Ein BCI verwendet Gehirnsignale um die Kommunikation mit jenen schwerbehinderten wiederherzustellen, welche jegliche Muskelkontrolle im Verlauf einer Erkrankungen des motorischen Nervensystems verloren haben und andere auf Muskelkontrolle basierende technischen Kommunikationshilfen nicht mehr verwenden können. Kortikale Gehirnfunktionen werden im Vorfeld der operativen Entfernung von krankhaften Gehirngewebe kartiert. Präoperative Planung der Entfernung bedingt die Abgrenzung des krankhaften Gehirngewebes sowie die Kartierung kortikaler Gehirnfunktionen in dessen Umfeld.

Diese Anwendungen könnten existierende klinische Verfahren ersetzen oder verbessern, jedoch wird dies durch niedrige Kommunikationsgeschwindigkeit und eine Abhängigkeit von Experten und nachfolgenden Analysen verhindert. Dies ist bedingt durch technologische Grenzen der Sensoren, Signalverarbeitung, Mustererkennung und Benutzerschnittstellen.

Das Ziel dieser Dissertation ist es Methoden zu entwickeln, welche die diese Probleme überwinden und die klinische Anwendung von Gehirnsignalen für Kommunikation und Diagnose ermöglichen. Die Resultate zeigen, daß die Kommunikationsgeschwindigkeit mittels kortikale Gehirnsignale um den Faktor 3-4 erhöht werden kann und dass kortikale Gehirnfunktionen ohne die zuvor notwendigen Experten und nachfolgenden Analysen kartiert werden können.

Zusammenfassend resultieren aus dieser Dissertation zwei technologische Fortschritte, welche essentiell für die klinische Anwendung von Gehirnsignalen für Kommunikation und Diagnose sind.

Schlagwörter: Elektroenzephalografie (EEG), Elektrokortikogramm (ECoG), brain-computer interface (BCI), technische Kommunikationshilfen, P300, Ereigniskorrelierte Potentiale (EKP), Visuell evoziertes Potential (VEP), Ereigniskorrelierte Synchronization (ERS), Ereigniskorrelierte De-synchronization (ERD), Epilepsie, Neurochirurgie, funktionelle Gehirnkartierung

Statutory Declaration

I declare that I have authored this thesis independently, that I have not used other than the declared sources / resources, and that I have explicitly marked all material which has been quoted either literally or by content from the used sources.

Place	Date	Signature

Eidesstattliche Erklärung

Ich erkläre an Eides statt, dass ich die vorliegende Arbeit selbstständig verfasst, andere als die angegebenen Quellen/Hilfsmittel nicht benutzt, und die den benutzten Quellen wörtlich und inhaltlich entnommene Stellen als solche kenntlich gemacht habe.

Ort	Datum	Unterschrift

Acknowledgments

This dissertation symbolizes another milestone on an endeavor that started 27 years ago when I first started school. I would like to thank those who gave me faith, inspiration, direction and impetus on this endeavor. This dissertation would not have been possible without the mentoring, support and patience of my advisors Drs. Horst Bischof and Gerwin Schalk. I also remain deeply indebted to Drs. Anthony Ritaccio and Jonathan Wolpaw who helped me bridge the gaps between theory and clinical practice. I remain grateful to Ms. Theresa Vaughan for her sincere support throughout all my years in the United States. I would like to thank Mr. Herbert Tanner, Drs. Rainer Graumann, Dieter Ritter and Matthias Mitschke for the insight and inspiration they gave me over the course of my industrial internships. I would also like to thank my high school teachers Mr. Franz Braunschmid and Herbert Kuttelwascher for showing me the value of flawless work in a competitive environment. I would like to acknowledge Griffin Milsap and Sean Austin for assisting in the programming and Drs. Timothy Lynch, Bridget Frawley, Matthew Adamo and Joseph Emrich for providing clinical support. Among all my colleagues at the Albany Medical Center and the Wadsworth Center, I would like to especially thank Dr. Aysegul Gunduz for all her support and helpful discussions. I would also like to thank all the human subjects and patients that participated in the studies of this dissertation for their time and patience. Finally, I would like to dedicate this dissertation to my parents who have provided me with their love and support.

This work was supported by the NIH (EB006356 (GS), EB00856 (JRW and GS)) and the US Army Research Office (W911NF-07-1-0415 (GS) and W911NF-08-1-0216 (GS)).

Contents

List of Figures

List of Tables

1 Introduction

Brain signals reflect neural activity in the central nervous system (CNS). These signals are expressed through chemical, electric, magnetic and metabolic modulations of neural activity in the brain and spinal cord.

For decades, brain signals have been used for three established clinical applications: (1) general diagnosis of epilepsy and other disorders of the central nervous system through visual inspection of electroencephalographic (EEG) signals (Gibbs et al. 1936, Fig. 1.1); (2) localization of epileptogenic cortex through visual inspection of interictal and ictal data in electrocorticographic (ECoG) signals (Penfield et al. 1942, Fig. 1.1); and (3) mapping of eloquent cortex[1] through electrical cortical stimulation (ECS) for presurgical planning of epileptogenic and lesional cortical tissue resection (Ojemann et al. 1989, Fig. 1.2).

Recent studies have shown promising emerging clinical applications. Such applications include ***brain-computer interface (BCI) communication*** (Vidal 1973), and ***passive mapping of eloquent cortex*** (Crone et al. 1998a).

A brain-computer interface, or BCI, is a system that measures CNS activity and converts it into an artificial output that replaces, restores, enhances, supplements, or improves natural CNS output, and thereby changes the ongoing interactions between the CNS and its external or internal environment (Wolpaw and Winter-Wolpaw 2011). Many people affected by debilitating neuromuscular disorders such as amyotrophic lateral sclerosis (ALS), brainstem stroke, or spinal cord injury are impaired in their ability to communicate. Conventional assistive devices (e.g., letter boards, cheek or tongue

[1] Areas of cortex that - if resected or lesioned - will cause sensory processing or linguistic impairment, minor paralysis, or paralysis.

Figure 1.1: **Visual inspection of brain signals.** This figure shows the evolution of procedures that use visual inspection of brain signals for clinical diagnosis and intervention. (A) The photograph on the left shows a mechanical stylus and paper instrumentation that records EEG signals up to 30 Hz from one patient. A physician inspects the signals in real-time while also observing the behavior of the patient. (B) The photograph on the right shows the evolution of this system into an automated video EEG instrumentation that simultaneously records neural signals and behavior (i.e., two video streams of the patient) from up to 6 patients. A technician observes the six streams of video EEG and marks interesting behavioral events for the post-hoc inspection through a physician.

switches, or eye trackers) that aim to restore communication functions all require muscular control, which is often lost in the progress of neuromuscular disorders. For these people, a brain-computer interface (BCI) that uses brain signals directly, rather than muscles, can re-establish communication with the outside world.

BCIs can be classified into exogenous and endogenous systems (Mason and Birch 2003). In an exogenous BCI the user communicates his intention through selectively attending to an external stimuli. A BCI then detects the user's intent from the neural response to the stimuli. As the neural response to the stimuli is time-locked to the stimuli and typically only depends on the attention to the stimuli, exogenous BCIs tend to be static machine-learning problems that require no user training or adaptation of the machine-learning algorithm. In an endogenous BCI, the user communicates his intent by selectively modulating neural activity. A BCI detects the user's intent from the neural modulation. As the neural activity is not time-locked to a known stimulus and typically depends on a mental strategy, endogenous BCIs tend to be co-adaptive machine-learning problems that require extensive user training.

Various different exogenous and endogenous BCI approaches have been proposed. An exogenous BCI approach that several groups have begun to test in clinical appli-

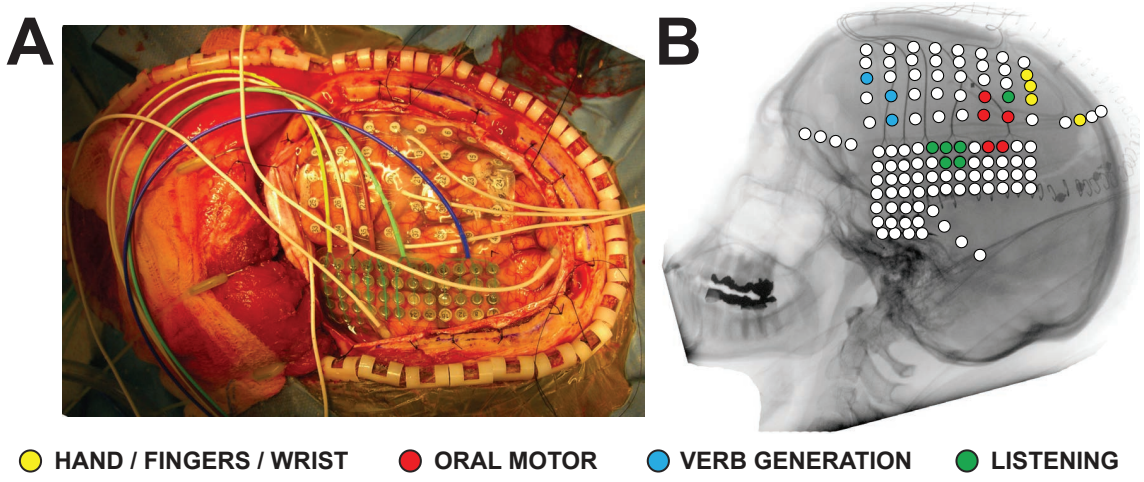

Figure 1.2: **Electrical stimulation mapping (ESM).** This figure shows the process of electrical stimulation mapping (ESM) prior to resective brain surgery. (A) The cortex is exposed through a craniotomy of the skull and an incision of the dura. An electrode grid is then placed on the cortex and connected to a cortical stimulator (not depicted in this figure). (B) A physician then uses the connected cortical stimulator to deliver pulses of electrical current that evoke a behavioral response. The observation of this response results in a map of eloquent cortex that is directly used by the neurosurgeon to delineate eloquent from abnormal tissue during resective surgery.

cations in humans (e.g., Nijboer et al. 2008; Sellers et al. 2006b, 2010; Vaughan et al. 2006; see Donchin and Arbel 2009 for a comprehensive review) is the EEG-based matrix speller originally described by Farwell and Donchin in 1988. This interface allows people to communicate at a rate of 4-5 characters per minute by selectively attending to external stimuli. Another exogenous approach is the EEG-based steady-state visual evoked potential (SSVEP)-based BCI. In such a paradigm, the subject performs a selection by focusing eye-gaze on the target character (i.e., one of multiple light sources flickering at different frequencies) while the BCI detects those frequencies in the EEG recorded over occipital cortex (Middendorf et al. 2000). This interface allows people to communicate at a rate of up to 19 characters per minute (Bin et al. 2009). An endogenous BCI approach is the EEG-based sensory-motor rhythm (SMR) BCI speller (McFarland et al. 2003; Müller et al. 2008; Pfurtscheller et al. 2003; Wolpaw et al. 1991). This interface allows people to communicate at a rate of 4-5 characters per minute by selectively modulating the sensory-motor rhythm (SMR).

Currently BCIs present the only way of communication for people affected by the late stages of debilitating neuromuscular disorders. However, people beyond this population, i.e., people that still posses residual motor control, find conventional assistive devices to provide a better communication performance (e.g., MyTobii P10 eye-tracker system, 10 words per minute at close to 100% accuracy). Consequently, BCIs need to improve in speed, accuracy, and consequently the perceived value to the user, if they were to become a viable alternative to conventional assistive devices.

The low communication performance of BCIs is due in part to the limitations in the signal fidelity of EEG signals (Schalk 2008). A growing number of recent studies (e.g., Felton et al. 2007; Leuthardt et al. 2006, 2004; Miller et al. 2010; Ritaccio et al. 2010; Schalk et al. 2008c; Vansteensel et al. 2010; Wilson et al. 2006) suggested that signals recorded from the surface of the brain (electrocorticography (ECoG)) are a promising platform for real-time BCI communication. This advantage is due in part to the high spatial, spectral, and temporal fidelity that characterize ECoG signals (Ball et al. 2009; Brunner et al. 2009; Leuthardt et al. 2004; Miller et al. 2007b, 2008). It is possible that these favorable signal characteristics may provide distinct advantages for the BCI communication performance, but this has not been explored.

In aim 1 of this dissertation, we investigate this possibility by evaluating the feasibility and online performance of the matrix speller using ECoG signals. We hypothesize that these experiments will provide evidence that the ECoG-based speller may support communication rates that are higher than those typically expected by EEG-based spellers.

Mapping of eloquent cortex is performed prior to resective brain surgery. Resective brain surgery is often performed in people with intractable epilepsy, congenital structural lesions, vascular anomalies, and neoplasms. Surgical planning of the resection procedure depends substantially on the delineation of abnormal tissue, e.g., epileptic foci or tumor tissue, and on the creation of a functional map of eloquent cortex in the area close to that abnormal tissue. Traditionally, different methodologies have been used to produce this functional map: electrical cortical stimulation (ECS) (Foerster, 1931; Hara et al., 1991; Ojemann, 1991; Uematsu et al., 1992), functional magnetic resonance imaging (fMRI) (Chakraborty and McEvoy, 2008), positron emission tomography (PET) (Bittar et al., 1999; Meyer et al., 2003), magnetoencephalography (MEG) (Ganslandt et al., 1999), or evoked potentials (EP) (Dinner et al., 1986). Each of these methods has problems that include morbidity, time consumption, expense, or practicality. However, be-

cause existing surgical protocols typically already include the placement of subdural electrodes, and because of its procedural simplicity, ECS has become the gold standard for mapping of eloquent cortex.

Recently, a number of studies showed that ECoG activity recorded from these electrodes reflect task-related changes (Aoki et al., 1999, 2001; Crone et al., 2001, 1998a,b; Fries, 2005; Graimann et al., 2002; Lachaux et al., 2003; Leuthardt et al., 2007; Miller et al., 2007b; Sinai et al., 2005; Varela et al., 2001). These studies showed that ECoG amplitudes in particular frequency bands carry substantial information about movement or language tasks. Furthermore, recent studies demonstrated that such ECoG changes, in particular those in the gamma band, were in general agreement with those derived using fMRI (Lachaux et al., 2007a) and with results determined using ECS (Leuthardt et al., 2007; Miller et al., 2007b; Sinai et al., 2005).

While a few recent studies have provided encouraging evidence that ECoG-based analyses could become more accessible to clinicians (Lachaux et al., 2007b,c; Miller et al., 2007a), passive mapping of eloquent cortex using ECoG has remained an academic demonstration. This is because the mapping procedure employs a discriminative approach that depends on post-hoc analysis and an expert to optimize the analyses for each individual patient. Generative approaches have been shown to overcome the requirement for expert supervised post-hoc analysis in related domains such as computer vision (Friedman and Russell 1997; Harville et al. 2001; Kuo et al. 2003; Lee 2005; Liyuan et al. 2004; Pless 2003; Stauffer and Grimson 1999; Toyama et al. 1999) and biosignal processing (Costa and Cabral 2000; Gardner et al. 2006; Harris et al. 2000; Pernkopf and Bouchaffra 2005).

In aim 2 of this dissertation, we investigate the feasibility of the use of a generative approach to passively map eloquent cortex using ECoG. We hypothesize that these experiments will provide evidence that a generative approach to passively map eloquent cortex using ECoG will provide results that are in general agreement to those derived using electrical stimulation and that mapping can be accomplished without expert oversight.

1.1 Techniques to Acquire Brain Signals

In the 80 years since Hans Berger first recorded electroencephalographic activity (EEG) from the scalp using silver wires and a galvanometer (Berger 1929), researchers and clinicians have continued to explore better techniques to acquire brain signals. This research has lead to invasive and non-invasive techniques that record brain signals either directly using electrophysiological signals or indirectly using metabolic changes that relate to neuronal activity. Non-invasive techniques include the recording of metabolic activity using functional near-infrared spectroscopy (fNIR), functional magnetic resonance imaging (fMRI) and the recording of electrophysiological activity using EEG and magnetoencephalography (MEG). Invasive techniques exclusively record electrophysiological activity using electrocorticography (ECoG), local field potentials (LFP), and single-unit activity (SUA) (see Fig. 1.3 and Table 1.1).

Clinical applications then translate these brain signals into outputs that provide value to the clinical investigator or the patient. This dissertation focuses on the application of brain signals for communication and diagnosis. The following sections describe the utility of each of the techniques to acquire brain signals for these two applications.

Table 1.1: **Comparison of techniques that acquire brain signals.** This table compares the utility of non-invasive (e.g., fMRI, MEG, fNRI, EEG) and invasive (e.g., eECoG, ECoG, LFP, SUA) techniques that acquire brain signals. In this comparison non-invasive techniques tend to provide comprehensive coverage at low risk, but suffer from high cost and low spatial resolution and signal to noise ratio.

	fMRI	MEG	fNIR	EEG	epidural ECoG	subdural ECoG	LFP	SUA
temporal resolution	sec	ms	sec	ms	ms	ms	ms	μs
spatial resolution	cm	cm	cm	cm	mm	mm	mm	μm
coverage	full	full	limited	full	limited	limited	limited	very limited
signal to noise ratio	low	low	low	low	medium	high	high	very high
number of sensors	1000	100	50	100	100	100	200	500
expert required	yes	yes	no	no	yes	yes	yes	yes
expensive equipment	very	very	no	no	no	no	no	no
susceptible to artifacts	yes	yes	yes	yes	no	no	no	no
variety of tasks	limited	high	limited	high	high	high	high	very high
invasive	no	no	no	no	yes	yes	yes	yes
infection risk	no	no	no	no	no	yes	yes	yes
recording time limit	hours	hours	hours	hours	years	months	months	days

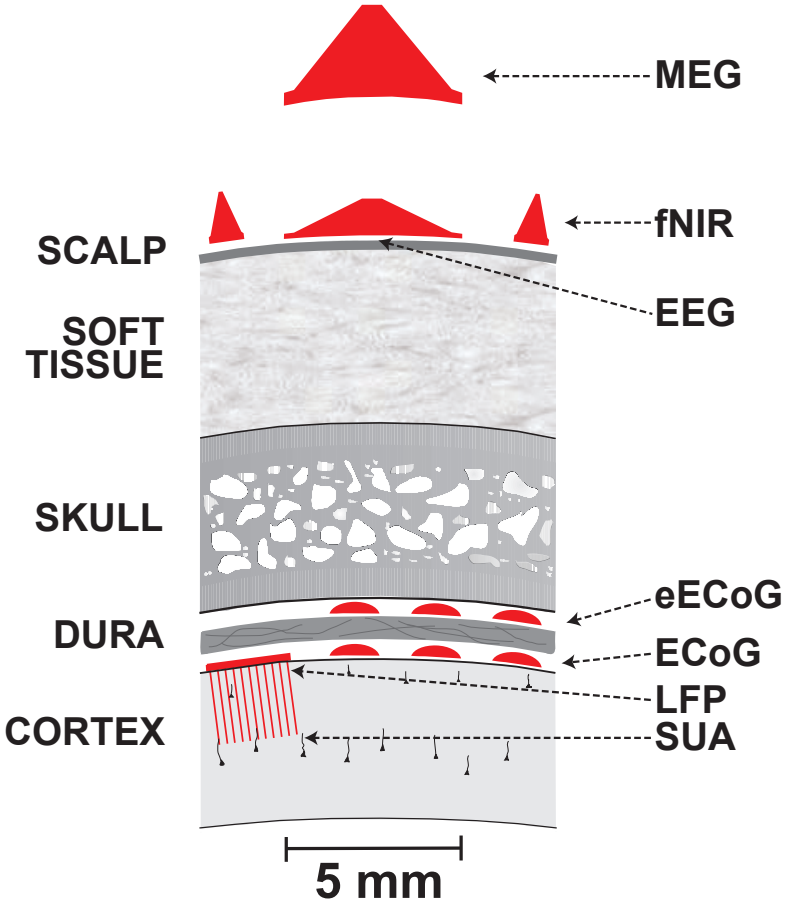

Figure 1.3: **Size and location of sensors that acquire brain signals** This figure shows the size and the location of sensors that acquire brain signals. Non-invasive sensors are located on (e.g., EEG, fNRI) or above (e.g., MEG) the scalp and typically are sized 10 mm or larger in diameter. Invasive sensors are located on the dura (e.g., eECoG), under the dura (e.g., ECoG) or within the cortex (LFP, SUA) and typically are sized 2 mm or smaller in diameter.

1.1.1 Non-Invasive Acquisition of Brain Signals

Non-invasive techniques acquire brain signals without penetrating the skin. This is accomplished by recording brain signals directly using the magnetic (MEG) or electric (EEG) field, or indirectly by recording the metabolic changes that relate to neural activity (fMRI, fNIR).

1.1.1.1 Functional Magnetic Resonance Imaging (fMRI)

Functional magnetic resonance imaging measures the change in blood flow (i.e., hemodynamic response) that is related to neural activity in the brain (Belliveau et al. 1991). The change in blood flow occurs through neurovascular coupling in capillaries that feed neurons engaged in neural activity, and induces a small magnetic field distortion that can be measured. fMRI therefore is a non-invasive and indirect measure of neural activity that provides excellent depth sensitivity. The temporal resolution of fMRI is limited because of two reasons. First, blood flow follows the change in neural activity only slowly and with a delay. This limits the temporal resolution of fMRI to a few seconds. Second, fMRI measures the change in blood flow sequentially (i.e., slice by slice) along the medial axis of the brain. Each sequential measurement (i.e., slice) takes approximately 100ms and a full measurement along the medial axis of the brain requires up to 150 slices. Consequently, the 15 seconds for one full measurement further limit the temporal resolution of fMRI. This limitation and the high cost (e.g., multiple million dollars) for the device restrict the utility of fMRI mainly to diagnostic applications. In these applications, baseline fMRI activity is contrasted to task-related activity, resulting in an fMRI image that shows the average neural activity during the task relative to baseline.

1.1.1.2 Magnetoencephalography (MEG)

Magnetoencephalography measures the weak magnetic fields that are created by synchronized neurons. MEG therefore is a direct measure of neural activity (Cohen 1968). As the magnetic field flux density attenuates exponentially with the distance to the neural source, the measured magnetic fields are most dominantly related to neural activity in the cortex rather than to neural activity in deeper cortical structures. The recorded magnetic fields are created by primary currents (i.e., currents directly related to neural activity) and secondary currents (i.e., surface currents that compensate primary currents). As the magnetic fields are not markedly affected by the geometry and conductivity of the scalp, skull, outer meningeal covering and brain, MEG can easily locate neural activity within the brain from the primary sources. Because this neural activity instantly creates magnetic fields, the temporal resolution of MEG is only limited by the sensitivity of the magnetic sensor technology. While the spatial coverage of MEG fully encompasses the brain, its spatial resolution is limited by the size of the sensors that measure the magnetic fields. As with fMRI, high cost (i.e., multiple million dollars) for the device limits MRI to diagnostic applications.

1.1.1.3 Functional Near-Infrared Spectroscopy (fNIR)

Functional near-infrared spectroscopy measures the change in concentration and oxygenation of hemoglobin in the brain (i.e., hemodynamic response) that is related to neural activity in the brain (Chance et al. 1998). Therefore fNIR, like fMRI, is a non-invasive and indirect measure of neural activity. In contrast to fMRI, fNIR can be more easily combined with other non-invasive techniques (e.g., fMRI, EEG, MEG), and is cheap and easy to acquire. The use of near-infrared spectroscopy allows the simultaneous acquisition of fNIR signals from multiple sensors. While this provides a somewhat higher temporal resolution than fMRI, light spread and absorption limit the spatial resolution to a few centimeters and the depth sensitivity to a few millimeters of the cortex. In addition, because hair markedly affects the signal quality, fNRI is typically limited in its spatial coverage to the forehead and the acquisition of neo-cortical brain signals. This limits fNIR mostly to basic research and applications that use the fNIR signals for communication.

1.1.1.4 Electroencephalography (EEG)

Electroencephalography measures electrical fields on the scalp that are created by synchronized neurons (Fig. 1.4). Therefore, EEG is a direct measure of neural activity (Berger 1929). As the electric field flux density attenuates exponentially with the distance to the neural source, the measured electric fields are most dominantly related to neural activity in the cortex rather than to neural activity in deeper cortical structures. These issues are compounded by the fact that the recorded electric fields are created by secondary currents (i.e., surface currents that compensate primary currents). In addition, the geometry and conductivity of the scalp, skull, outer meningeal covering and brain, markedly affect the electric field (Fig. 1.6). Therefore, it is difficult for EEG to locate neural activity within the brain, effectively limiting its spatial sensitivity.

In contrast to techniques that measure changes in metabolic activity or magnetic fields, techniques that measure changes in electrical fields require a reference to which the electrical field is measured. While an "indefinite" reference (e.g., on the leg) would be roughly equidistant to all possible sources within the brain, the electrical noise (e.g., line-noise) between the "indefinite" reference and the measurement site would markedly affect the quality of the measured electrical signal. This limits the choice of the reference to unipolar (e.g., one reference for all measurement sites) and bipolar (e.g., one reference for each measurement site). Depending on the reference, unipolar EEG (e.g., linked ear-

lobes as reference) tends to measure changes in global neural activity while bipolar EEG tends to measure changes in local neural activity.

Neural activity instantly creates electric fields, and therefore the temporal resolution of EEG is only limited by the sensitivity of the electric sensor technology and the electric filter characteristics of the volume conductor (i.e., the scalp, skull, outer meningeal covering and brain). As MEG, the spatial coverage of EEG also fully encompasses the brain, but the spatial resolution is mainly limited to the spatial filter characteristics of the volume conductor. In contrast to fMRI and MRI, EEG is inexpensive and easy to use. For that reason, EEG is used beyond diagnostic applications (see 1.3.1).

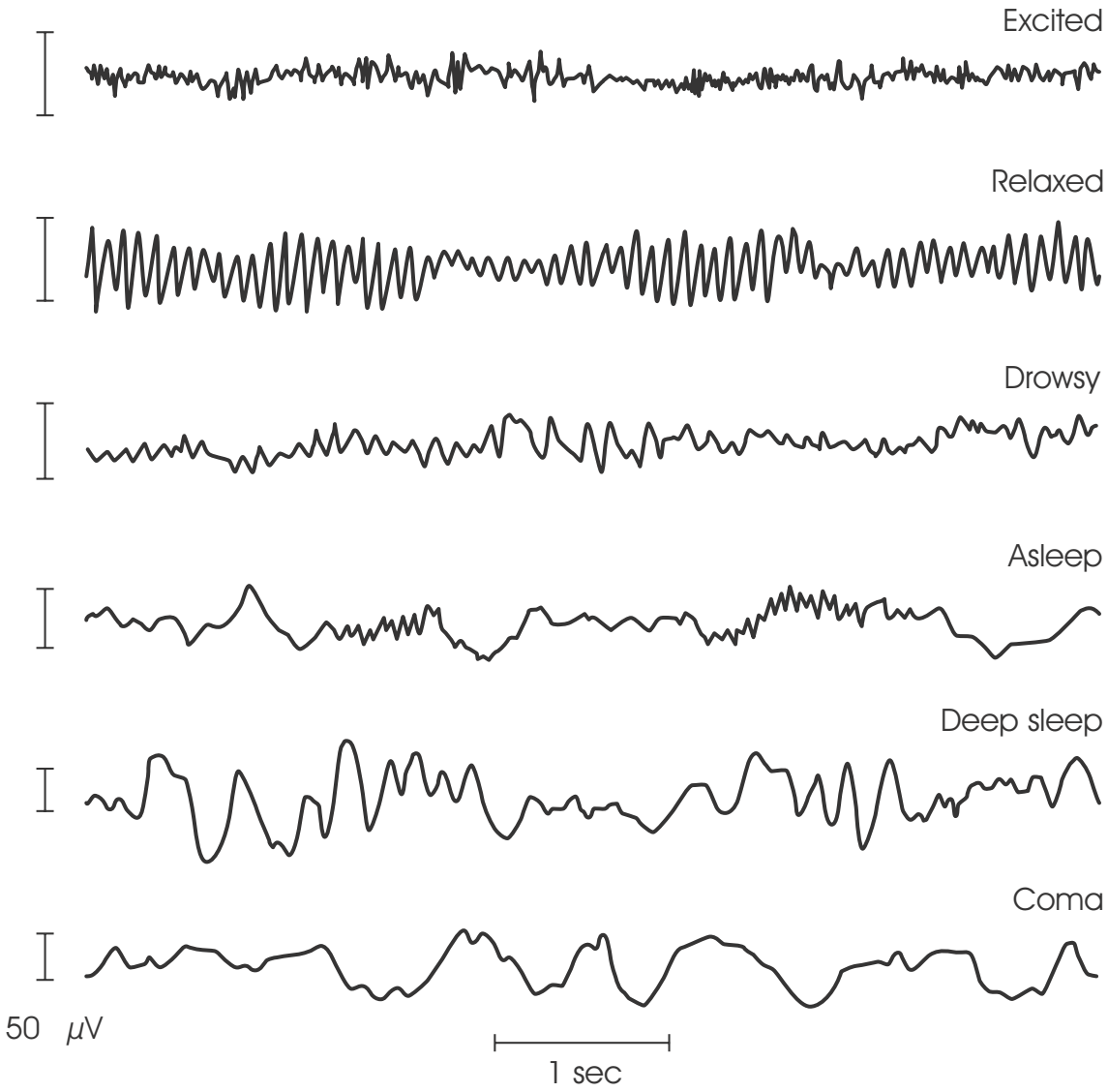

Figure 1.4: **Examples of characteristic EEG signals recorded during various behavioral states in humans.** These signals show the beta brain-wave pattern in an awake, alert person (Excited); the alpha rhythm associated with relaxing with the eyes closed (Relaxed); the slowing in frequency and increase in amplitude of theta waves associated with a drowsy condition (Drowsy); the slow, high-amplitude delta waves associated with sleep (Asleep); the larger, slow waves associated with deep sleep (Deep sleep); and the further slowing of electroencephalographic waves associated with coma (Coma). (After Epilepsy and the Functional Anatomy of the Human Brain by W. Penfield and H. H. Jasper. Boston: Little, Brown, 1954, p. 12.)

1.1.2 Invasive Acquisition of Brain Signals

Acquiring brain signals invasively involves making an incision in the subject's body and inserting electrodes to record electrophysiological signals. This procedure entails additional costs and risks, which currently limit the utility of invasive brain signals to applications in clinical diagnosis and basic research.

1.1.2.1 Electrocorticography (ECoG)

Electrocorticography measures electrical fields that are created by synchronized neurons using a grid of electrodes on the cortex (i.e., subdural ECoG) or on the dura (i.e., epidural ECoG). Therefore, ECoG is a direct measure of neural activity (Penfield and Boldrey 1937).

To place the electrode grid and record ECoG, the cortex is accessed through a craniotomy of the skull and an incision of the outer meningeal covering, i.e., the dura. In acute (i.e., intra-operative) ECoG, the cortex is left exposed. In chronic (i.e., inter-operative) ECoG, the grid is sealed under the dura, skull and scalp, with the cables tunneled through the incision in the dura, to exit the scalp distant to the incision (see Fig. 1.5). Subdural ECoG requires penetration of the skull and the dura. This is important for clinical application of this method, because the penetration of the dura increases the risk of bacterial infection (Davson 1976; Fountas and Smith 2007; Hamer et al. 2002; Van Gompel et al. 2008; Wong et al. 2009). Epidural electrodes (i.e., electrodes placed on top of the dura mater) provide signals of approximately comparable fidelity (Torres Valderrama et al. 2010) and do not penetrate the dura.

ECoG recordings are typically referenced to electrocorticographically silent electrodes (i.e., locations that were not identified as eloquent cortex by electrocortical stimulation mapping). Similar to EEG, the measured electric fields are most dominantly related to neural activity in the cortex rather than to neural activity in deeper cortical structures. However, ECoG provides better temporal and spatial resolution than EEG (Fig. 1.6, Ball et al. 2009), as the signals are not attenuated and spread by the electric filter characteristics of the volume conductor (i.e., the scalp, skull and outer meningeal covering). Despite these advantages, current ECoG technology requires the brain to be exposed, effectively limiting spatial coverage of ECoG to part of one hemisphere.

As with all invasive methods, the entailed cost and risks currently limit the application of ECoG to applications in clinical diagnosis and basic research.

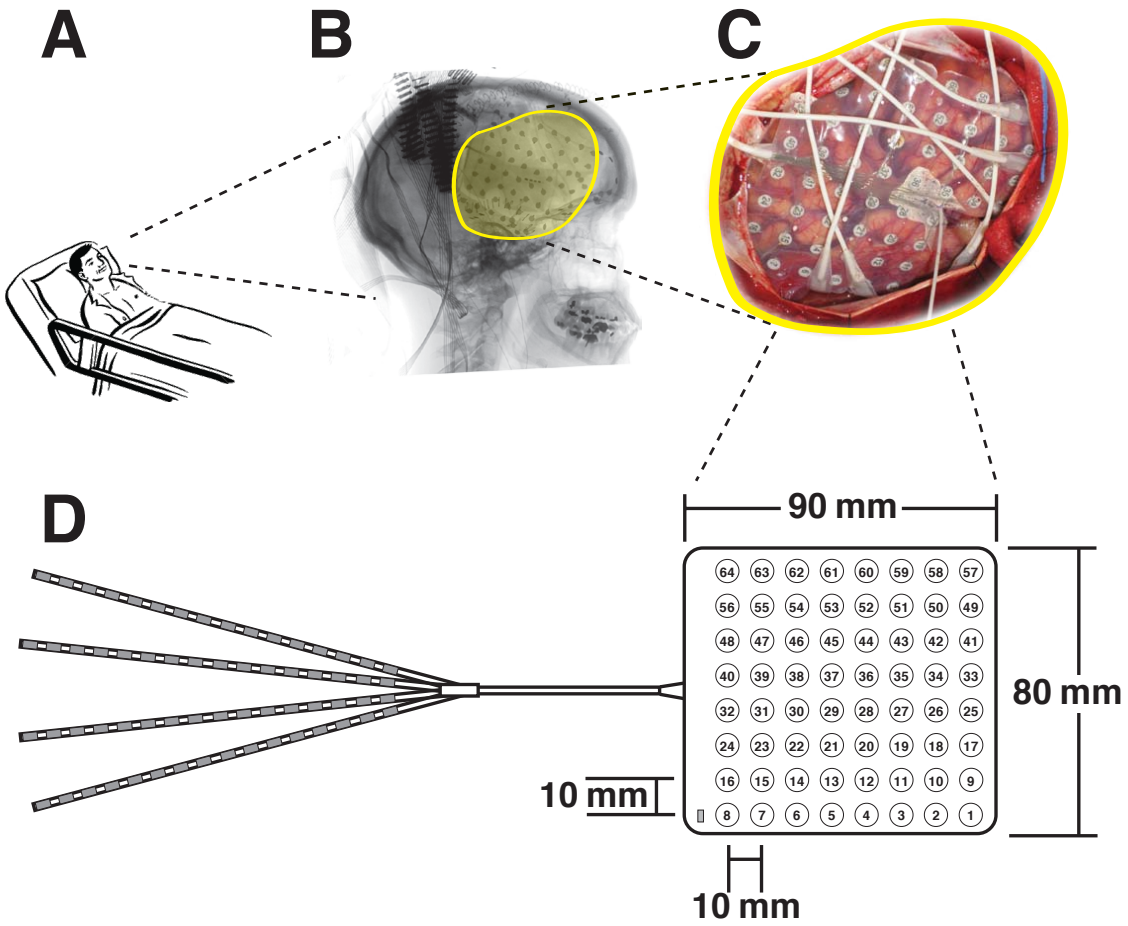

Figure 1.5: **Details of ECoG implant.** This figure shows the patient (A) with a craniotomy (B) and a subdural (C) ECoG implant (D). The cortex is accessed through a craniotomy of the skull (B) and an incision of the outer meningeal covering, i.e., the dura (C). In acute (i.e., intra-operative) ECoG, the cortex is left exposed. In chronic (i.e., inter-operative) ECoG, the grid is sealed under the dura, skull and scalp, with the cables tunneled through the incision in the dura to exit the scalp distant to the incision.

1.1.2.2 Local Field Potentials (LFPs)

Local field potentials (LFPs) are electrical fields within the cortex that are created by synchronized neurons. LFPs therefore are a direct measure of neural activity (Kennedy 1989; Legatt et al. 1980). To record LFPs, the cortex is exposed and microelectrodes are implanted into the cortex. As microelectrodes are close to the neural activity, can be spaced tightly and extend into deeper cortical structures, LFPs have excellent temporal, spatial and depth resolution. However, current LFP technology limits the spatial coverage of LFPs in two ways. First, as with ECoG, implantation of microelectrodes requires

the exposure of the cortex. Second, as the implantation process causes tissue damage and inflammation around the microelectrode, extensive spatial coverage poses an increased risk for infection and thus morbidity associated with this procedure (Jackson et al. 2010; Krüger et al. 2010; Leach et al. 2010; Marin and Fernández 2010).

The additional cost and risks over other invasive techniques (e.g., ECoG) currently limit the application of LFPs to applications in basic research.

1.1.2.3 Single-Unit Activity (SUA)

Single-unit activity is composed of action potentials that are created by individual neurons. Therefore, SUA is a direct measure of neural activity (Fetz 1969). SUA activity is recorded in the same way as local field potentials, however using smaller tipped microelectrodes (Cham et al. 2005; Fee and Leonardo 2001). From recorded signals, action potentials from individual neurons are isolated (Hochberg et al. 2006; Velliste et al. 2008). As LFPs, SUA provides excellent temporal, spatial and depth resolution at the cost of limited spatial coverage. However, SUA activity recordings suffer in their long-term recording stability from inflammation and displacement of the electrodes relative to cortex (Jackson et al. 2010; Krüger et al. 2010; Leach et al. 2010; Marin and Fernández 2010).

The additional cost and risks over other invasive techniques (e.g., ECoG) currently limit the application of SUA to applications in basic research.

1.1.3 Conclusions

The comparison of fMRI, MEG, fNIR, EEG, ECoG, LFP and SUA shows that broad acceptance of a technique to acquire brain signals for communication and diagnosis mainly depends on the ability to provide high temporal and spatial resolution without entailed cost and risks (see Table 1.1). For example, MEG provides good temporal and spatial resolution, but high cost impedes its utility for communication and diagnosis. SUA, as an alternative, is more cost effective and provides even higher temporal and spatial resolution, however the associated risks and limited practicality impede its utility for communication and diagnosis.

ECoG represents an appealing compromise between high spatial and temporal resolution, and entailed cost and risks (Ball et al. 2009; Chao et al. 2010). This makes ECoG well suited for overcoming the bandwidth limitation of brain-computer interfaces and the conceptual limitations in mapping eloquent cortex.

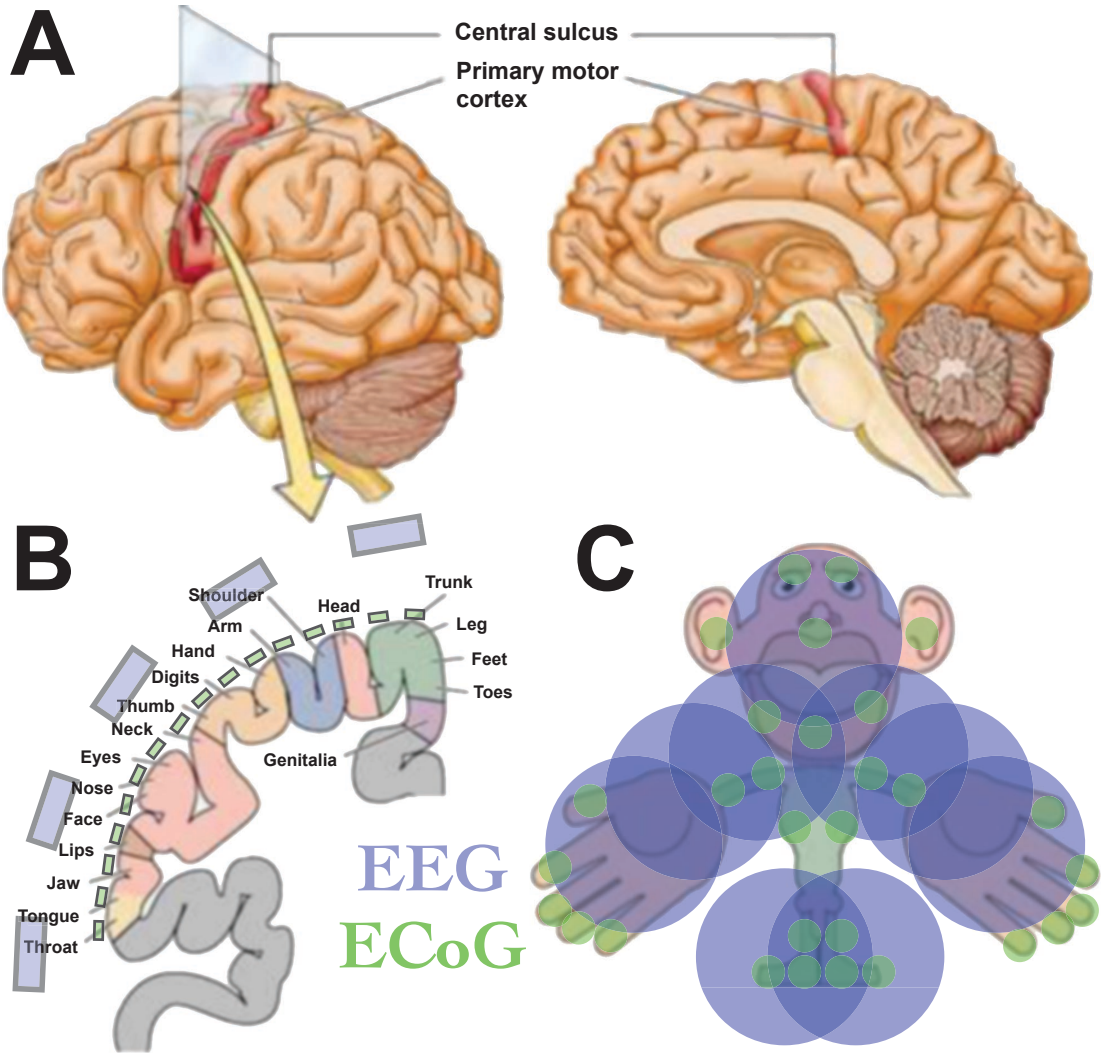

Figure 1.6: **Somatosensory map of EEG and ECoG.** This figure shows the somatosensory map of EEG (blue) and ECoG (green). Primary motor cortex (A) is structured (B) into different somatosensory modalities that can be mapped (C) using EEG (blue) or ECoG (green). The distance of EEG electrodes to the somatosensory cortex (B) results in extensive overlapping coverage in the somatosensory map (C), limiting the ability to dissociate the different somatosensory modalities. In contrast, ECoG electrodes are located on the somatosensory cortex (B) and provide the ability to dissociate the different somatosensory modalities (C).

1.2 Techniques to Analyze Brain Signals

Traditional clinical applications that use brain signals all depend on visual inspection to provide value to the clinical investigator or the patient. In such applications, a highly trained clinical investigator would base his/her diagnosis on the visual inspection of recorded behavioral patterns and neurophysiological signals (Fig. 1.1).

This concept has been recently challenged by studies that have shown promising emerging clinical applications that could replace and enhance established visual inspection-based procedures. Two of these applications are ***brain-computer interface (BCI) communication*** (Vidal 1973), and ***passive mapping of eloquent cortex*** (Crone et al. 1998a). In these applications, traditional visual inspection is replaced by signal processing, feature extraction and machine learning techniques.

So far, brain-computer interfaces and passive mapping of eloquent cortex employed supervised feature extraction and discriminative techniques that depend on post-hoc analysis and an expert to optimize the analyses for each individual patient. Unsupervised and generative approaches have been shown to overcome the requirement for expert supervised post-hoc analysis in related domains such as computer vision (Friedman and Russell 1997; Harville et al. 2001; Kuo et al. 2003; Lee 2005; Liyuan et al. 2004; Pless 2003; Stauffer and Grimson 1999; Toyama et al. 1999) and biosignal processing (Costa and Cabral 2000; Gardner et al. 2006; Harris et al. 2000; Pernkopf and Bouchaffra 2005).

This dissertation focuses on the application of brain signals for communication and diagnosis. The following sections describe the signal processing steps that are necessary to translate brain signals into an output that provides value to the clinical investigator or patient.

1.2.1 Signal Preprocessing

Brain signals are time-varying quantities that are modulated by either the subject's intent (e.g., in the case of communication) or by the subject's cognitive state (e.g., in the case of diagnosis). This context-dependent modulation is considered as information that provides value to the clinical investigator. Signal processing is the process of extracting this information from raw brain signals (1.7).

For example, raw electrophysiological brain signals (e.g., EEG and ECoG) are measurements of potential differences between two electrodes, i.e., a recording and a reference electrode. The signals in these field potentials then reflect activity from both

electrodes. Adding to this, the wiring between electrodes and amplifier is typically susceptible to external electromagnetic noise (e.g., 50/60 Hz line noise). Leading to all electrodes being affected by the same external electromagnetic noise.

To extract and enhance information from such brain signals signal preprocessing employs two fundamental signal processing approaches: (1) Spatial filtering to remove noise common to all electrodes and to extract local and global activity from brain signals by re-referencing them. (2) Averaging brain signals across epochs, to augment the information correlated across epochs and to attenuate uncorrelated noise.

1.2.2 Feature Extraction

For brain signals to be useful in communication and diagnosis, they need to be modulated by relevant information that provides value to the investigator. For example, for the diagnosis of eloquent cortex, those signals are relevant, that are modulated by behavioral tasks. Similarly, for communication, only those signals are relevant that are modulated by the subject's intent. However, such modulations are typically not accessible to visual inspection based procedures and require feature extraction and selection techniques (Fig. 1.7, Fig. 1.8).

Brain signal features are typically extracted in the time or frequency domain, depending on how the signals are modulated. EEG and ECoG signals are modulated in response to exogenous stimuli or to endogenous intent. The response to an exogenous stimulus is typically time and phase locked and therefore best represented in the time domain. In contrast, an endogenous intent remains covert to the observer and is thus neither time nor phase locked and therefore best represented in the frequency domain.

Time domain feature extraction techniques range from simple area under the curve or peak amplitude to the amplitude at a specific time point relative to the exogenous stimulus. In the frequency domain, spectral power is typically determined as a feature through parametric or non-parametric filters.

Such techniques provide the basis to characterize one task-related response or simultaneous intent. Multi-dimensional communication and control and the diagnosis of eloquent cortex require multiple independent features. Feature independence occurs through separation of the modulation in time, frequency, code and space domains.

The following paragraphs describe the necessary signal processing steps to extract relevant features from brain signals in the time and frequency domain.

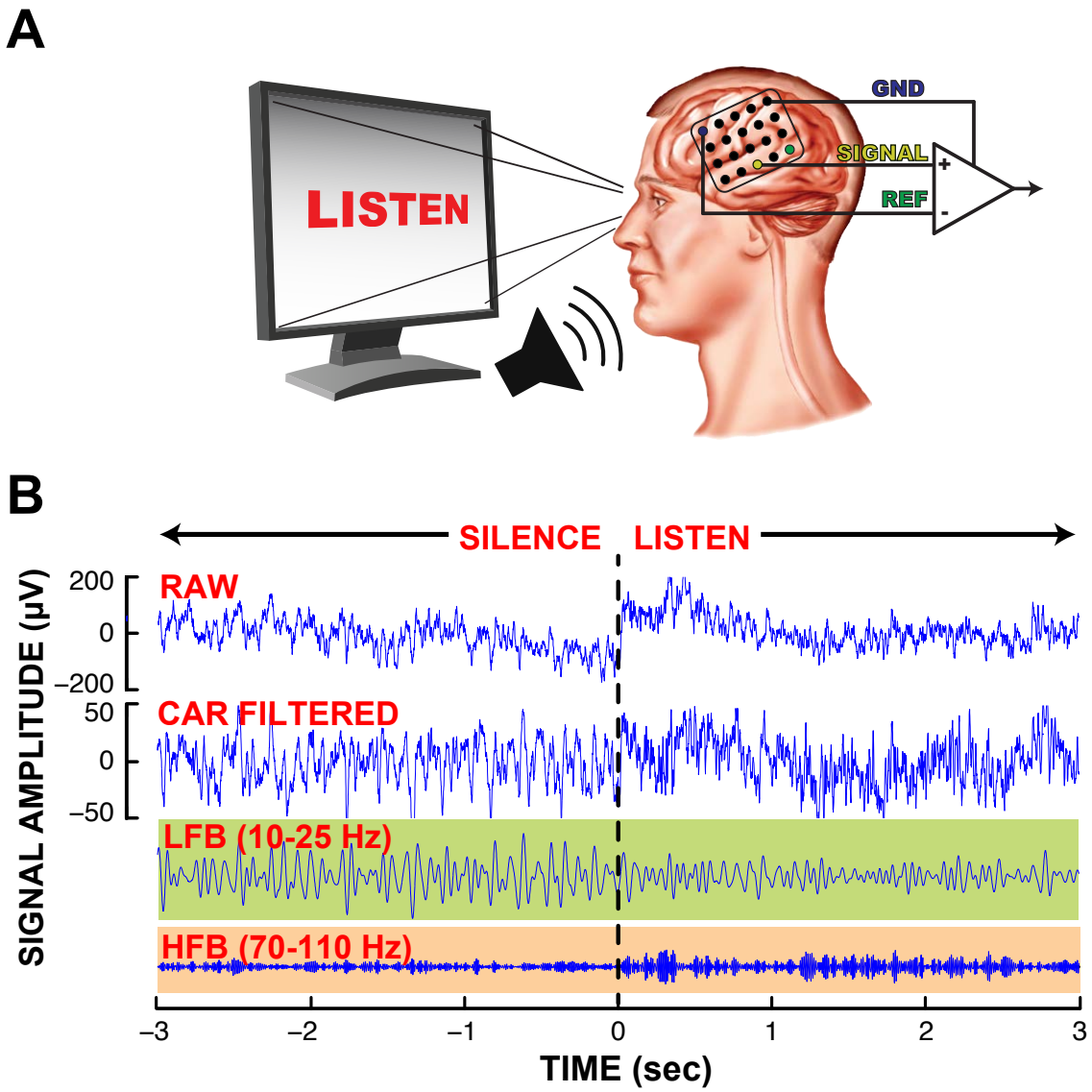

Figure 1.7: **Signal modulation in the time domain.** This figure shows signal modulation in the time domain in response to a listening task. (A) After some silence, the subject is presented with listening task, while electrocorticographic (ECoG) signals are recorded from the superior temporal gyrus. (B) The task-related modulation of the raw ECoG signals cannot be revealed by visual inspection. However, re-referencing (i.e., subtracting the common-average-reference signal) and band-pass filtering reveals the task-related modulation in the LFB (i.e., low frequency band) and HFB (i.e., high frequency band).

1.2.2.1 Time Domain

Brain signals that are time- and phase-locked to an external stimulus are best represented in the time domain. Event related responses (ERP) are such signals that in theory

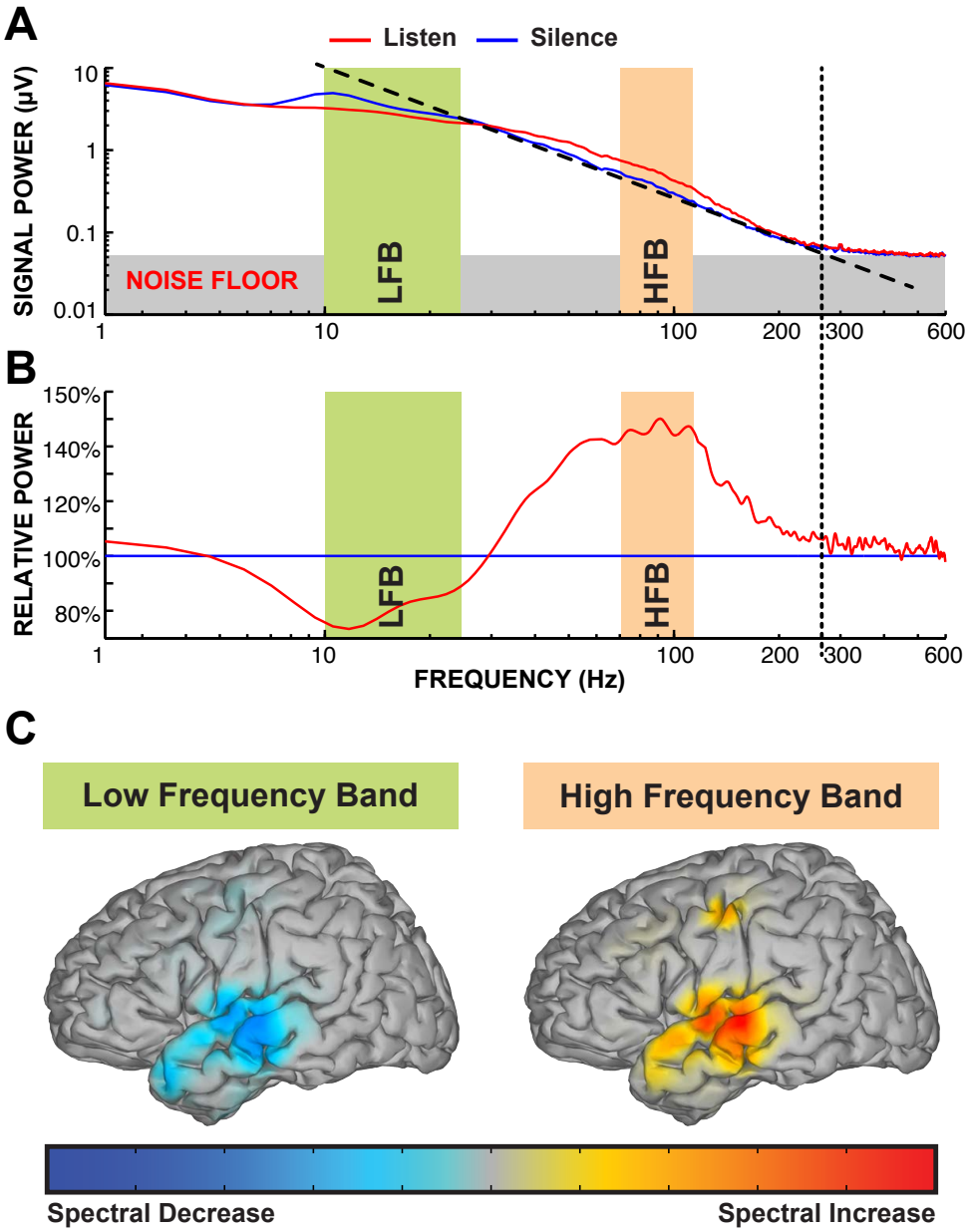

Figure 1.8: **Signal modulation in the frequency domain.** This figure shows the signal modulation in the frequency domain in response to a listening task as presented in Fig. 1.7. (A) Frequency analysis of ECoG signals recorded during listening (red line) and silence (blue line) reveal power-law characteristics (dashed line) that limit the useful signal modulation (i.e., signal-to-noise > 1) to the 0-300 Hz range (dotted line). (B) Within this range, the listening task induces a power decrease in the low frequency band (LFB) and a power increase in the high frequency band (HFB). (C) A topographic representation of these power augmentations reveals the involvement of the superior temporal gyrus (STG) in the listening task.

can be characterized through a matched filter or linear regression. However, variance in the ERP's amplitude and associated noise often require a reduction of the dimensionality. This is achieved either through feature selection (e.g., stepwise linear regression) or feature projection (e.g., area under the curve, energy, peak to peak value).

1.2.2.2 Frequency Domain

Brain signals that are constituted by power augmentations of multiple damped harmonic oscillators are best represented in the frequency domain. Event-related synchronizations and de-synchronizations (ERS/ERD) are such signals. Methods that estimate the spectrum of these oscillations can be divided into parametric (e.g., moving average, auto-regressive methods) and non-parametric methods (e.g., periodogram and other FFT-based methods). Parametric methods estimate the parameters of stochastic process that describes that signal; Non-parametric methods estimate the spectrum without assuming any particular structure. The damped nature of the oscillator makes the frequencies of ERS/ERD non-stationary in their phase, adversity affecting FFT-based methods. This makes parametric methods well suited to estimate the spectral power of these brain signals.

1.2.2.3 Time-Frequency Domain

Brain signals constituted by power augmentations that are time- and phase-locked to multiple external oscillators are best represented in the time-frequency domain. Steady-state evoked potentials (SSEPs) are such signals. The fixed relationship to an external oscillator makes the frequencies of SSEPs stationary in their phase. This makes FFT-based methods well suited to estimate the spectral power of these brain signals.

1.2.3 Dimensionality Reduction

The extraction of features from multiple signal channels in the time, frequency and time-frequency domain typically results in a exorbitant number of features. For example, for 64 signal channels, an FFT-based time-frequency feature extraction (e.g., 1s $\times$ 100Hz with 100ms temporal, and 1Hz frequency resolution) would result in 64.000 features. This exorbitant number of features makes modeling and classification with a limited number of samples (e.g., 200 samples) infeasible. Feature projection and feature selection are two strategies that aim to reduce the number of features while preserving the information content.

1.2.3.1 Feature Projection

This strategy combines the original features into a lower-dimensional subspace. This can be achieved in a supervised and unsupervised fashion. Supervised feature projection uses the data labels to maximize the discriminability and minimize the dimensionality of the data. For example, common spatio-temporal patterns (CSTP) determine an optimal spatio-temporal filter that combines features from each channel into a new feature. In the previous example, CSTP would reduce the number of features from 64.000 to 64. In contrast unsupervised feature projection maximize a statistical property of the data without using the labels of the data. For example principal component analysis (PCA) transforms the features into a set of uncorrelated orthogonal features. Independent component analysis (ICA) de-correlates the features even more by transforming the features into a set of maximally independent non-orthogonal features. As PCA and ICA don't reduce the dimensionality of the data, they require subsequent feature selection.

1.2.3.2 Feature Selection

Features can be selected in a supervised and unsupervised fashion. Supervised feature selection uses the data labels to maximize the discriminability and minimize the dimensionality of the data. For example, stepwise linear regression is an iterative algorithm that adds features if they significantly benefit the model (e.g., p-value < 0.05) and removes them otherwise. To promote dimensionality reduction, an information criterion penalizes larger models over smaller ones. In contrast, unsupervised feature selection maximizes an objective function of the data. For example, a PCA decomposes the data into eigenvectors (i.e., the principal components) that each have an eigenvalue associated (i.e., the variance in the data explained by the corresponding principal component). Unsupervised feature selection then minimizes the dimensionality by selecting those principal components as the feature subspace that explains a certain portion (e.g., 90%) of the variance in the data.

1.2.4 Modeling and Classification

1.2.4.1 Discriminative Techniques

Discriminative techniques use a combination of signal features to separate two or more categories. The combination of features is determined through a machine learning algorithm that calculates the coefficients of a linear or non-linear function (i.e., classifier)

that is predictive of the categories. The employed machine learning algorithms typically require a supervised data set to determine the classifier.

Such supervised and discriminative techniques work well on data that is stationary and for which all classes are known, but fail when data is non-stationary or not all classes are known. Applications that use brain signals can be classified into exogenous and endogenous systems (Mason and Birch 2003). For exogenous systems, the neural response to the stimuli is time-locked to the stimuli and typically only depends on the attention to the stimuli. Therefore, exogenous systems tend to produce supervised and stationary data for which supervised and discriminative techniques work well. In contrast, while endogenous systems may cue the subject to produce a neural response, the evoked neural activity is not time-locked to a known stimulus and typically depends on a mental strategy. Therefore, exogenous systems tend to produce weakly-supervised and non-stationary data which is sub-optimal for supervised and discriminative techniques.

Many different approaches, including adaptation and more robust learning algorithms, have been proposed to address these problems. However, each of these approaches adds complexity and additional parameters that impede its successful application to brain signals in a clinical environment.

In summary, discriminative techniques are best suited for exogenous systems for which all classes are known and stationary. One such exogenous system is the matrix-based speller originally described by Farwell and Donchin in 1988. In aim 1 of this dissertation, we use discriminative techniques to investigate for the first time the online performance of the matrix speller using ECoG signals.

1.2.4.2 Generative Techniques

Generative techniques use a combination of signal features to model the statistical properties of the data. The parameters of the model are typically determined through a machine learning algorithm that maximizes the data likelihood. The employed machine learning algorithms may use supervised or unsupervised data sets to determine the model.

Unsupervised generative techniques work well on data for which statistical properties are stationary and known, but fail when statistical properties are non-stationary. Consequently, generative techniques are best suited for endogenous systems for which one stationary condition exists. One application of an endogenous system is the passive mapping of eloquent cortex using ECoG signals (Crone et al. 1998a). In this applica-

tion, one known stationary condition (e.g., ECoG activity during rest) is discriminated from multiple unknown non-stationary conditions (e.g., ECoG activity during activation of eloquent cortex). In aim 2 of this dissertation, we investigate the feasibility of a generative approach to passively map eloquent cortex using ECoG.

1.2.5 Conclusions

In conclusion, brain signal analysis aims to describe the information contained in neural signals through a limited number of variables. This entails, removing common noise, extracting meaningful features, reducing the dimensionality and modeling the data.

1.3 Applications that Make Use of Brain Signals

1.3.1 Applications for Communication

In the 80 years since Hans Berger first recorded electroencephalographic activity (EEG) from the scalp using silver wires and a galvanometer (Berger 1929), researchers and clinicians have continued to develop better instrumentation and clinical applications that can detect and/or use EEG and other brain signals. One of these clinical applications is a brain-computer interface (BCI) (Vidal 1973) that might restore communication to people with severe motor disabilities. BCI instrumentation consists of hardware and software. BCI hardware records brain signals either non-invasively (e.g., EEG, magnetoencephalography (MEG), functional near-infrared spectroscopy (fNIR)) or invasively (e.g., electrocorticography (ECoG), local field potentials (LFP), single-unit activity) using a series of devices (i.e., sensor, biosignal amplifier and analog-to-digital converter). BCI software then translates these brain signals into device output commands and provides feedback to the user.

Up to the present, BCI research and development has mainly focused on basic research and laboratory demonstrations of various BCI applications (Bin et al. 2009; Birbaumer et al. 1999; Coyle et al. 2007; Farwell and Donchin 1988; Gao et al. 2003; McFarland et al. 2010b; Müller et al. 2008; Pfurtscheller et al. 1993, 2003; Schwartz et al. 2006; Taylor et al. 2002; Velliste et al. 2008; Wolpaw and McFarland 2004; Wolpaw et al. 1991, see Wolpaw et al. 2002 for review). As BCI research is evolving from isolated demonstrations to systematic investigations, it has become clear that BCI hardware and software require features, such as real-time capability (Berger et al. 2007; Cincotti et al. 2006; Guger et al. 2001, 1999; Mason and Birch 2003; Schalk et al. 2004; Wilson et al. 2010) and high bandwidth and sensitivity (Crone et al. 1998a; Schalk 2008), that existing hardware and software often did not provide. In response, different vendors (e.g., g.tec, Brain Products, Tucker-Davis Technologies, Ripple, etc.) have produced hardware devices that are optimized for BCI or related research. These research systems can capture EEG, ECoG or single-neuron activity in real time from up to 512 channels and sample these signals at up to 50 kHz with very high sensitivity (e.g., 24-bit resolution, 250-mV sensitivity). This BCI hardware is interfaced with BCI software that is based either on general-purpose BCI frameworks such as BCI2000 (Mellinger and Schalk 2007; Schalk et al. 2004; Schalk and Mellinger 2010) or OpenVIBE (Renard et al. 2010), or on custom software. Using these research-grade systems, groups around the world are now beginning to demonstrate clinical efficacy of BCIs in patients with severe motor disabilities

(Cincotti et al. 2008; Guger et al. 2009; Kübler et al. 2005; Nijboer et al. 2008; Sellers et al. 2006b, 2010; Stavisky et al. 2009; Vaughan et al. 2006, see Mak and Wolpaw 2009 for review), thereby beginning the translation of research findings into clinical practice.

In addition to these academic efforts that focus on clinical applications of BCI technology, some commercial vendors have begun to provide consumer-grade applications to both able-bodied and disabled people. Such consumer applications include augmented communication devices (IntendiX, `http://www.intendix.com`) and gaming systems (MindFlex, `http://www.mindflexgames.com`, Allison et al. 2007; Blankertz et al. 2010; Fairclough 2008, see Reuderink 2008 for review). Other types of commercial applications may use BCI technology to detect different covert states in a subject (Baernreuther et al. 2010; Bahramisharif et al. 2010; Zander and Jatzev 2009). This approach provides the basis for emerging applications such as neuromarketing (e.g., Neurofocus, `http://www.neurofocus.com`, Pradeep 2010) or defense applications (e.g., Honeywell, AugCog helmet, Dorneich et al. 2009; Kotchetkov et al. 2010; St. John et al. 2005).

In summary, applications of BCI technology fall into the following four categories: Basic Research, Clinical/Translational Research, Consumer Products, and Emerging Applications. These four categories all use BCI hardware and software, but have different sets of requirements. For example, while basic research needs to explore a wide range of system configurations, and thus requires a wide range of hardware and software capabilities, applications in the other three categories may be designed for relatively narrow purposes and thus may only need a very limited subset of capabilities. The following sections summarize different technical issues for these four categories of BCI applications.

1.3.1.1 Basic Research

Basic BCI research and development is based predominantly on recording and analysis of electrophysiological brain signals. These brain signals can be classified into three categories that depend on the source of the signal recordings: (i) EEG signals, which are recorded from electrodes on the scalp; (ii) ECoG signals, which are recorded from electrode grids on the surface of the brain; and (iii) single-unit activity that is recorded from electrode arrays implanted within the brain.

The number of channels that are recorded usually varies from 8-64 for EEG (Sharbrough et al. 1991), to 32-192 for ECoG (Lesser et al. 2010), to 100-300 for single-unit recordings (Maynard et al. 1997). The brain signals recorded from these modalities vary substantially in their amplitudes and frequencies (EEG: 50 μV, 0-50 Hz; ECoG: 500 μV,

0-300 Hz; extracellular single unit activity: 100 μV, 0.3-30 kHz, see Niedermeyer and Lopes da Silva 1993 for review). Because signals also vary substantially in amplitude across frequencies (Miller et al. 2010, 2008), it is difficult to acquire these three signal categories with the same amplifier and analog/digital converter. This issue is compounded by safety requirements that are prescribed by regulatory authorities such as the Food and Drug Administration (FDA) in the US, the European Commission (CE) in Europe, and the Ministry of Health, Labor, and Welfare (MHLW) in Japan. For that reason, current BCI hardware is usually tailored for only one category of signals and the extraction of one set of features. In consequence, laboratories may need to purchase a dedicated set of BCI hardware for each of these signals. At a system cost of several hundred to one thousand dollars per channel, this becomes an expensive proposition.

The integration of these dedicated sets of acquisition hardware into the laboratory requires connecting different hardware interfaces to electrodes and behavioral sensors. This usually requires additional hardware (e.g., head stages, pre-amplifiers and behavioral data acquisition) to acquire signals from other sources and to prevent artifacts that affect the signal-to-noise ratio.

The coordinated acquisition, analysis, and storage of brain and behavioral signals recorded by these sets of acquisition hardware remain complex. It requires communication between and synchronization of various software interfaces. These interfaces may be synchronous (e.g., stream-based) or asynchronous (e.g., event-based) and their timing and sampling-rate may vary (Wilson et al. 2010). General-purpose BCI software frameworks such as BCI2000 (Mellinger and Schalk 2007; Schalk et al. 2004; Schalk and Mellinger 2010) or OpenVIBE (Renard et al. 2010) provide readily available solutions to acquire, analyze and store brain and behavioral signals. However, standardization of software beyond such packages does not yet exist.

In summary, standardization and integration of hardware and software continues to remain an issue for BCI research and development.

1.3.1.2 Clinical/Translational Research

The translation of BCIs into clinical practice provides a primary impetus and focus for BCI research, and is thus of high interest to funding institutes such as the National Institutes of Health (NIH). Groups around the world are demonstrating the clinical efficacy of BCIs (Cincotti et al. 2008; Guger et al. 2009; Kübler et al. 2005; Nijboer et al. 2008; Sellers et al. 2006b, 2010; Stavisky et al. 2009; Vaughan et al. 2006, see Mak and Wolpaw 2009 for review), and the NIH lists 11 active investigational clinical BCI trials

(http://clinicaltrialsfeeds.org).

These investigational studies currently use experimental-grade BCI hardware and software that were developed for basic research and suffer from high cost and complexity, proprietary standards, and lack of robustness (Cincotti et al. 2006). The translation of this experimental-grade BCI hardware and software into product-grade clinical BCI instrumentation is challenging. It requires the integration of BCI hardware and software into clinical environments as well as improvements to clinical applicability, robustness, usability, and cost/benefit ratio (Kübler et al. 2006). Beside these engineering tasks, the development of clinical certification (Higson 2002), reimbursement (Raab and Parr 2006), and dissemination procedures all require attention.

In addition to the difficulties in translating BCI technologies, it remains unclear whether clinical BCI systems will ever be a viable alternative to other established (i.e., muscle-based) and emerging (e.g., bionic) assistive devices. Currently established and emerging assistive clinical devices tend to provide a better cost/benefit ratio and are easier to use and disseminate (Berger and Glanzman 2005; Majaranta and Räihä 2002; Pylatiuk and Döderlein 2006; Schalk 2008).

If clinical BCI systems are to become widely used, they need to either improve on their performance or complement established and emerging assistive devices. Hybrid BCIs, i.e., the combination of a BCI with other BCIs or existing assistive systems, follow a current trend that addresses this issue (Allison et al. 2010; Millán et al. 2010; Pfurtscheller et al. 2010; Zander et al. 2010). In any case, the current lack of product-grade BCI hardware and software and standardized procedures impedes the translation of BCIs into clinical practice.

1.3.1.3 Consumer Products

The growing interest in and maturity of the field of BCI research have opened up different avenues for application of BCI technology in commercial contexts.

Commercial BCI devices measure signals from the brain and turn them into outputs that provide value to the customer. As with many other novel technologies, it is currently unclear in which situations BCI devices can provide maximum value for the largest number of users. Several manufacturers are currently exploring these questions by offering commercial BCI-like devices. These companies include Emotiv (http://www.emotiv.com), Neurosky (http://www.neurosky.com) and OCZ Technology (http://www.ocztechnology.com).

Success of widespread dissemination of commercial BCI devices depends on reduc-

ing the barriers to acquiring and using these systems. This requirement entails several challenges that relate mainly to cost and ease of use. The cost of a typical (i.e., research-based) BCI system is usually at least 5000 dollars – too much for most consumer products. Reducing these costs is mainly a technical problem that can be solved, but does require appropriate resources. Improving ease of use mainly relates to improving EEG electrode technology. Typical EEG electrodes are wet, i.e., they require the application of conductive electrode gel, and usually have to be applied by trained experts who abrade the skin mildly. In contrast, widespread application requires that electrodes can be applied without gel and the associated mildly abrasive procedures. Different strategies have been proposed to address this problem. The first strategy is to create "dry" electrodes, i.e., electrodes that can function with a dry interface between electrodes and the scalp. Different types of dry electrodes have been proposed (Gargiulo et al. 2010; Matthews et al. 2007; Popescu et al. 2007; Sellers et al. 2009; Sullivan et al. 2008) and are currently distributed by commercial vendors (e.g., Nouzz (`http://nouzz.com`), Quasar (`http://www.quasarusa.com`)), but at least some still have unsolved problems with robustness. The second strategy is to create "active" electrodes, i.e., electrodes that do require the application of conductive gel, but amplify the EEG signal at the electrode, which minimizes the need for skin abrasion. Active electrodes are provided by many commercial vendors of EEG equipment, but typically are quite expensive and still require an additional biosignal amplifier and analog-to-digital converter. The third strategy is to actively shield the connection between the electrode and the distant biosignal amplifier. This possibility is currently only implemented by one commercial vendor (Twente Medical Systems International (`http://www.tmsi.com`)). Their system utilizes actively shielded cables that prevent capacitive coupling that also minimizes the need for abrading the skin.

Finally, improving ease of use also requires that operation of the BCI software should be as easy as possible. This requires that it can adapt efficiently to fluctuations in brain signals caused by changes in the subject's brain state or environmental or other noise.

In summary, it is currently unclear to what extent BCI performance will further improve, and when and to what extent BCI technologies will find commercially viable applications in consumer areas.

1.3.1.4 Emerging Applications not related to Communication and Control

Since their origin, BCIs have focused mainly on communication and control. The resulting studies have developed a body of knowledge and technology, including portable

hardware and novel methods for extracting and reliably classifying relevant aspects of brain signals. This knowledge has applications beyond the development of traditional BCIs. Some of these applications challenge the current definition of BCIs.

BCI technology can also provide the basis for novel applications that go beyond restoration of function. Such novel and emerging applications that are not related to communication and control may include detection of covert behavior (Baernreuther et al. 2010; Bahramisharif et al. 2010; Zander and Jatzev 2009), biofeedback, sleep control, treatment of learning disorders, functional and stroke rehabilitation, and the use of brain signals as biomarkers for diagnosis of diseases or their progression (Georgopoulos et al. 2007). Some of these opportunities have begun to be exploited commercially, e.g., neuromarketing (Neurofocus, `http://www.neurofocus.com`, Pradeep 2010) and defense applications (Honeywell, AugCog helmet, Dorneich et al. 2009; St. John et al. 2005). The ability of BCI feedback to induce cortical plasticity (Carmena et al. 2003; Fetz 1969; Leuthardt et al. 2004; Miller et al. 2010; Taylor et al. 2002; Wolpaw and McFarland 2004) may provide the basis for therapeutic tools that restore brain function. Such therapeutic tools are currently under development for reducing seizures (Monderer et al. 2002; Sterman and Egner 2006; Walker and Kozlowski 2005), treating attention deficit or hyperactivity disorders (Monastra et al. 2005), improving cognitive function in elderly (Angelakis et al. 2007), managing pain (deCharms et al. 2005), and improving motor function in stroke patients (Ang et al. 2010; Buch et al. 2008; Daly et al. 2009, see Daly and Wolpaw 2008 for review). One of the characteristics of these emerging applications is that they are often targeted toward larger markets than traditional BCIs.

In summary, emerging applications not related to communication and control may provide additional drive for development of BCI hardware and software.

1.3.1.5 Standardization

As described in the previous sections, the translation of BCI hardware and software from isolated demonstrations to systematic investigations and commercial products requires efforts in different disciplines (Berger et al. 2007). The lack of defined technical standards has become an important impediment to the integration of those efforts. As an example, it is currently difficult to mix and share hardware devices (e.g., EEG headsets, amplifiers), tools (e.g., Bianchi et al. 2009), and software modules (e.g., classifiers) that originate from different laboratories or manufacturers. While there have been isolated efforts to define and implement a common model for BCI operation (Mason and Birch 2003), a standard way in which they exchange information through well-defined

interfaces (Quitadamo et al. 2008), and general-purpose BCI software (Bianchi et al. 2003; Renard et al. 2010; Schalk and Mellinger 2010), these efforts do not yet completely encompass all aspects of hardware connectivity, file formats for storing any kind of information (e.g., biosignals, classifiers outputs, feedback rules), or all software interfaces (in particular with third-party software).

Standardization of the technical basis for hardware and software interfaces has been shown to facilitate the translation from isolated demonstrations to systematic investigations and commercial products (Tassey 1997). On the other hand, standardization, if poorly designed or timed, impedes innovation (Tassey 2000). However, if well designed and timed, standardization will facilitate the coordinated development of future BCI hardware and software. For example, as a first step, connectors between EEG caps and biosignal amplifiers could easily be standardized without overly stifling innovation.

1.3.1.6 Conclusions

BCI applications for communication are currently in a transition from isolated demonstrations to systematic research and commercial development. Successful and continuing transition requires that BCI technology further improve in speed, accuracy, price, and robustness, and consequently the cost/benefit ratio. For example, to match the cost/benefit ratio of conventional assistive communication devices, product-grade BCI spelling devices may require maintenance-free spelling performance of more than 10 words per minute at close to 100% accuracy for less than 15 thousand dollars (e.g., MyTobii P10 eye-tracker system, Tobii Technology AB, Sweden, `http://www.tobii.com`). To facilitate necessary improvements, an ecosystem of product-grade BCI systems and components needs to be developed. The requisite efforts include the development of better integrated and more robust BCI hardware and software, the definition of standardized interfaces, and the development of certification, dissemination and reimbursement procedures.

We expect that these efforts will create an ecosystem of increasingly compatible BCI hardware and software that will enable the translation of BCIs into clinical practice, as well as the rapid development and dissemination of commercial consumer applications and additional applications that are not related to communication and control. The detailed aspects for creating an ecosystem of product-grade BCI hardware and software, and the likely societal impact of this ecosystem, require further investigation.

The creation of this ecosystem may be hindered by factors such as defensive intellectual property strategies, and the lack of patent pools and commercial interests. It is

also possible that unresolved ethical considerations, such as privacy and liability, will eventually impede the proliferation of BCIs (Haselager et al. 2009; Kübler et al. 2006).

In summary, the successful and continuing transition of BCI technology from isolated demonstrations to systematic research and commercial development requires significant improvements in speed, accuracy, price, and robustness, and consequently the cost/benefit ratio. In aim 1 of this dissertation, I will begin to address this problem by developing and validating methods for increased speed of matrix speller BCIs.

1.3.2 Applications for Diagnosis

Electrophysiological brain signals have been used for decades for three established clinical diagnostic applications: (1) general diagnosis of epilepsy and other disorders of the central nervous system through visual inspection of EEG signals (Gibbs et al. 1936); (2) localization of epileptogenic cortex through visual inspection of interictal and ictal data in ECoG signals (Penfield et al. 1942); and (3) mapping of eloquent cortex through electrical cortical stimulation (ECS) for presurgical planning of epileptogenic and lesional cortical tissue resection (Foerster 1931).

These three applications (i.e., visual inspection of EEG or ECoG, or ECS mapping) have evolved from mechanical stylus- and paper-based instrumentation to fully computerized clinical bedside monitoring systems (Fig. 1.9). In this evolution, clinical bedside monitoring systems were designed to deliver a visual impression comparable to that of mechanical systems. Such systems record EEG or ECoG signals from 0.1 to 50 Hz sampled at 256 Hz with 12-bit resolution (i.e., sensitivity of 100 μV). To acquire these signals, EEG recordings typically use 20-64 surface electrodes arranged according to the 10/20 international electrode system (Jasper 1958). ECoG recordings may use arrays of subdural electrodes in numbers from several to 200 arranged in 1-cm spacing on multiple grids and strips and implanted above or below the dura. A biosignal amplifier with analog-to-digital converters and a workstation comprise the clinical bedside monitoring system. The workstation stores the recorded signals along with a video stream of the subject's behavior. A clinical investigator then bases his/her diagnosis on the visual inspection of recorded behavioral patterns and neurophysiological signals.

The focus of these devices on only those aspects important to visual inspection has recently begun to show its limitations. For example, recent studies have shown promising emerging clinical applications that could replace and enhance established visual inspection-based procedures. One of these applications is the passive mapping of eloquent cortex using functional magnetic resonance imaging (fMRI) (Chakraborty and McEvoy, 2008), positron emission tomography (PET) (Bittar et al., 1999; Meyer et al., 2003), magnetoencephalography (MEG) (Ganslandt et al., 1999), evoked potentials (EP) (Dinner et al., 1986) or electrocorticography (ECoG) (Crone et al. 1998a).

Each of these methods has problems that include morbidity, time consumption, expense, or practicality (Table 1.2). However, because existing surgical protocols typically already include the placement of subdural electrodes, and because of its procedural simplicity, ECS has become the gold standard for mapping eloquent cortex. The following sections summarize different practical issues related to the application of fMRI, PET,

MEG, EP and ECoG for passive mapping of eloquent cortex.

Table 1.2: **Comparison of techniques that map eloquent cortex.** This table compares the utility of techniques that map eloquent cortex. In this comparison, ECS tends to entail the most issues associated with risks, limitations, requirements and results. In contrast, ECoG tends to entail fewer risks and limitations, but still suffers from issues associated with the requirements and results of this procedure.

Risks	**ECS**	**PET/fMRI**	**MEG**	**ECoG**
can induce seizures	yes	no	no	no
increased morbidity	yes	no	no	yes
Limitations	**ECS**	**PET/fMRI**	**MEG**	**ECoG**
limited spatial resolution	yes	yes	yes	no
limited temporal resolution	yes	yes	no	no
limited variety of tasks	yes	yes	yes	no
limited to adult patients	yes	yes	no	no
Requirements	**ECS**	**PET/fMRI**	**MEG**	**ECoG**
requires expert†	yes	yes	yes	yes†
requires expensive equipment	no	yes	yes	no
requires much time†	yes	yes	yes	yes†
requires patient compliance	yes	yes	yes	yes
Results	**ECS**	**PET/fMRI**	**MEG**	**ECoG**
suffer from expert variability†	yes	yes	yes	yes†
suffer from artifacts problems	yes	yes	yes	no
require post/hoc analysis†	no	yes	yes	yes†

Note: † Issues addressed in this dissertation.

1.3.2.1 Electrical Cortical Stimulation (ECS)

Electrical cortical stimulation (ECS) maps eloquent cortex by applying electrical current onto the cortical surface while observing the evoked behavioral response (Foerster 1931). The electric current is delivered in pulses (e.g., 0.5-15 mA, 0.3 ms 50 Hz pulses, 2-5 sec stimulation, see Ojemann 1991 for details) through a grid of electrocorticographic electrodes (2.4 mm diameter, 1 cm spaced). The stimulation evokes an excitatory or inhibitory neural and consequently behavioral response that is observed by the clinical investigator. Stimulation of motor, sensory or visual cortex typically evokes an excitatory response, while stimulation of auditory, memory or language cortex evokes an inhibitory response. The stimulation thresholds for motor and sensor cortex are lower (e.g., 2-4 mA) than those for auditory, memory and language cortex (e.g., 8-15 mA).

As such, ECS is a lesional and non-physiological approach that can be applied in the operating room under local anesthesia (i.e., intraoperatively) or at the bedside. The results, i.e., the electrodes that are labeled as eloquent cortex, are directly used by the neurosurgeon to delineate eloquent from abnormal tissue during resective surgery.

Since ECS has three quarters of a century of historical and clinical relevance (Foerster, 1931), and perhaps also due to its relative procedural simplicity and low cost, ECS has become the gold standard in mapping eloquent cortex. It has gained broad acceptance despite limited data to support efficacy (Hamberger, 2007) and despite of several substantial issues. For example, ECS is time consuming because it requires a comprehensive search, i.e., stimulation of each grid contact, while simultaneously determining the appropriate stimulation amplitude. ECS can also produce after-discharges that may trigger seizures or even status epilepticus. This can result in substantial delays, aborted procedures, and patient morbidity. The results derived using ECS may also not be correct because: 1) stimulation may produce inhibitory responses that cannot readily be observed; 2) propagation of stimulation current is affected by the anatomy and potential after-discharges, and thus variable; 3) there may be substantial procedural variability; and 4) stimulation-based mapping is based on a lesional and not a physiological model. Finally, ECS depends on patient compliance and thus cannot easily be used in some patient populations (such as pediatric patients). The characteristics of ECS are reviewed in (Devinsky et al., 1993) and (Ojemann et al., 1989). The problems described above increase the risk to the patient and the time and cost associated with surgical planning.

1.3.2.2 Positron Emission Tomography (PET) and Functional Magnetic Resonance Imaging (fMRI)

Positron emission tomography (PET) and Functional magnetic resonance imaging (fMRI) map eloquent cortex by measuring the task-related increase in metabolic activity relative to a baseline (Bittar et al. 1999; Chakraborty and McEvoy 2008; Meyer et al. 2003). As such, PET and fMRI represent physiological non-lesional (i.e., passive) approaches that are limited to pre-surgically assessment of eloquent cortex. The result of this assessment is a 3-dimensional volume of eloquent cortex that requires a translation into the 2-dimensional coordinate system that is used by the neurosurgeon to delineate eloquent from abnormal tissue during resective surgery. This typically requires a multimodal acquisition (PET-CT) and subsequent co-registration with anatomical structures (MRI).

PET-CT (Beyer et al. 2000) and fMRI (Belliveau et al. 1991) have only been recent advances in medical imaging, require expensive instrumentation (e.g., multiple million

dollars) and trained personnel. This is compounded by the technological limitations of the fMRI and PET: 1) the procedure is not available at the bedside or in the operating room when surgical decisions are most critical; 2) the low temporal resolution of fMRI and PET prevents the assessment of eloquent cortex that is not continuously activated (e.g., language, memory); Because of these reasons, PET and fMRI have not gained broad acceptance as techniques to map eloquent cortex.

1.3.2.3 Magnetoencephalography (MEG)

Magnetoencephalography (MEG) maps eloquent cortex by measuring the task-related increase in the weak magnetic field that is created by synchronized neurons (Cohen 1968). As such, MEG represents a physiological non-lesional (i.e., passive) approach that is limited to pre-surgically assessment of eloquent cortex. The measured magnetic field follows neural activity instantly and is not markedly affected by the geometry and conductivity of the scalp, skull, outer meningeal covering and brain. Consequently MEG provides the high spatial and temporal resolution (Ganslandt et al. 1999) necessary to map eloquent cortex that is not continuously activated (e.g., language, memory).

However, MEG mapping suffers from two substantial disadvantages: 1) it requires expensive instrumentation (e.g., multiple million dollars) and trained personnel; 2) it is not available at the bedside or in the operating room; In consequence, MEG has not gained broad acceptance as a technique to map eloquent cortex.

1.3.2.4 Electrocorticography (ECoG)

Electrocorticography (ECoG) maps eloquent cortex by measuring the task-related increase in electrical fields on the cortex (i.e., subdural) or on the dura (i.e., epidural) that are created by synchronized neurons (Aoki et al. 1999, 2001; Crone et al. 2001, 1998a,b; Fries 2005; Graimann et al. 2002; Lachaux et al. 2003; Leuthardt et al. 2007; Miller et al. 2007b; Sinai et al. 2005; Varela et al. 2001). These fields are typically recorded from the same electrocorticographic grids that are used for ECS mapping (2.4 mm diameter, 1 cm spaced). While the spatial resolution of ECoG mapping is limited by these grids, it provides excellent temporal resolution that allows to map eloquent cortex that is not continuously activated (e.g., language, memory). As such, ECoG represents a physiological non-lesional (i.e., passive) approach that is suited for intraoperative (i.e., within the operating room) and bedside assessment of eloquent cortex. ECoG mapping typically uses task-related increases in the gamma band and its results have been shown

to be in general agreement with those derived using fMRI (Lachaux et al., 2007a) and ECS (Leuthardt et al., 2007; Miller et al., 2007b; Sinai et al., 2005). The results, i.e., the electrodes that are labeled as eloquent cortex, are directly used by the neurosurgeon to delineate eloquent from abnormal tissue during resective surgery.

While a few recent studies have provided encouraging evidence that ECoG-based analyses could become more accessible to clinicians (Lachaux et al., 2007b,c; Miller et al., 2007a), passive mapping of eloquent cortex using ECoG has remained an academic demonstration due to the dependence on post-hoc analysis and an expert to optimize the analyses for each individual patient.

1.3.2.5 Conclusions

The comparison of ECS, PET, fMRI, MEG, and ECoG shows that broad acceptance of a technique to map eloquent cortex mainly depends on cost, availability and limitations. For example, while the high temporal, spatial, and task fidelity of MEG overcomes many limitations that are associated with ECS, high cost and the dependence on co-registration with anatomical structures impede broad acceptance. Interestingly, ECoG represents a cost-effective and readily available technique that overcomes many limitations of ECS (see Table 1.2). However, because of the dependency on post-hoc analysis, ECoG has not become a widely accepted technique to map eloquent cortex.

In aim 2 of this dissertation, I will develop techniques that remove the need for post-hoc analysis by using a generative approach to passively map eloquent cortex using ECoG.

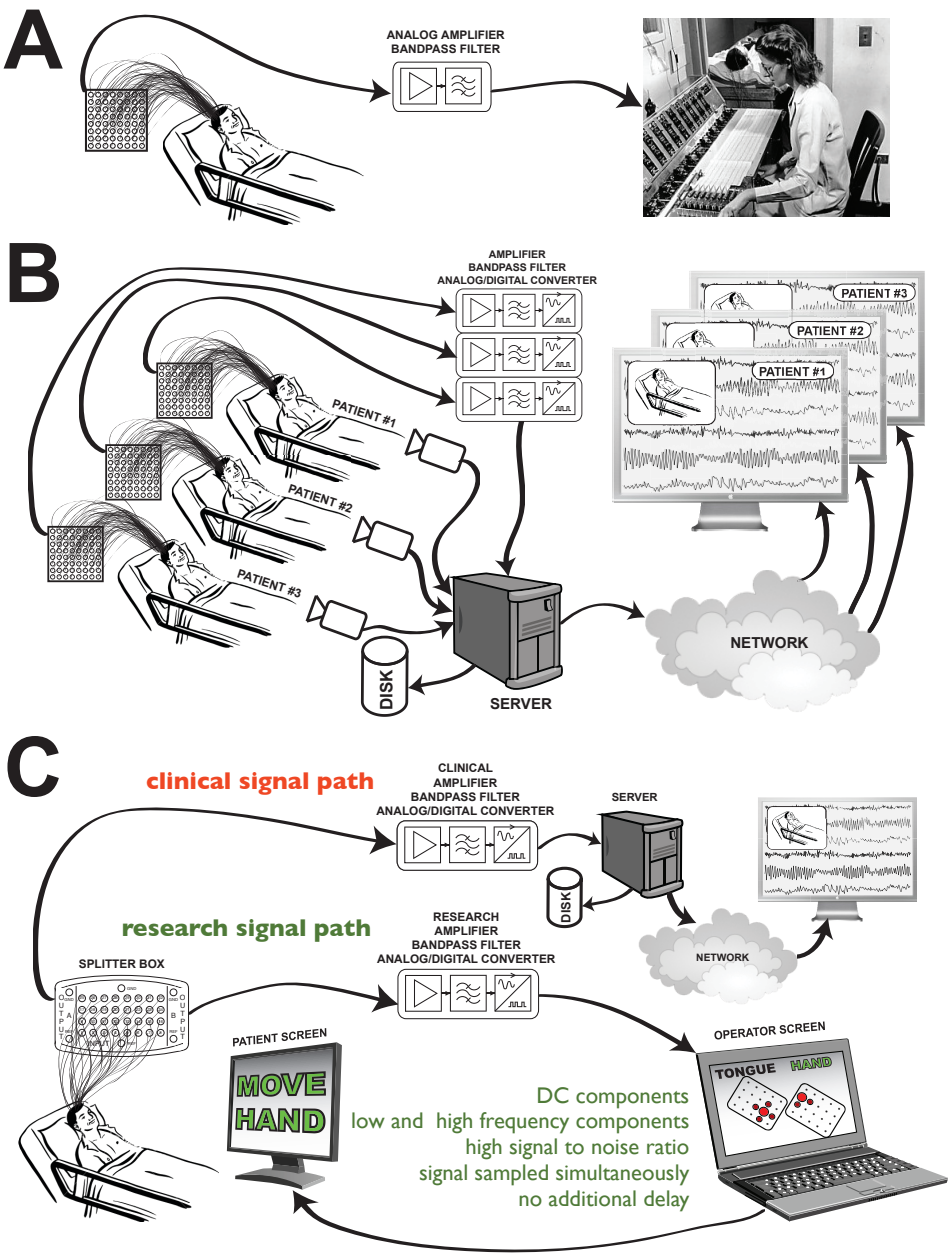

Figure 1.9: **Evolution of clinical bedside monitoring systems** This figure shows the evolution of clinical bedside EEG and ECoG monitoring systems with the patient (left), the instrumentation (center), and the interface to the investigator (right). In this evolution, clinical bedside EEG and ECoG monitoring systems have evolved from mechanical stylus and paper systems (A) over video-EEG (B) to dedicated clinical research systems (C) which in addition to monitoring the EEG and ECoG also provide feedback to the patient.

1.4 The Two Aims in this Dissertation

The introduction of this dissertation identified two major limitations of emerging clinical applications that use brain signals for communication and diagnosis. These limitations are: (1) low communication performance; (2) dependence on experts and post-hoc analysis for diagnosis of eloquent cortex. This dissertation aims to overcome these limitations by improving communication performance and by eliminating the need for experts and post-hoc analysis in clinical diagnosis.

In Chapter 2, Brain Signals for Communication, we aim to improve the performance of clinical applications that use brain signals for communication. We hypothesize that a ECoG-based matrix speller may support communication rates that are higher than those typically expected by EEG-based spellers. We test this hypothesis in real-time experiments (study 1) and subsequently investigate the applicability of this BCI approach to the target population, i.e., to people that suffer from severe neuromuscular diseases and are unable to shift eye-gaze (study 2). The results demonstrate that an ECoG-based speller could provide a sustained communication rate of 17 characters per minute (69 bits/min), which is 3-4 times higher than what had previously been reported. Our investigation of the applicability to the target population unequivocally showed, that the performance of the matrix speller BCI depends on the ability to fixate on the intended character. While this finding effectively limits the utility of increased spelling performance to people that are able to fixate on the target, this has created an awareness on this dependency and has since sparked scientific interest to develop exogenous BCI systems that do not depend on eye-gaze.

In Chapter 3, Brain Signals for Diagnosis, we aim to eliminate the need for experts and post-hoc analysis in applications that use brain signals for clinical diagnosis. We hypothesize that a generative approach, to passively map eloquent cortex using ECoG will provide results that are in general agreement to those derived using expert-supervised electrical stimulation. We develop a diagnostic tool that uses ECoG and generative models to passively map eloquent cortex and test our hypothesis in a multi-center study. The results show that this system does not need experts or post-hoc analysis to provide maps of eloquent cortex that are in general alignment with those obtained from the current gold standard. This could extend the clinical option for mapping eloquent cortex prior to resective surgery.

1.5 Overview of Contributions

The work described in this Dissertation produced a number of important contributions to the clinical application of brain signals for communication and diagnosis, as well as to basic and applied neuroscience. These contributions have been reported in 22 peer-reviewed journal papers (see Appendix A) and are described in detail in Chapters 2 and 3, and are summarized here.

CHAPTER 2: Brain Signals for Communication At present, the translation of assistive BCI communication devices into clinical practice has been impeded by poor speed and accuracy, and by the unclear applicability to the target population.

The work described in Chapter 2 provided three contributions that will help to overcome these impediments: first, I implemented the first ECoG-based speller BCI system. Second, using this system, I showed that an ECoG-based speller can provide a sustained communication rate of 17 characters per minute (69 bits/min), which is 3-4 times higher than what had previously been reported. Third, I showed that the performance of the matrix speller BCI depends on the ability to fixate on the intended character. These results should facilitate the translation of assistive BCI communication devices from laboratory demonstrations into clinical practice.

CHAPTER 3: Brain Signals for Diagnosis The clinical application of brain signals to map eloquent cortex has been impeded by the dependency on experts and post-hoc analysis. The work described in Chapter 3 provided three contributions that will help to overcome this impediment: first, I developed a generative technique to model brain signals and to detect task-related changes. Second, I implemented this technique in a software tool that maps eloquent cortex in real-time at the bedside, and provides the results in an intuitive interface to the clinical investigator. Third, I validated the technique in a multi-center study that showed that the results are in general agreement to those derived using electrical stimulation. These results should facilitate the clinical application of brain signals to map eloquent cortex.

2 Brain Signals for Communication

2.1 Summary of Contributions and Approach

This chapter discusses improvements in speed and applicability of **Brain Signals for Communication**. At present, the translation of assistive BCI communication devices into clinical practice has been impeded by poor speed and accuracy, and by the unclear applicability to the target population (i.e., people with severe motor-disabilities). Consequently, if BCI communication was to be become a viable alternative to conventional assistive devices it needs to improve in speed, accuracy, and the applicability to the target population.

The main contribution presented in this chapter is the improvement in speed and accuracy in BCI communication and the finding that the most commonly used BCI communication interface may not be applicable to the target population. The improvement in speed and accuracy in BCI communication encompasses the development of techniques and protocols for chronic real-time recording of ECoG signals from the surface of the brain. The determination of applicability to the target population encompasses the development of techniques and protocols for real-time operant conditioning to simulate the target population, i.e., people with sever motor-disabilities that are unable to control their eye-gaze. The associated work is described in section 2.2 for the improvement in speed and accuracy in BCI communication and in section 2.3 for the determination of the applicability to the target population. The results provide evidence that brain signals recorded from the surface of the brain (ECoG) could provide a sustained communication rate that is 3-4 times higher than what had previously been reported, and that the performance of the "P300" matrix speller BCI depends on the ability to fixate

on the intended character. The work accomplished in this chapter should help to overcome the speed and accuracy barriers that currently impede the translation of assistive BCI communication devices into clinical practice. At the same time, the finding that the most commonly used BCI communication interface may not be applicable to the target population should spark scientific interest to develop exogenous BCI systems that do not depend on eye-gaze.

The work in this chapter was highly multidisciplinary and depended on the integration of methodologies from different areas of engineering and science, such as experimental psychology, neurosurgery, electrophysiology, electrical engineering, computer science and signal processing. For example, I used computer science methodologies to implement the software interfaces that enabled the real-time operant conditioning of the subject's eye-gaze.

2.2 Rapid Brain-Computer Interface (BCI) Communication Using Electrocorticographic Signals (ECoG)

2.2.1 Introduction

Many people affected by neurological or neuromuscular disorders such as amyotrophic lateral sclerosis (ALS), brainstem stroke, or spinal cord injury, are impaired in their ability to or even unable to communicate. A brain-computer interface (BCI) uses brain signals to restore some of the lost function. A BCI approach that several groups have begun to test in clinical applications in humans (e.g., Nijboer et al. 2008; Sellers et al. 2006b, 2010; Vaughan et al. 2006; see Donchin and Arbel 2009 for a comprehensive review) is the matrix-based speller originally described by Farwell and Donchin (Farwell and Donchin 1988). This speller uses different event-related potentials (ERPs) including the P300 evoked response. In this system, the user attends to a character in a matrix while each row or column flashes rapidly and pseudo-randomly. The brain produces a response to the row or column that contains the intended character (i.e., the oddball); this response is different for the other rows or columns. The BCI can detect the desired character by determining the row and column that produces the largest evoked response. Using this approach, recent electroencephalography (EEG)-based studies (Guger et al. 2009; Lenhardt et al. 2008; Nijboer et al. 2008; Sellers et al. 2006a, 2010; Serby et al. 2005) reported real-time accuracies from 79% to 91% (6x6 matrix of 36 characters; 2.8% chance) at 13 to 42 seconds per selection.

A growing number of recent studies (e.g., Felton et al. 2007; Leuthardt et al. 2006, 2004; Miller et al. 2010; Ritaccio et al. 2010; Schalk et al. 2008c; Vansteensel et al. 2010; Wilson et al. 2006) suggested that signals recorded from the surface of the brain (electrocorticography (ECoG)) are a promising platform for real-time BCI communication. This advantage is due in part to the high spatial, spectral, and temporal fidelity that characterize ECoG signals (Ball et al. 2009; Brunner et al. 2009; Leuthardt et al. 2004; Miller et al. 2007b, 2008). It is possible that these favorable signal characteristics may provide distinct advantages in the context of the matrix speller, but this has not been explored.

In this study, we investigated this possibility by evaluating the feasibility and online performance of the matrix speller using ECoG signals recorded from frontal, parietal, and occipital areas in one human subject. We hypothesized that these experiments will provide evidence that the ECoG-based speller may support communication rates that are higher than those typically expected by EEG-based spellers. The results demonstrate that ECoG allows for accurate single-trial detection of evoked responses, and thereby

supports very high communication rates. Thus, with additional verification in more subjects, these results may further extend the communication options for people with serious neuromuscular disabilities.

2.2.2 Methods

2.2.2.1 Human Subject

The subject in this study was a 29 year old right handed woman with intractable epilepsy who underwent temporary placement of subdural electrode arrays (see Fig. 2.1A) to localize seizure foci prior to surgical resection. The subject had corrected-to-normal vision and gave informed consent through a protocol reviewed and approved by the review board of Albany Medical College.

A neuropsychological evaluation revealed a full-scale IQ score of 122 (93rd percentile, Wechsler 1997), superior visuomotor scanning performance (92nd percentile, Trail Marking Test, Reitan 1958), and average visual search capacity (75th percentile, WAIS-III: Symbol Search Subtest, Wechsler 1997).

The subject had a total of 96 subdural electrode contacts (i.e., one 8 x 8 64-contact grid, one 23-contact grid, and two strips in 1 x 6 and 1 x 3 configuration, respectively). These grids/strips were placed over the left hemisphere in frontal, parietal, temporal and occipital regions (see Fig. 2.1B for details). The implants consisted of flat electrodes with an exposed diameter of 2.3 mm and an inter-electrode distance of 1 cm, and were implanted for one week. Grid placement and duration of ECoG monitoring were based solely on the requirements of the clinical evaluation without any consideration of this study. Following placement of the subdural grid, postoperative CT imaging verified grid location (Talairach and Tournoux 1988).

2.2.2.2 Data Collection

We recorded ECoG from the implanted electrodes using 6 g.USBamp amplifier/digitizer systems (g.tec, Graz, Austria) and the BCI software platform BCI2000 (Mellinger and Schalk 2007; Schalk et al. 2004; Schalk and Mellinger 2010). Simultaneous clinical monitoring was implemented using a connector that split the cables coming from the patient into one set that was connected to the clinical monitoring system and another set that was connected to the g.USBamp devices. Thus, at no time was clinical care or clinical data collection compromised. Two electrocorticographically silent electrodes (i.e., locations that were not identified as eloquent cortex by electrocortical stimulation mapping)

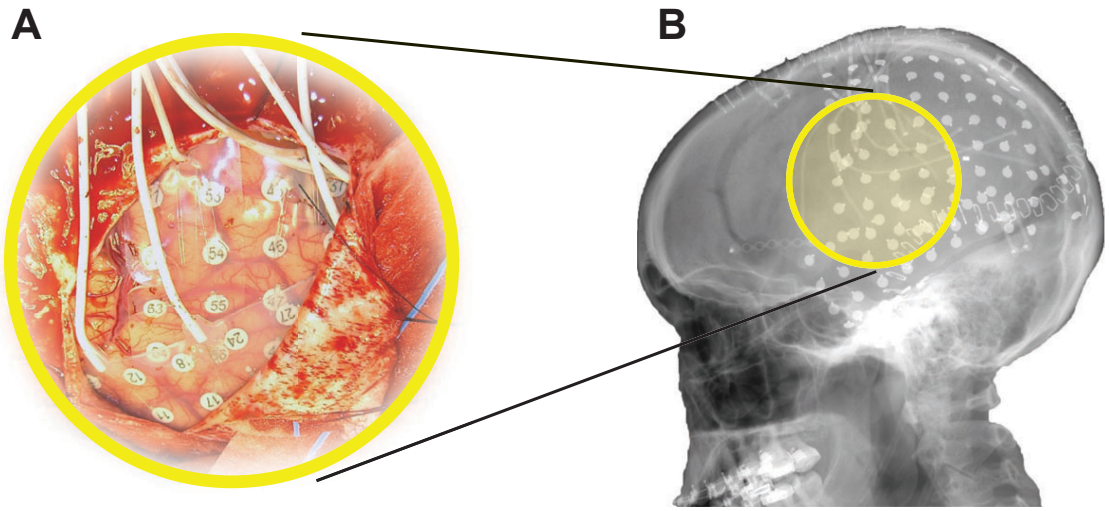

Figure 2.1: **Implant.** The subject had 96 subdural electrodes (2 grids and 2 strips in different configurations) implanted over left frontal, parietal, temporal, and occipital regions. A: Photograph of the craniotomy and the implanted grids in this subject. B: Lateral x-ray of the subject, showing an 8x8 grid over frontal/parietal cortex, a 23 contact grid over temporal cortex, and several strips.

over inferior and superior posterior parietal cortex served as ground and reference, respectively. We used a grounding connection between the g.USBamp systems and the patient's skin to dissipate any electric currents generated by external electromagnetic fields and to block electromagnetic interference. The amplifiers sampled the signal at 512 Hz and used a high pass at 0.1 Hz and a notch filter at 60 Hz.

2.2.2.3 Experimental Paradigm

The subject sat 60 cm in front of a flat-screen monitor. She was presented with a matrix of alphanumeric characters that was centered on the screen and arranged in a 6x6 configuration (see Fig. 2.2). At this distance, the matrix subtended ± 7.1 degrees of the horizontal and vertical visual field.

The subject participated in a recording session that consisted of offline and online experiments. In the offline (i.e., calibration) experiments, the BCI2000 matrix speller flashed each of the 12 rows or columns in a pseudo-random sequence. Flashes occurred at a rate of 16 Hz. Each flash lasted 1/64 s (16 ms) to 3/64 s (46.8 ms), followed by a 1/64 to 3/64 s inter-stimulus period. The intensity contrast between a flash and a non-flash was 3:1. 15 flash sequences comprised one trial. The subject's task in each trial was to pay attention to the highlighted character in the words "THE QUICK BROWN," and to

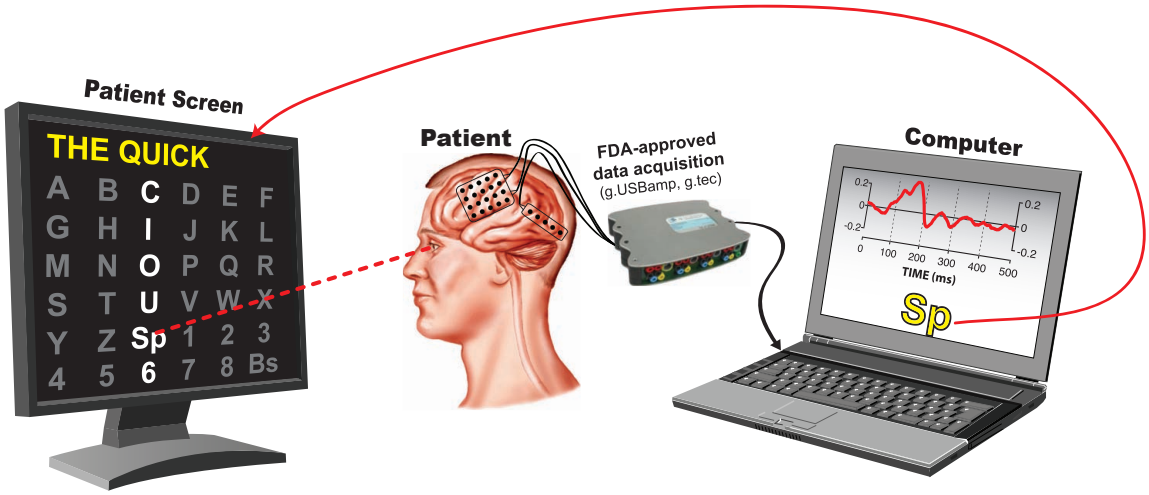

Figure 2.2: **Experimental setup.** The subject sat 60 cm in front of a flat-screen monitor that presented a centered 6x6 matrix containing alphanumeric characters as well as space (Sp) and backspace (Bs). The rows and columns in the matrix flashed rapidly and pseudo-randomly. The subject's task was to pay attention to the intended character. The computer determined the intended character from the subject's ECoG responses.

make a mental note (i.e., to count) each time the correct row/column flashed. A 3-sec pause (i.e., "flight time") between characters gave the subject time to shift her attention onto the next character. We used the ECoG data collected in this calibration experiment to establish a classifier using the stepwise regression method reported in Krusienski et al. 2006. We then configured the BCI to use this classifier in online experiments.

During each of the 7 online experiments, the subject copy-spelled the sentence "THE QUICK BROWN FOX JUMPS OVER THE LAZY DOG." The BCI system provided feedback of the characters predicted from the ECoG signals. The subject selected "backspace" to correct incorrect selections. In the 7 online experiments, the subject spelled a total of 301 characters (i.e., 444 characters including "backspace" and subsequent corrections) using different stimulation parameters that are described in more detail in the Results section.

2.2.2.4 Offline Analyses

In offline analyses of data from each of the calibration experiments, we first filtered the signal between 0.1 and 20 Hz and downsampled it to 40 Hz. We then extracted the stimulus response, i.e., the ECoG signals from all 96 channels for 500 ms after stimulus onset (see Fig. 2.3). This yielded 20 features (i.e., $40 \times 0.5 = 20$) per channel or a total

of 1920 features for all 96 channels. We define a sequence to be 12 flashes, i.e., flashes of 6 rows and 6 columns of the presented matrix. Of these 12 flashes, two (i.e., the row and column that contained the desired character) are expected to elicit a target evoked response (i.e., oddball ERP) and 10 are not. With 15 flash sequences in each trial, this yielded 30 target ERPs and 150 non-target ERPs. As we recorded 13 trials (i.e., each character in "THE QUICK BROWN") during a calibration experiment, this resulted in a total of 390 target and 1950 non-target ERPs for calibration.

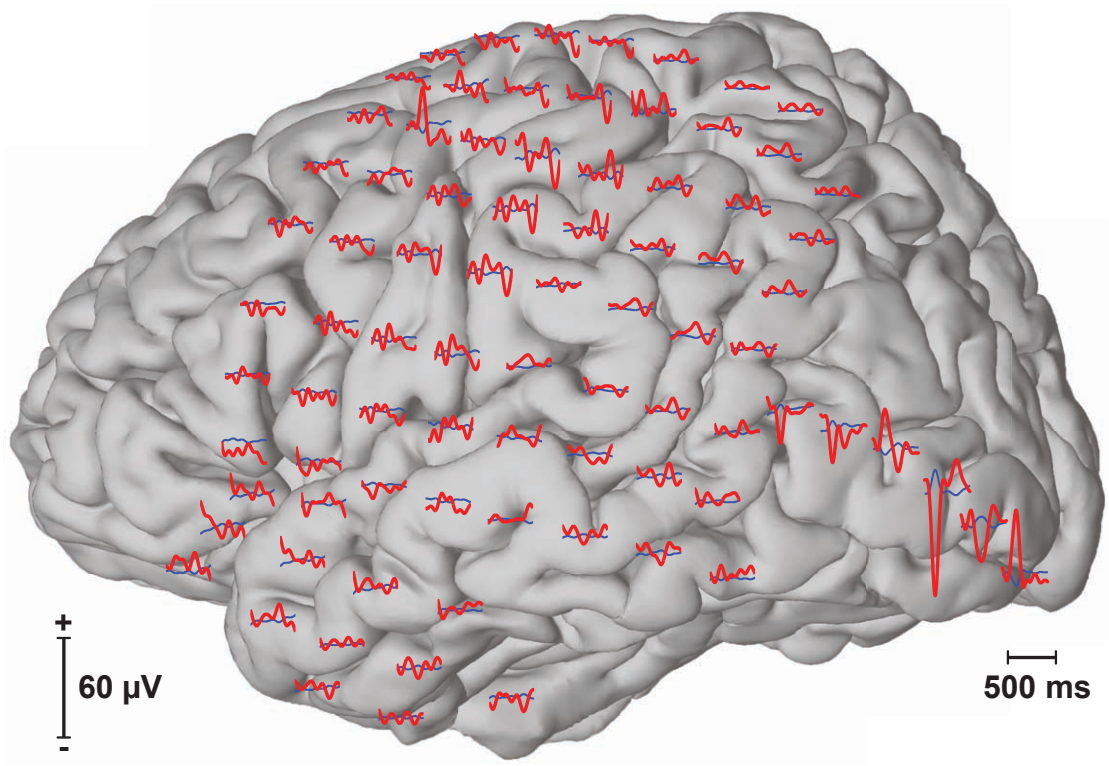

Figure 2.3: **Event-related potentials (ERPs).** The figure above shows averaged event-related responses to target (red) and non-target (blue) flashes at each of the 96 recorded locations.

2.2.2.5 Stepwise Regression Model

In the matrix speller paradigm, the subject's selection is predicted by the intersection of the row and column that elicits the largest target-related response. In 1988, Farwell and Donchin proposed multiple approaches to determine the target-related response from data for which the intended selection is known (i.e., calibration data, Farwell and

Donchin 1988). These approaches included stepwise regression, peak picking, area under the curve measurements, and the covariance. In our study, we used a stepwise regression procedure that has been described in detail in Krusienski et al. 2006. In brief, we first filtered the brain signal from each channel between 0.1 and 20 Hz and downsampled it to 40 Hz. The downsampled ECoG amplitude of all 96 channels for 500 ms after stimulus onset resulted in a total of 1920 potential signal features. A stepwise procedure then produced a linear model that predicted, given a subset of all features, whether or not the stimulus associated with these features was a target or non-target. In this iterative procedure, each step added the most significant and/or removed the least significant feature based on the p-value of a F-statistic ($p_{add} = 0.1$, $p_{remove} = 0.15$, Jennrich 1977). To prevent overfitting, the stepwise procedure limited the number of features to 60 and terminated when a step did not further improve the regression model or when the maximum number of iterations (5000) was reached. In summary, this procedure reduced the 1920 potential ECoG features to a maximum of 60 features, and resulted in a linear model that was predictive of target or non-target. This linear model was applied to the ECoG response to each stimulus (i.e., row or column flash). The row and column with the highest model output defined the predicted character. Because there were 36 characters, chance accuracy was 2.8%.

2.2.2.6 Online Experiments

For each online experiment, we used one of three different flash durations (i.e., 1/64, 2/64, 3/64 s). For each flash duration, we collected calibration data ("THE QUICK BROWN") and performed the offline analyses described above to establish a regression model. We then used this model to evaluate online system performance. In these online experiments, we asked the subject to use the matrix speller BCI system to spell "THE QUICK BROWN FOX JUMPS OVER THE LAZY DOG". The BCI system provided feedback on the predicted characters as shown in Fig. 2.2. The subject performed a "backspace" selection to correct for incorrect selections.

2.2.3 Results

2.2.3.1 Optimization of System Performance

Over the course of online experimentation, we continually optimized system parameters (i.e., the flash duration and number of flash sequences) so as to optimize the subject's information transfer rate. The results are shown in Fig. 2.4 and Table 2.1. For one flash sequence, spelling accuracy reached a maximum of 81% (see Fig. 2.4) at a flash duration of 3/64 s. We then used a flash duration of 3/64 s (i.e., 47 ms) and increased the number of flash sequences. The accuracy reached 98% at 3 flash sequences, while the actual information transfer rate (i.e., bit rate), which was calculated including stimulation- and flight-time, peaked at 60.5 bits/min and 2 flash sequences (i.e., a selection every 4.5 s).

In a subsequent seventh 3.5 minute run, we reduced the time between selections to 2 seconds. The subject achieved a selection every 3.5 s at 86.4% accuracy. This represents an information transfer rate of 69 bits/min or 17 characters per minute.

In a final run, we further decreased the number of flash sequences to one. In this run, the subject spelled the word "FLOWER" at rate of 2.75 s/character (i.e., 22 characters/min or 113 bits/min).

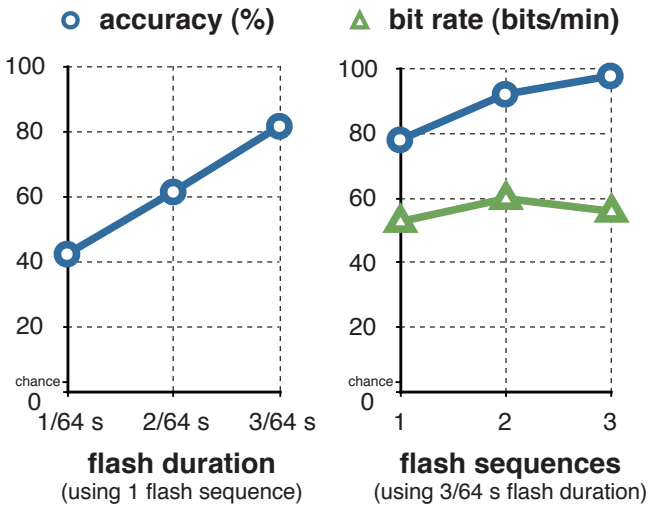

Figure 2.4: **Optimizing accuracy and information transfer rate.** The figure on the left shows the relationship between the flash duration and classification accuracy with a single flash sequence (i.e., single-flash accuracy). The figure on the right shows the relationship between the number of flash sequences and classification accuracy using a flash duration of 3/64 seconds (i.e., 46.9ms). The subject reached a maximum of 98% classification accuracy at three flash sequence, and a maximum of 60.5 bits/min at 92.2% accuracy (i.e., a selection every 4.5 s) at two flash sequences.

Table 2.1: **Optimizing accuracy and information transfer rate.** The table on the top shows the relationship between flash duration and classification accuracy with a single flash sequence (i.e., single-trial accuracy). The table below shows the relationship between the number of flash sequences and classification accuracy using a flash duration of 3/64 seconds (i.e., 46.9 ms). The data in these tables corresponds to the traces in Fig. 2.4.

flash duration	flash sequences	accuracy	bit rate
1/64 s	1	42%	
2/64 s	1	61%	
3/64 s	1	81%	
3/64 s	1	78%	53 bits/min
3/64 s	2	92%	60 bits/min
3/64 s	3	98%	56 bits/min

2.2.3.2 Cortical Locations With Significant Evoked Responses

The results presented in the previous section demonstrated that the BCI system successfully predicted the intended character online with an accuracy of 81% using only one flash of each row/column. We were interested in the physiological basis for this successful demonstration, i.e., in the cortical locations and ERP components that held significant information. To do this, we trained the classifier separately on each location using the calibration data with a flash duration of 3/64 s, and evaluated performance on the online data with the same flash duration and 1-3 flash sequences. Fig. 2.5 shows the locations of all 96 subdural electrodes (blue dots) and the corresponding color-coded classification accuracies. Accuracy ranged from chance level ($\frac{1}{6*6} = 2.8\%$) to 50% for the best electrode location.

Statistical comparisons (two-sample t-test, Bonferroni corrected for the number of features (i.e., 1920)) of each extracted feature (ECoG amplitudes at a given time and location) between target and non-target conditions revealed statistically significant ($p<<0.001$) differences over wide-spread areas in secondary visual cortex (see locations marked with A,B,C,D in the brain plot in Fig. 2.5), associative visual cortex (E), angular gyrus (F) and somatosensory association cortex (G). The traces below show the correlation of the ECoG signals following the flash with the type of the ERP (i.e., target vs. non-target). This correlation analysis for locations A-G showed dominant peaks between 125 and 175 ms after the flash. The amplitude of these peaks were reversed between the neighboring electrodes C, D, and E. Furthermore, signals recorded from angular gyrus (F), but not other locations, were sensitive to the orientation (i.e., row or column) of the attended flash ($p=0.00003$).

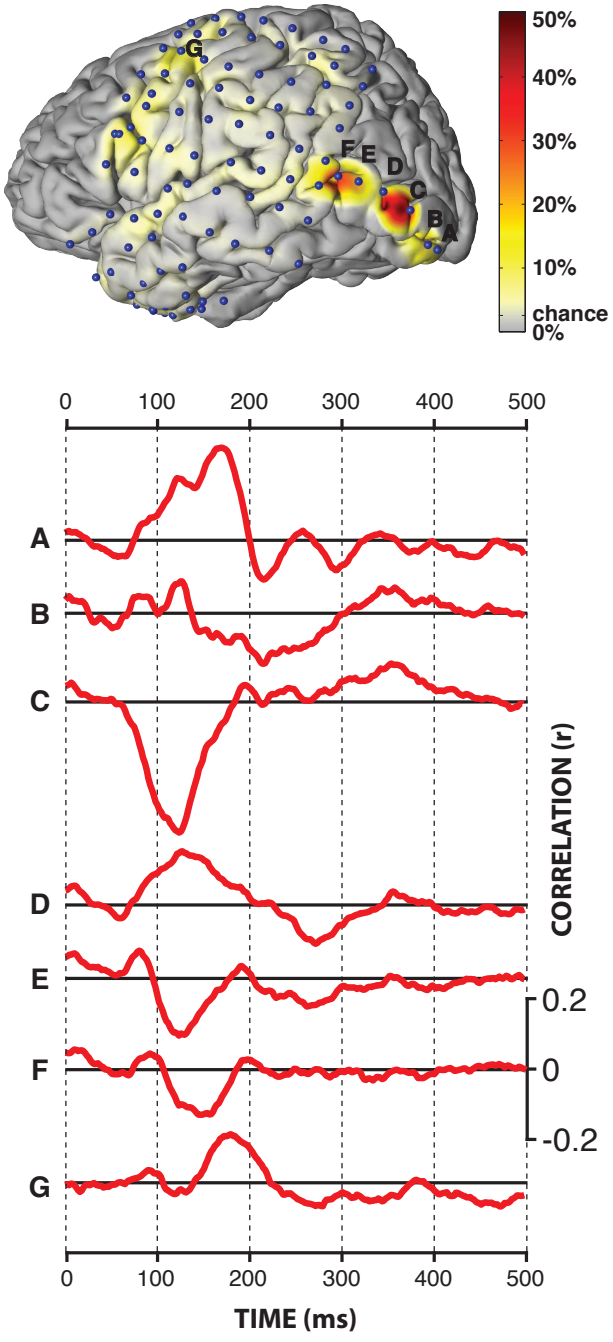

Figure 2.5: **Qualitative Results.** The figure at the top shows the locations of the 96 subdural electrodes (blue dots), as well as the color-coded single-flash classification accuracy at each individual electrode. The traces at the bottom show evoked responses (i.e., the correlation between ECoG amplitude and the type of the ERP (target/no target) for cortical locations A-G.

2.2.3.3 Optimizing Number of Electrodes

The results presented in the previous section show that, in this particular subject, ERPs recorded from electrodes over visual cortex contribute significantly to the performance of the matrix speller BCI system. This suggests that a similar level of performance may be achieved using recordings from only a few electrodes over a relatively small area, which is important for potential clinical application of this approach. Thus, we were interested in the relationship between the number of utilized electrodes over visual cortex and spelling performance.

To do this, in offline post-hoc analyses, we evaluated spelling performance using 1-6 electrodes over visual cortex (i.e., locations A-F in Fig. 2.5) and 1-3 flash sequences. In these analyses, we used the same calibration data as in the online experiment (i.e., "THE QUICK BROWN", 15 flash sequences, 3/64 s flash duration). We then established one classifier for each possible combination of the 1-6 electrodes over visual cortex. For each combination, we then applied the corresponding classifier to the data from the online experiments. The results in Fig. 2.6 and Table 2.2 show the relationship between the best combinations of 1-6 electrodes and spelling performance, i.e., accuracy and bit rate, for 1-3 flash sequences. The results suggest that this particular subject could achieve a maximum of 100% classification accuracy at three flash sequences and four electrodes, and a maximum of 64 bits/min at two flash sequences and five electrodes. Furthermore, one bipolar derivation (i.e., between locations C and A) may already allow for 57 bits per minute or 90% of the peak spelling performance supported by five electrodes (see Table 2.2).

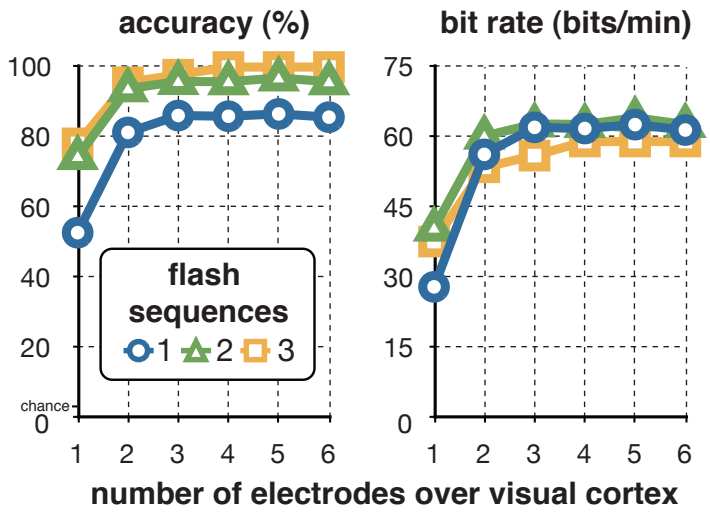

Figure 2.6: **Optimizing number of electrodes.** The two figures show the relationship between the number of electrodes over visual cortex and accuracy (left) or bit rate (right) that this subject may achieve with these electrodes at one (blue circle), two (green triangle), and three (orange square) flash sequences. The subject may achieve a maximum of 100% classification accuracy at three flash sequences and four electrodes, and a maximum of 64 bits/min at two flash sequences and five electrodes.

Table 2.2: **Optimizing number of electrodes.** This table shows the relationship between the number of electrodes over visual cortex and accuracy (left) or bit rate (right) that this subject can achieve with these electrodes at 1-3 flash sequences. The data in these tables corresponds to the traces in Fig. 2.6; locations A-F correspond to the electrode locations and evoked responses in Fig. 2.5.

		accuracy (%)			bit rate (bits/min)		
number of		flash sequences			flash sequences		
locations	location(s)	1	2	3	1	2	3
1	C	53	75	78	28	41	38
1*	C-A	75	91	93	50	57	51
2	C,A	81	94	96	56	60	54
3	C,B,A	86	96	98	62	63	56
4	E,C,B,A	86	96	100	62	63	59
5	E,D,C,B,A	87	97	100	63	64	59
6	F,E,D,C,B,A	86	96	100	62	63	59

Note: * Bipolar derivation.

2.2.4 Discussion

The results of this study show that ECoG can support matrix BCI spelling at a sustained rate of 17 characters per minute (i.e., 69 bits/min) and a peak rate of 22 characters per minute (i.e., 113 bits/min). In line with recently completed studies by us (Brunner et al. 2010a,b, see section 2.3) and others (Treder and Blankertz 2010), our offline analyses show that visual areas provided important contributions to the subject's performance. The results also indicate that only one bipolar derivation over visual cortex could support almost the same level of performance. In conclusion, with verification of our results in more subjects, these findings may increase the BCI-based communication options for people with serious motor disabilities.

The spelling rate reported for the one subject in this ECoG-based study (i.e., 17 sustained characters per minute or 69 bits/min) is 3-4 times higher than what had previously been reported in EEG-based P300 BCI studies (i.e., 1.4 to 4.5 characters per minute) (Guger et al. 2009; Lenhardt et al. 2008; Nijboer et al. 2008; Sellers et al. 2006a, 2010; Serby et al. 2005)[1] or in EEG-based sensory motor rhythm (SMR) BCI studies (1.7 to 4.9 characters per minute) (McFarland et al. 2003; Müller et al. 2008; Pfurtscheller et al. 2003; Wolpaw et al. 1991). Furthermore, the sustained performance demonstrated in this study is within the same range of previously reported EEG-based SSVEP studies (15.8 to 18.7 character per minute) (Bin et al. 2009; Gao et al. 2003). Finally, to the best of our knowledge, the peak performance shown here is the highest BCI performance demonstrated in humans to date.

The spelling rate of the ECoG-based matrix speller BCI shown here is beginning to match or even exceed that of conventional assistive devices. These devices are often either intrusive (e.g., cheek or tongue-switch), cumbersome (e.g., letter board) or susceptible to fatigue (e.g., video-based eye-trackers using the corneal reflection). Thus, while invasive, the BCI method presented here may provide distinct advantages over those conventional assistive devices.

While the spelling rate shown here is very high, it is still at least one order of magnitude slower than conventional communication (e.g., 200 to 400 characters using keyboard or voice; Majaranta and Räihä 2002; Schalk 2008). Although the spelling rate of the matrix speller could be further improved, there are fundamental limitations to these potential improvements. These limitations are due to the required dwell time (e.g., the time during which the rows/columns are intensified) and the flight time (e.g.,

[1] Some of these EEG-based studies used software and analysis methods that were identical to those used here.

the time between two characters). In our study, we used single-trial flash presentation/classification (i.e., the smallest possible number) and a dwell time (i.e., the time the subject sustained eye-gaze/attention) of as little as 0.75 s. While this dwell time compares favorably to what is used in other assistive devices (e.g., 0.6 to 1.0 s for a modern eye-tracker, Majaranta and Räihä 2002), these other devices tend to provide higher communication performance. This is because the matrix spelling paradigm used here also requires a flight time during which the subject produces brain responses, the computer evaluates the responses, and the subject shifts gaze/attention to the next character. It appears impractical to further substantially decrease either the 2-sec flight time duration, or the 0.75 s dwell time. Thus, the paradigm presented here should be limited to a spelling rate that is only modestly higher than what we report here. This limitation appears to have two reasons. First, the current paradigm is synchronous, i.e., the subject has to synchronize his/her behavior with the timing of the BCI. This requires the subject to shift eye-gaze/attention onto the intended character within the 2-sec flight time duration and to sustain eye-gaze/attention for the 0.75 s dwell time. One potential solution to overcome this limitation is an asynchronous paradigm, i.e., a paradigm in which the subject does not have to synchronize behavior with the system. Steady-state visual evoked potential (SSVEP)-based BCIs often use such asynchronous paradigms. In such a paradigm, the subject performs a selection by focusing eye-gaze to the target character (i.e., one of multiple light sources flickering at different frequencies) while the BCI detects those frequencies in the EEG recorded over occipital cortex (Middendorf et al. 2000). These paradigms not only overcome the synchronization requirement, they also permit stimulating each potential target independently for the whole dwell time (i.e., by using individual frequencies for each potential target). Using such a paradigm, Bin et al. 2009 reported 18.7 character per minute for EEG. The use of this paradigm with ECoG may further increase performance.

The results suggest that ERPs over visual areas (VEPs) contribute significantly to the performance of the matrix speller BCI system. Recent studies (Bin et al. 2009; Martens et al. 2009) suggest that a time-, frequency-, and code-based stimulation may elicit a wide range of VEPs while minimizing the flight time and obtrusive flickering that currently limits the utility of P300- and SSVEP-based BCIs. However, generation of a VEP depends on foveation of the target character. This is of critical relevance to clinical application of this BCI method, because eye movements are often impaired or lost in the target population. For example, although some people with ALS maintain residual eye movement for years (Birbaumer and Cohen 2007; Cohen and Caroscio 1983; Palmowski

et al. 1995), others progress to near-complete or complete paralysis. The distance to foveation influences visual acuity and also VEP amplitude (De Keyser et al. 1990; Sherman 1979) and thus would reduce the performance of any BCI that depends at least in part on VEPs.

An interesting finding was the polarity reversal of VEPs recorded from neighboring electrodes. While recording at the cortical surface (ECoG) can record these polarity reversed VEPs, EEG recordings may only record the canceled superposition (Di Russo et al. 2002; Makeig et al. 2002). This cancelation effect may be one reason why the performance of EEG-based matrix speller systems, despite wider cortical coverage (e.g., 64 scalp locations of an extended 10-20 montage (Sharbrough et al. 1991)), appears to be lower than that shown here.

While quite encouraging, the results shown here are based on only one subject who had coverage of large cortical areas including visual areas. Thus, it is currently unclear whether the results presented here will generalize to other subjects. Furthermore, while we were able to make general performance comparisons of this ECoG-based study with previously published EEG-based studies, we did not compare performance of ECoG and EEG within this subject.

The linear relationship between the flash duration and the accuracy, as well as the fact that only one electrode was sensitive to the orientation (i.e., row or column) of the attended flash, suggests that, in this particular subject, the magnitude of the ERP in response to visual stimulation was determined mostly by luminance. However, many previous studies have shown that the cortex performs neuronal processing of other features of visual stimuli, such as spatial frequency, orientation, motion, direction, speed, and many other spatiotemporal features (Hubel and Wiesel 1959, 1962; Zeki et al. 1991). A recent study (Martens et al. 2009) showed that these properties of the visual system can be exploited to increase the amplitude of the EEG response, and thereby increase overall classification accuracy. This suggests that more extensive electrode coverage may yield higher performance.

While in this study we only recorded signals from electrodes over the left hemisphere, it is known that visual cortex has bilaterally symmetric retinotopic maps (Engel et al. 1997, 1994; Yoshor et al. 2007). Thus, some of the ERPs may only reflect right visual field stimulation (Daniel and Whitteridge 1961) and therefore bilateral coverage might further increase performance. As a related point, the electrode placement in this study was based solely on the requirements of the clinical evaluation, without any consideration of this study. Pre-surgical mapping of visual cortex using functional magnetic

resonance imaging (fMRI) (Engel et al. 1997, 1994; Vansteensel et al. 2010) could be used to optimize electrode location.

In this study we used subdural electrodes (i.e., electrodes placed underneath the dura mater). This placement requires penetration of the skull and the outer meningeal covering, i.e., the dura. This is important for clinical application of this BCI method, because the penetration of the dura increases the risk of bacterial infection (Davson 1976; Fountas and Smith 2007; Hamer et al. 2002; Van Gompel et al. 2008; Wong et al. 2009). Epidural electrodes (i.e., electrodes placed on top of the dura mater) provide signals of approximately comparable fidelity (Torres Valderrama et al. 2010) and do not penetrate the dura. Thus, epidural placement may increase safety and thus clinical practicality of an ECoG-based matrix speller BCI.

Success of widespread clinical application of ECoG-based matrix speller BCI systems depends mainly on costs and risks (Higson 2002; Raab and Parr 2006). The results presented here are of critical relevance to these issues, because they suggest that effective ECoG-based matrix speller BCI systems may be realized by using only one bipolar and possibly epidural electrode.

Our results provide encouraging evidence that ECoG can provide high spelling rates, and recent results (Chao et al. 2010; Schalk 2010) suggest that ECoG has good long-term stability. Moreover, an ECoG-based system reduces the patient's dependence on a caregiver to set up EEG electrodes or other external conventional assistive devices. At the same time, the clinical value of an ECoG-based matrix speller BCI remains unclear. Compared to non-invasive approaches, an ECoG-based approach entails additional costs and risks. More generally, despite some encouraging successes of non-invasive matrix spellers (Nijboer et al. 2008; Sellers et al. 2006b), it is still unclear to what extent matrix spellers can serve the needs of people with disabilities, in particular those in who eye gaze is compromised: two recent studies (Brunner et al. 2010b; Treder and Blankertz 2010) demonstrated that the performance of the matrix speller depends substantially on the subject's ability to fixate the target character. It is also unclear whether similar fast stimulation rates (i.e., 16 Hz) can be used in people with disabilities. Even if the high speed suggested by this study could be translated to clinical applications, it is unclear to what extent end users will find this increased spelling rate desirable. Furthermore, it is currently unknown whether the added benefit of increased robustness and/or increased spelling rate will outweigh the additional cost of surgical implantation. More generally, it is still debated whether people with complete paralysis can even achieve and maintain brain-based control, irrespective of whether EEG or ECoG is used (Hill et al. 2006; Kübler

and Birbaumer 2008).

2.2.5 Conclusions

In summary, the results shown in this study demonstrate that ECoG supports spelling performance exceeding 20 characters per minute. In consequence, with additional verification in more subjects, our results may further extend the communication options for people with severe motor disabilities.

2.2.6 Recommendations

While the results of this study unequivocally support our hypothesis, i.e., that a ECoG-based matrix speller may support communication rates that are higher than those typically expected by EEG-based spellers, the results also raised questions. For example, the results suggest that ERPs over visual areas (VEPs) contribute significantly to the performance of the BCI communication system. This is of critical relevance to clinical application of this BCI method, because the target population may be impaired in their ability to fixate on the target and thus to generate VEPs. This raises the question whether the performance of matrix speller BCI depends on fixating the target.

In response to this issue, my next study, which is described in the next section (2.3), investigates whether the performance of the matrix speller BCI depends on fixating the target.

2.3 Does the "P300" Speller Depend on Eye Gaze?

2.3.1 Introduction

Many people affected by debilitating neuromuscular disorders such as amyotrophic lateral sclerosis (ALS), brainstem stroke, or spinal cord injury are impaired in their ability to or even unable to communicate with their family and caregivers. A Brain-Computer Interface (BCI) uses brain signals directly, rather than muscles, to re-establish communication with the outside world. One well-known BCI approach is the so-called "P300 matrix speller" that was first described by Farwell and Donchin in 1988. In this system, the user pays attention to a character in a matrix while each row and column is intensified in a random sequence. The brain produces a response to the row or column that contains the intended character (i.e., the oddball); this response is not present for the other rows or columns. The BCI typically averages several responses, detects the row and column with the strongest responses, and thereby identifies the character the user wants to select.

The individual parameters of the "P300" matrix speller have each been studied and optimized extensively. This includes the matrix size (Allison and Pineda 2003), stimulation frequency (Sellers et al. 2006a), stimulation intensity (Takano et al. 2009), classification algorithm (Krusienski et al. 2006) and electrode locations (Krusienski et al. 2008). It has been recently shown that more than 80% of the population can use such a BCI (Guger et al. 2009). The "P300" speller has also been used for a variety of applications, such as web browser navigation (Mugler et al. 2008), control of ambient environment (Edlinger et al. 2009), wheelchair navigation (Rebsamen et al. 2007), and mouse movement (Citi et al. 2008), which demonstrates the broad utility of this approach. Most important to the eventual goal of BCI research, several studies have also begun to show mounting evidence that the "P300" speller is a feasible, practical, and useful method to restore function in severely disabled individuals (Nijboer et al. 2008; Sellers et al. 2006b, 2010; Vaughan et al. 2006; see Donchin and Arbel 2009 for a comprehensive review). Interestingly, clinical studies with ALS patients (e.g., Nijboer et al. 2008; Sellers et al. 2006b, 2010; Vaughan et al. 2006) show lower spelling performance (i.e., 1.4-3 selections per minute, 79-83% accuracy) than laboratory demonstrations with healthy subjects (Lenhardt et al. 2008; Serby et al. 2005, 4-4.6 selections per minute, 79-83% accuracy).

Since the original description of the "P300" speller in 1988, it has been unclear whether this method relies primarily on the P300 evoked potential, and minimally if

at all on other EEG features, such as the visual evoked potential (VEP), that strongly depend on eye-gaze direction (Donchin et al. 2000; Sellers et al. 2006b; Serby et al. 2005). Omitting visual crowding (Korte 1923; Strasburger 2005), a P300 is not markedly affected by whether the target is foveated, whereas a VEP is larger when the target is foveated. This distinction is important for clinical application of this BCI method, because eye movements are often impaired or lost in the target population. For example, although some people with ALS maintain residual eye movement for years (Birbaumer and Cohen 2007; Cohen and Caroscio 1983; Palmowski et al. 1995), others progress to near-complete and complete paralysis. It has been shown that the distance to foveation influences visual acuity (see Fig. 2.7) and also VEP amplitude (De Keyser et al. 1990; Sherman 1979).

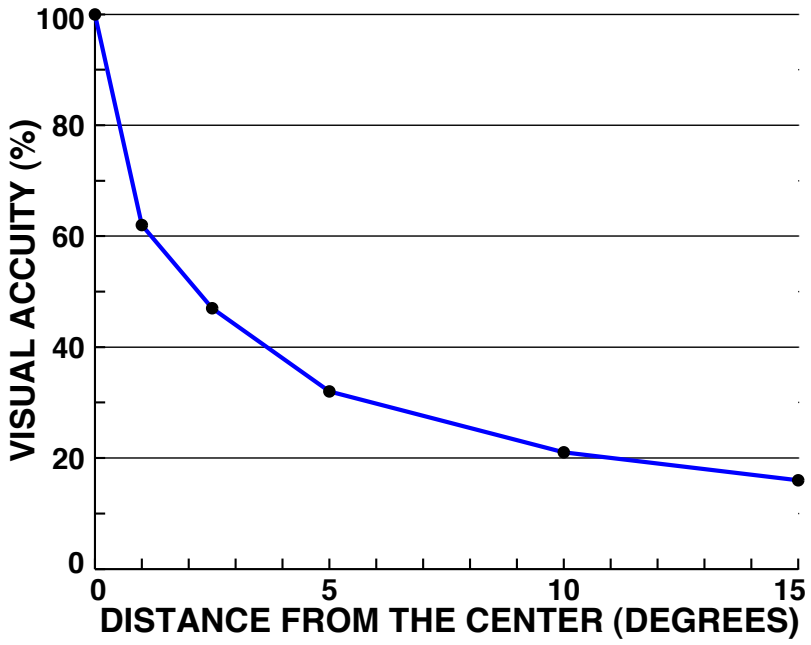

Figure 2.7: **The effects of the distance to the center (eccentricity) on visual acuity.** This figure shows the degradation of visual acuity at increasing angles from a centered focus point. The visual acuity (expressed as the Snellen fraction, i.e., 20/20 equals 100%) quickly declines to approximately 20% at 10 degrees eccentricity. (Modified from Westheimer 1965.)

The goal of this study was to determine to what extent performance in a "P300" speller depends on eye gaze. We hypothesized that fixation of the target item would produce both a P300 and a VEP, while fixation of a location other than that of the target would produce a P300 and a much smaller VEP. We also hypothesized that the 8-channel montage that had previously been optimized for target fixation is suboptimal when the eyes do not fixate the target. Furthermore, we hypothesized that the richer information (i.e., about target or non-target stimuli) in the target fixation condition would result in better speller performance (i.e., higher accuracy). Our results from 15 subjects unequivocally support these hypotheses, and thereby disprove the assumption that the performance of the "P300" speller does not depend on the subject's ability to fixate the target character.

2.3.2 Methods

2.3.2.1 Human Subjects

We collected a total of 17 datasets of 8- or 64-channel EEG from 15 right-handed subjects (two subjects participated twice) using the general-purpose BCI software platform BCI2000 (Mellinger and Schalk 2007; Schalk et al. 2004; Schalk and Mellinger 2010). The subjects were 6 females and 11 males, aged 20 to 62. All subjects had normal or corrected-to-normal vision, and gave informed consent through a protocol reviewed and approved by the Wadsworth Center Institutional Review Board.

2.3.2.2 Experimental Paradigm

Subjects sat 60 cm ($\pm$ 6 cm) in front of a flat-screen monitor. They were presented with a 6x6 matrix of 36 alphanumeric letters and numbers that was centered on the screen (see Fig. 2.8). At this distance, the matrix subtended $\pm$ 7.1 degrees of the visual field both horizontally and vertically. Eye gaze was measured 60 times per second by an eye tracker (Tobii T60, Tobii Technology, Inc., Sweden) that was integrated with the flat-screen monitor. These eye-gaze coordinates were acquired by BCI2000 along with the ongoing EEG and stored to disk. In addition, they were also used online to control for gaze direction as described below.

Each subject participated in one two-hour session. In this session, we collected data during two experimental conditions. In Condition 1, the "letter" condition, the subject was asked to gaze at the target item. In Condition 2, the "center" condition, the subject was asked to gaze only at a fixation cross located in the center of the screen while paying

Table 2.3: **Subject profiles.** We collected 8 channels of EEG in subjects A1-10, and 64 channels of EEG in subjects B1-B10.

Subject	Age	Handedness	Gender	Race	Glasses	Vision	Channels
A1	62	right	female	caucasian	yes	nearsighted	8
A2	28	right	female	caucasian	yes	nearsighted	8
A3	31	right	male	caucasian	no	normal	8
A4	26	right	male	caucasian	no	normal	8
A5	30	right	male	caucasian	yes	nearsighted	8
A6	25	right	male	caucasian	yes	nearsighted	8
A7†	29	right	male	caucasian	no	normal	8
A8	23	right	male	caucasian	yes	nearsighted	8
A9†	52	right	male	caucasian	no	normal	8
A10	38	right	female	asian	yes	nearsighted	8
B1	35	right	female	african	no	normal	64
B2	20	right	male	caucasian	no	normal	64
B3	28	right	female	asian	no	normal	64
B4	35	right	female	caucasian	no	normal	64
B5†	29	right	male	caucasian	no	normal	64
B6	22	right	male	caucasian	no	normal	64
B7†	52	right	male	caucasian	no	normal	64

Note: † Subjects A7 and A9 participated in group B as subjects B5 and B7.

attention to the target item. In both conditions, the subject was asked to note every time the target flashed. The fixation cross was color- and intensity-matched to the matrix elements and, in Condition 2, it rotated by 45 degrees if the subject shifted eye gaze more than 2.8 degree from the cross for more than 300 ms. Appropriate eye gaze in these two conditions was also verified offline as described later.

The subjects performed a total of 24 runs – 12 for each task – in an alternating fashion. Each run presented four different target items in succession (i.e., four trials), using 15 flashes (i.e., 15 flashes of each row and each column for each of the four targets). Each intensification lasted 125 ms and was followed by an interval of 125 ms at a contrast ratio of 5:1. An 8-sec pause between trials gave the subject time to shift attention (and, in Condition 1, eye gaze also) to the new target, which was presented in the center (i.e., (instead of the fixation cross) for the first 5 sec of the 8-sec pause, and was also present throughout the trial on the top left of the screen.

Each run was balanced and block randomized such that it contained one target from each matrix quadrant and one target at each of four of the six possible distances from the center (i.e., the fixation cross). The sequence of 12 runs was presented in the opposite direction for the two experimental conditions (i.e., the first run of the first set of four

targets for the "letter" condition was the last run for the "center" condition). All subjects that participated in this study had successfully used the "P300" matrix speller prior to this study. Because Condition 2, the "center" condition, may be a more complicated task than that in Condition 1, one practice run familiarized them with both conditions prior to the actual data collection.

2.3.2.3 Data Collection

In 10 subjects (Group A), we recorded EEG from 8 scalp locations (Fz, Cz, P3, Pz, P4, PO7, Oz, PO8) using an 8-channel analog amplifier (g.MOBIlab, g.tec, Austria). In 7 subjects (Group B), we recorded EEG from 64 scalp locations (extended 10-20 montage (Sharbrough et al. 1991)) using a 64-channel digital amplifier (g.USBamp, g.tec, Austria). For both groups, the left and right mastoids served as ground and reference, respectively (see Fig. 2.8). The 8-channel Group A montage had previously been shown to provide performance on the "P300" speller similar to that of the full 64-channel Group B montage (Krusienski et al. 2006, 2008). The 64-channel data of Group B allowed us to define the topographies of the responses to the flashing stimuli. Both amplifiers sampled the signal at 256 Hz and used a high pass filter and a notch filter to remove frequency components be low 0.1 Hz and at 60 Hz, respectively. In addition to the 8 or 64 EEG channels, eye gaze coordinates were independently acquired 60 times per second for the left and right eyes, aligned with the EEG data, and stored.

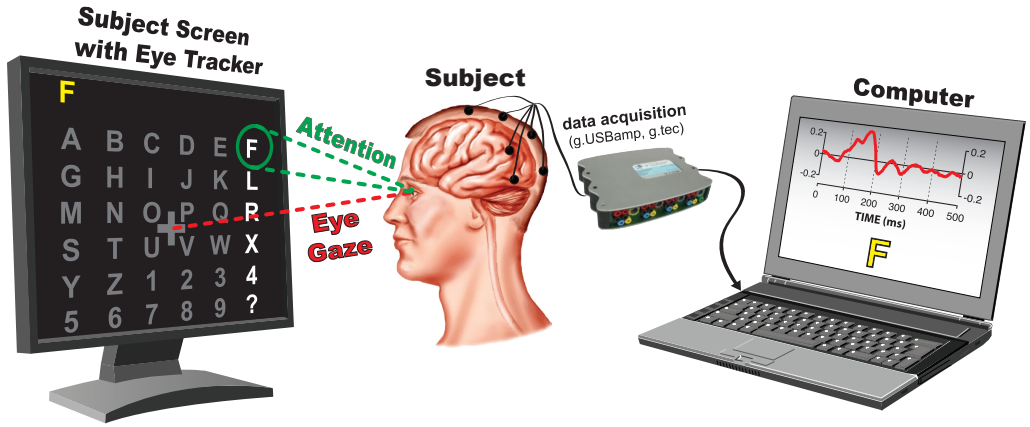

Figure 2.8: **Experimental setup.** Subjects were presented with a matrix on a computer screen. There were two experimental conditions. In condition 1 ("letter"), the subject was free to gaze at the target (e.g., the letter F). In condition 2 ("center"), the subject was asked to gaze at a fixation cross in the center of the matrix. Fixation was verified in real time by an eye tracker.

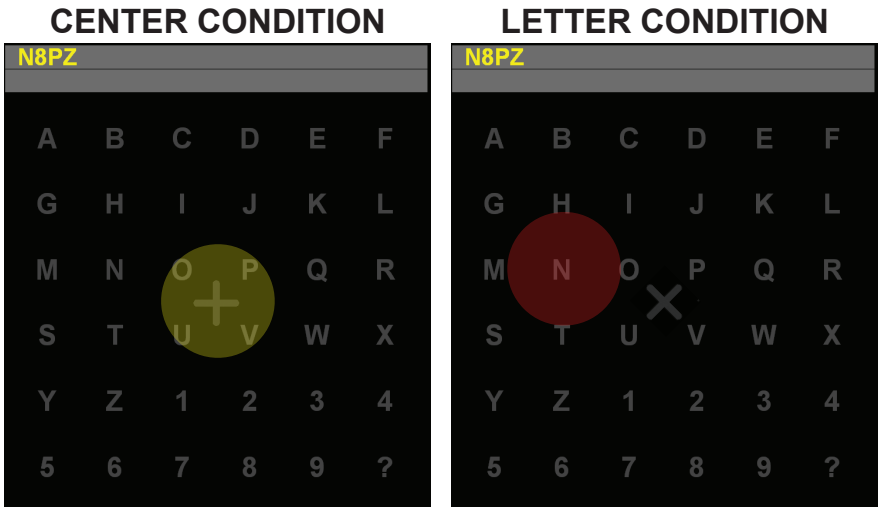

Figure 2.9: **Behavioral task.** Subjects performed two behavioral tasks. In condition 1 ("letter", see right figure), the subject was free to gaze at the target (e.g., the letter N). In condition 2 ("center", see left figure), the subject was asked to gaze at a fixation cross in the center of the matrix. Fixation was verified in real time by an eye tracker.

2.3.2.4 Feature Extraction

In offline analyses, we first filtered the signal between 0.1 and 20 Hz and downsampled it to 40 Hz. We then extracted the stimulus response, which was defined as the 750 ms of EEG after stimulus onset from all eight channels of the optimized montage (i.e., the same channels whether 8 or 64 channels were recorded). This yielded 30 features (i.e., $40 \times 0.75 = 30$) per channel or a total of 240 features for all 8 channels. Each sequence had 12 stimuli, i.e., flashes of 6 rows and 6 columns of the matrix. Of these 12 flashes, two included the target and thus elicited a target evoked potential (EP), while the other ten did not include the target and thus elicited a non-target EP. The 15 sequences in each trial (i.e., with each target) yielded 30 target EPs and 180 non-target EPs. Because a subject performed 48 trials in each of the two conditions, we had a total of 1320 target EPs and 7920 non-target EPs from each subject.

2.3.2.5 Modeling and Evaluation

We used previously established methods (Krusienski et al. 2006) to discriminate target EPs from non-target EPs. In particular, we used a stepwise regression ($p_{enter} = 0.1$, $p_{remove} = 0.15$, Jennrich 1977) to reduce the 240 features to a maximum of 60 features. The regression established a linear model that predicted from the selected features

A

RUN#	TEXT	TASK
1	N8PZ	Center
2	T3OF	Letter
3	Q74H	Center
4	AWUE	Letter
5	YKC?	Center
6	RV5B	Letter
7	VG5D	Center
8	6MK?	Letter
9	2ALU	Center
10	H9SJ	Letter
11	O1F3	Center
12	PIXZ	Letter
13	PIXZ	Center
14	O1F3	Letter
15	H9SJ	Center
16	2ALU	Letter
17	6MK?	Center
18	VG5D	Letter
19	RV5B	Center
20	YKC?	Letter
21	AWUE	Center
22	Q74H	Letter
23	T3OF	Center
24	N8PZ	Letter

B

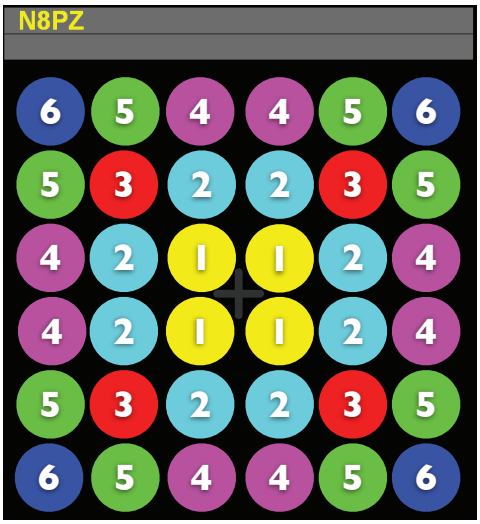

C

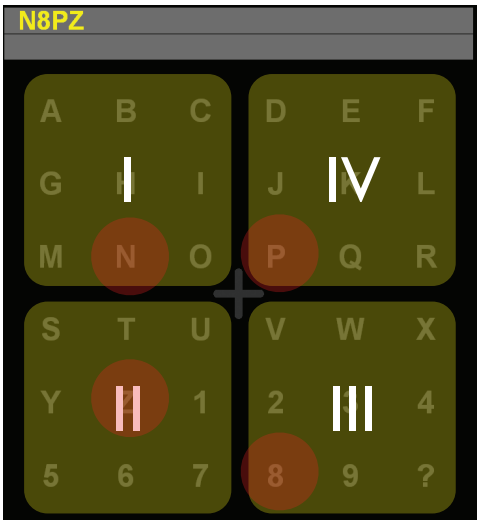

Figure 2.10: **Experimental design.** (A) The subjects performed a total of 24 runs – 12 for each task – in an alternating fashion. Each run presented four different target items in succession (i.e., four trials). (B) The 6x6 matrix of 36 alphanumeric letters and numbers that was centered on the screen and each target was presented in 1 of 6 possible distances from the center. (C) Each run presented one target from each distance from the center and each of the four 3x3 quadrants of the 6x6 matrix.

whether a particular row or column did or did not contain the target. This model was constructed and evaluated using a leave-one-out cross validation scheme. Thus, in each of the 12 folds of this cross validation, a model was constructed using 11 out of 12 runs (i.e., 44 targets) and was tested on the remaining run. Each run served once as the test run. For each trial, the intersection of the row and column that analysis indicated produced a target EP defined the predicted target. Chance accuracy was 1/36, or 2.8% ($\frac{1}{6*6} * 100$). We calculated the average classification accuracy for the 12 cross validation folds.

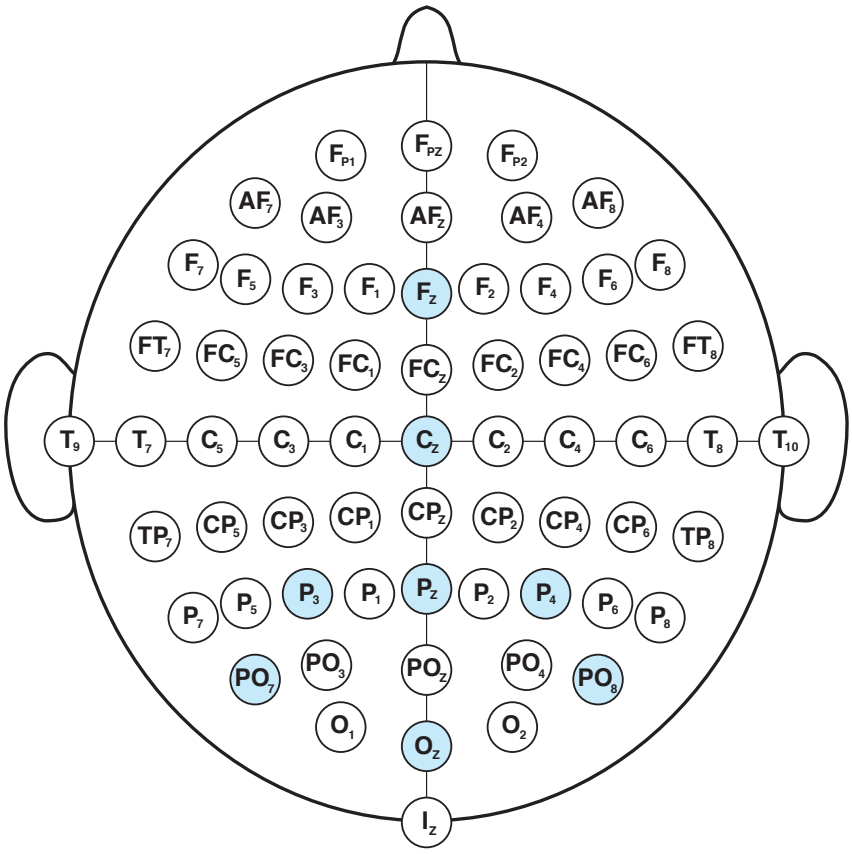

Figure 2.11: **Electrode montage for groups A and B.** EEG from group B was recorded from the 64 locations shown here (extended 10-20 montage (Sharbrough et al. 1991)). EEG from group A was recorded from an optimized subset of 8 electrodes (shown in blue) (Krusienski et al. 2006, Krusienski et al. 2008).

2.3.2.6 Verification of Behavioral Compliance

Because the two experimental conditions in this study were set up to assess differences in the EEG that were related to the gaze location, it was critical to verify that the subjects actually fixated on the target in the "letter" condition and on the fixation cross in the "center" condition. As described above, in the "center" condition the subjects received immediate visual feedback if they looked away from the fixation cross for more than 300 ms, but the trial was not aborted. To verify that the subjects did maintain gaze as instructed, we also analyzed the gaze data offline. The results are summarized in Fig. 2.12. The traces show the distributions of the horizontal (for the six columns) or vertical (for the six rows) distances of gaze location from the fixation cross for the two conditions. The red trace ("letter" condition) shows six peaks for the six rows/columns, while the blue trace ("center" condition) shows only one peak sharply focused on the fixation cross. These data show that the subjects did follow the instructions, that is, they looked at the target in the "letter" condition and at the fixation cross in the "center" condition. It is relevant to note that the subject's behavior during the "letter" condition (i.e., looking at the target) using the instructions used in this study (i.e., to fixate on the target) was comparable to that using the common instructions (i.e., to focus attention on the target, see Fig. 2.13).

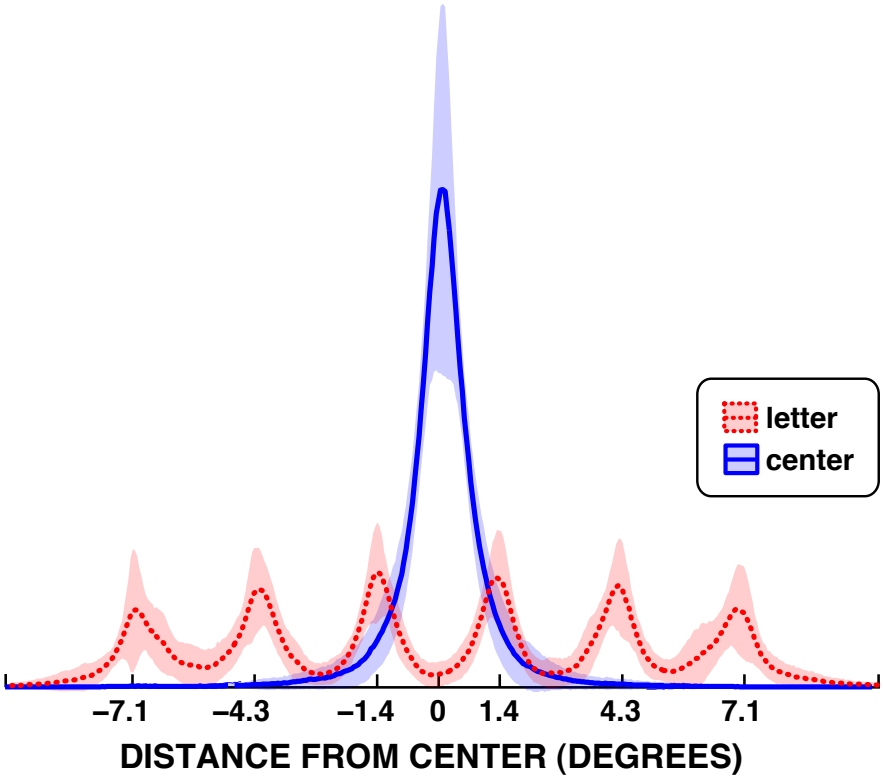

Figure 2.12: **Distributions of the distance of eye gaze from the center during the two conditions.** The traces show the distributions of the horizontal (for the six columns) or vertical (for the six rows) distances of gaze location from the fixation cross for the "letter" condition (red) and the "center" condition (blue). Shading shows standard deviation across subjects.

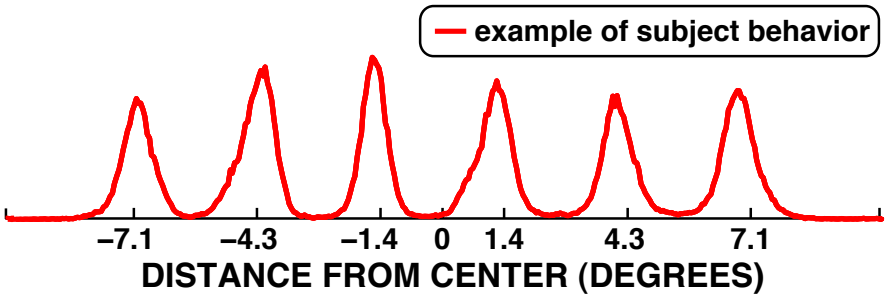

Figure 2.13: **Distributions of the distance of eye gaze from the center when given normal "P300" matrix speller usage instructions.** The traces show the distributions of the horizontal (for the six columns) or vertical (for the six rows) distances of gaze location from the fixation cross for one subject that was given the instruction to "focus attention" on the intended letter.

2.3.3 Results

2.3.3.1 Effect of Condition on Classification Accuracy

The main results of this study are shown in Fig. 2.14. This figure shows the classification accuracy (i.e., the accuracy in identifying the target) for the two conditions as a function of stimulus repetitions. All subjects performed significantly better (pairwise t-test, $p < 0.001$) for Condition 1, the "letter" condition, than for Condition 2, the "center" condition. The final classification accuracy after 15 stimulus repetitions (i.e., the rightmost data point in each trace) ranged from 80% to 100% for the "letter" condition and from 2.8% (i.e., chance level) to 90% for the "center" condition. These offline analyses showed that the target could be identified with 100% accuracy for the majority (53%) of subjects for the "letter" condition. In contrast, accuracy did not reach 100% for any subject during the "center" condition, and reached at least 50% in only 47% of the subjects.

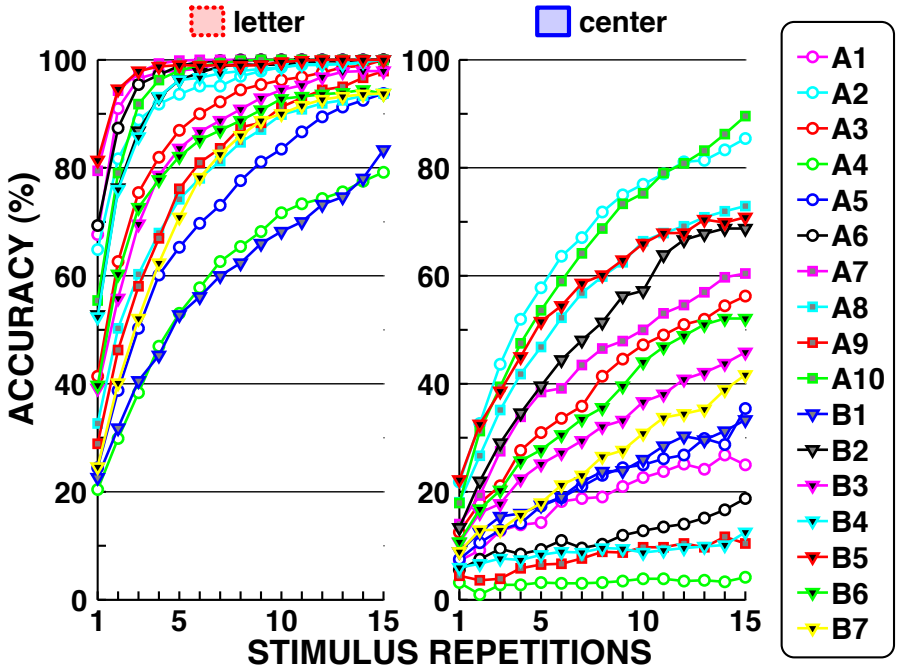

Figure 2.14: **Classification accuracy as a function of the number of stimulus repetitions.** As expected, classification accuracy steadily increases with number of stimulus repetitions. Accuracy is substantially greater for the "letter" condition than for the "center" condition.

2.3.3.2 Effect of Gaze Distance from the Center on Accuracy

Expanding on the results shown in the previous section, we determined whether accuracy depended on the distance between the target and the fixation cross. We hypothesized that this distance would not affect classification accuracy when the subjects fixated on the target (Condition 1), but would adversely affect accuracy when the subject fixated on the center (Condition 2). Blue and red traces in Fig. 2.15 show for Conditions 1 (red) and 2 (blue) the accuracy for all subjects for whom accuracy with 15 stimulus repetitions was $> 50\%$ as a function of distance of eye gaze from the center. The results confirm our hypothesis: in Condition 2 only, accuracy declined as the distance of the target from the center increased (i.e., as the target moved from near the center of the visual field toward the periphery).

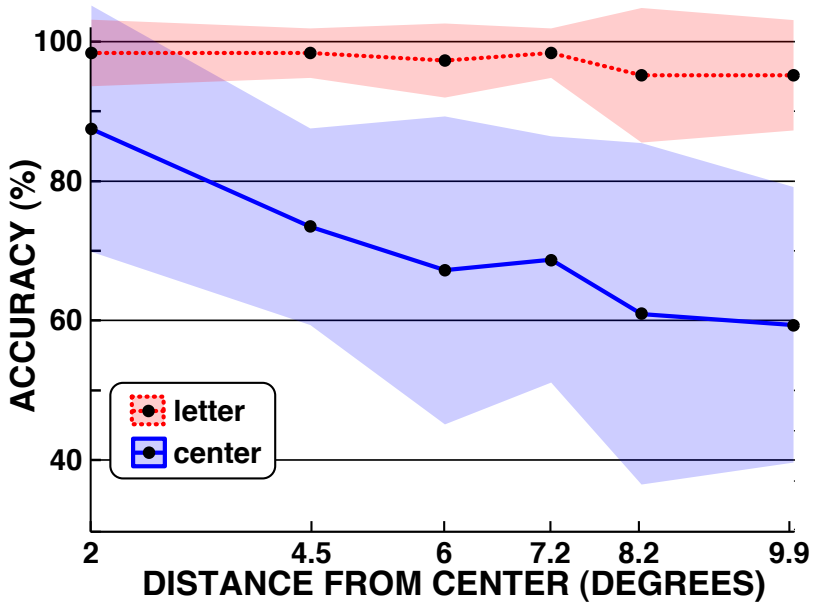

Figure 2.15: **Accuracy as a function of the distance of eye gaze from the center.** Red and blue traces show results for Conditions 1 and 2, respectively. Shading indicates standard deviation across subjects.

2.3.3.3 Effect of Electrode Montage on Classification Accuracy

We also determined whether accuracy would be increased by a larger number of electrodes. As described above, in the 10 subjects of Group A we recorded EEG using an 8-channel montage that had previously been optimized for the "P300" speller (Krusienski et al. 2006, 2008), while in the 7 subjects of Group B we used a full 64-channel extended 10-20 montage (Sharbrough et al. 1991). In offline analysis of the Group B data, we compared accuracies for the optimized 8-channel montage and the full 64-channel montage (see Fig. 2.11). The results are shown in Fig. 2.16 for the two montages and the two conditions. For both conditions, the 64-channel montage consistently yielded higher accuracies. Consistent with a previous study (Krusienski et al. 2008), the superiority of the 64-channel montage over the optimized 8-channel montage was modest (4.4%, $p = 0.34$, pairwise t-test) for Condition 1 (red). In contrast, the improvement with the larger montage was much greater for Condition 2 (18.7%, $p < 0.01$, pairwise t-test). These results suggest that when a subject does not fixate the target, a different (or larger) montage may be helpful.

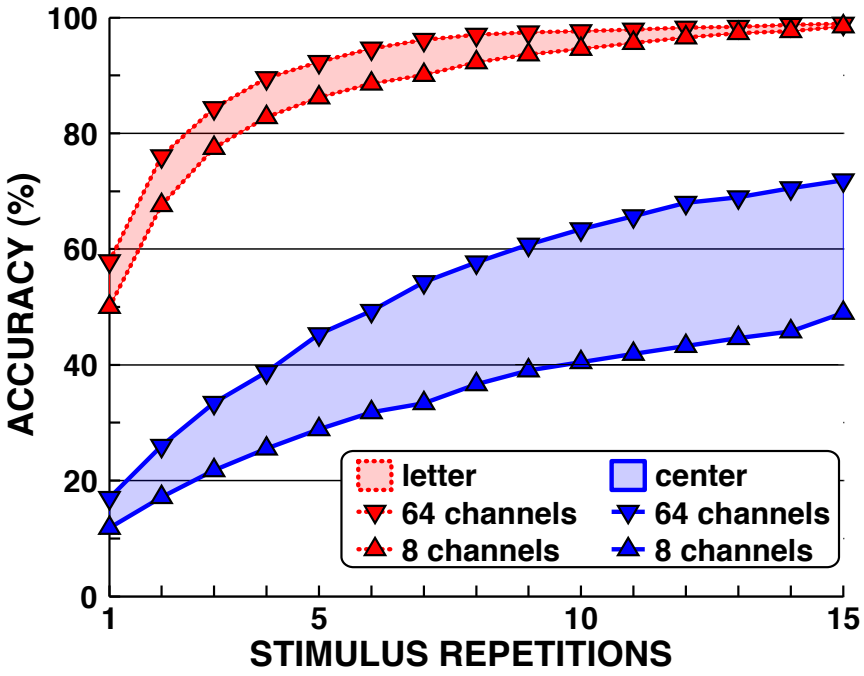

Figure 2.16: **Accuracy as a function of stimulus repetitions for the 8-channel (red) and 64-channel (blue) montages for Condition 1 (down-pointing triangles) and Condition 2 (up-pointing triangles) for the subset of subjects with 64-channel recordings.**

2.3.3.4 Effect of Fixation Task on EEG Responses

The results presented in Section 2.3.3.1 show that all subjects performed significantly better in Condition 1 than in Condition 2 (pairwise t-test, $p < 0.001$). We were interested in the physiological basis for this difference. To assess the effect of condition on the actual responses to the target and non-target stimuli, we calculated, for each subject's data under each condition, signed squared correlation coefficient (r^2) values for each time segment of the target and non-target responses at each of the 8 electrodes of the optimized montage. We then calculated the average Condition 1 and Condition 2 results across all subjects. The results are shown in Fig. 2.17. Fig. 2.17A and Fig. 2.17B show the signed r^2 time courses and raw EEG time courses, respectively, for Condition 1 (red) and Condition 2 (blue). The Condition 1 traces show early components around 180 ms after stimulus onset that are absent in the Condition 2 traces. The P3 components appear to be delayed and smaller in amplitude for the "center" task. Fig. 2.17C-D show color-coded topographies for the 8-channel and 64-channel datasets, respectively. The topographies are consistent for the 8-channel and 64-channel datasets. They show an early VEP component that is focused on visual/occipital areas, with polarity reversal over central and frontal locations, as well as a following P3 component that is focused on central-parietal areas. The early VEP component is missing for the "center" task. We quantified the impact of this early VEP component on classification accuracy by running similar analyses as before, except that we excluded all data between 0 and 250 ms post stimulus. Compared to the results that included all data, the results show a significant reduction in classification accuracy (16%, $p < 0.01$) for Condition 1, the "letter" condition, and no change (0%, $p = 0.9$) for Condition 2, the "center" condition.

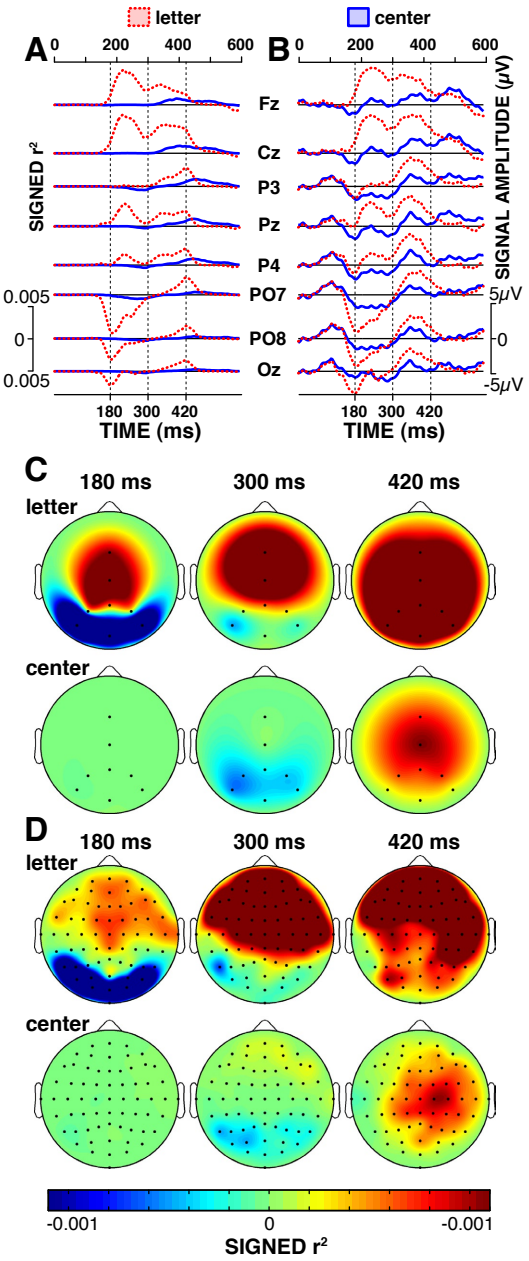

Figure 2.17: **Average traces and topographies for the two tasks.** Average signed r^2 traces (A) and wave forms (B) for the two tasks. The traces show negative early VEP components around 180 ms post stimulus for the "letter" task (red traces). P3 components appear to be delayed and smaller in amplitude for the "center" task (blue traces). (C,D): Topographies show an early VEP component (topographies at 180 and 300 ms) for the "letter" task that is absent for the "center" task. Topographies also show a classical P300 response (topographies at 420 ms).

2.3.4 Discussion

This study shows that accuracy of the "P300" speller is affected by gaze direction: fixating on the target (as in Condition 1) produces substantially better classification than fixating on a center point (as in Condition 2). These results suggest that online performance of a "P300" speller-based BCI can be expected to be substantially reduced when subjects do not gaze at the desired item. We also found that accuracy decreases as the distance between the gaze fixation point and the target increases. Finally, we found that the 8-channel montage, which focuses on central parietal and occipital areas and has previously been optimized for the "P300" matrix speller (Krusienski et al. 2008), is suboptimal when subjects do not gaze at the target. Detailed analysis of the target and non-target responses indicates that the decreased performance when the subject does not gaze at the target is due mainly to the lack of an early response over posterior (i.e., visual) cortex. These findings are in general alignment with a recently performed study (Treder and Blankertz 2010). In Figure A1, we demonstrate that task-related ERPs between 50-400 ms are negatively correlated with distance to the center point. Together with the fact that P300 evoked responses have not been reported to occur around 180 ms and over visual areas, these results suggest that the matrix speller BCI usually depends, as has been previously shown, on the P300 ERP that is evoked by the recognition of the desired stimulus, but also on a visual ERP that is evoked by the flashing target stimulus.

Our results may explain in part why "P300" speller performance in ALS patients tends to be lower than that in healthy subjects (Nijboer et al. 2008; Sellers et al. 2006b; Vaughan et al. 2006). At the same time, further studies are needed to determine the relationship of gaze and performance in ALS patients, and to optimize the montage for this population. In summary, our findings suggest that the clinical applicability of the "P300" matrix speller in subjects with impaired gaze may be limited. In such subjects, an auditory "P300" matrix speller (e.g., Furdea et al. 2009; Klobassa et al. 2009; Schreuder et al. 2010) may prove useful.

The percent of subjects (94%) with high accuracy (i.e., 80-100% correct) in Condition 1 was similar to that found in a recently published study (Guger et al. 2009) that allowed the subjects to gaze directly at the target.

The accuracy shown in this study declines with increasing distance of the target from the center of foveation due mainly to the lack of an early response over posterior (i.e., visual) cortex. Because of the relationship between the visual acuity and the VEP amplitude (De Keyser et al. 1990; Sherman 1979; Westheimer 1965), we expected a more extensive decline in accuracy. This was not the case. Fig. 2.18 shows a decline over

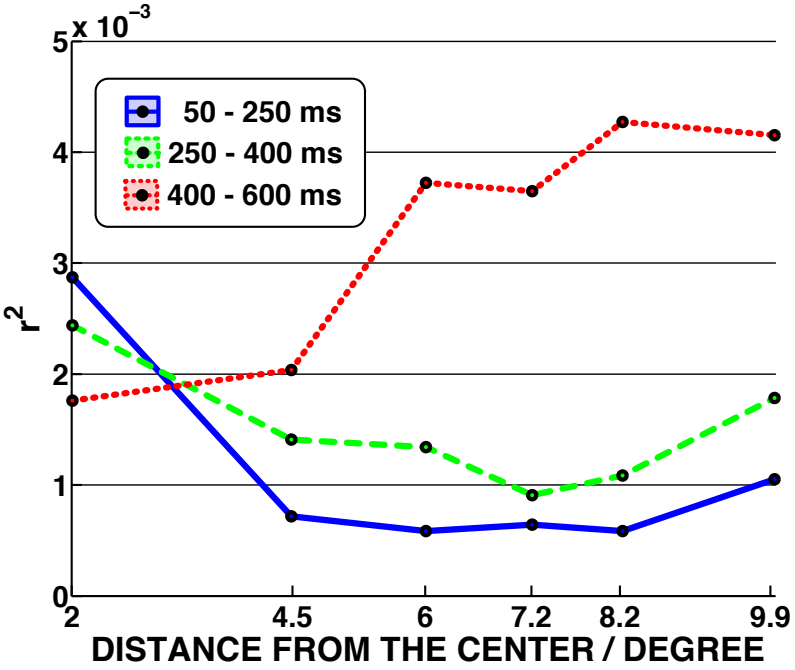

Figure 2.18: **Average squared correlation coefficient r^2 values of the target and non-target responses as a function of the distance of gaze from the center.** The traces show the r^2 averaged over all 8 electrodes of the optimized montage and all subjects that achieved more than 50% in Condition 2, the "center" condition. The traces show a decline of the r^2 value over the distance for the 50-200 ms (i.e., VEP) and the 250-400 ms (i.e., P300) period, while the r^2 value for the 400-600 ms (i.e., late ERP) period increases.

the distance for the VEP (i.e., 50-200 ms) and the P300 (i.e., 250-400 ms) responses, while the amplitude of the late ERP (i.e., 400-600 ms) response increases. This increase in amplitude of the late ERP may explain the less extensive decline in accuracy with increasing distance of the target from the center of foveation. As a side note, this change of the ERP component amplitude with increasing distance of the target from the center of foveation did not affect the generalization of the classifier as Fig. 2.19 shows.

Hubel and Wiesel (1959, 1962) showed that the visual cortex performs neuronal processing of spatial frequency, orientation, motion, direction, speed, and many other spatiotemporal features. A recent study (Martens et al. 2009) showed that these properties of the visual system can be exploited to increase the amplitude of the EEG response, and thereby the overall classification accuracy. Di Russo et al. 2002 showed the same polarity reversal of the early VEP components between visual/occipital cortex and central and frontal locations that we observed in Condition 1 (see Section 2.3.3.4).

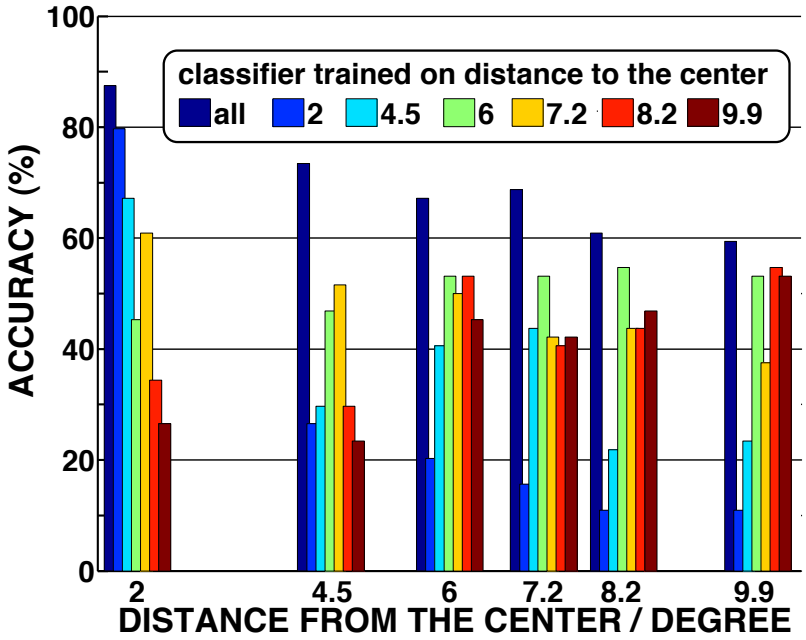

Figure 2.19: **Classification accuracy, based on distance specific classifiers, as a function of the distance of gaze from the center.** The bars show the classification accuracy in Condition 2, the "center" condition, for classifiers specifically trained on each of 6 distance of gaze to the center. The distance specific classifiers poorly generalize to other distances (e.g., trained on 2 degree, tested on 9.9 degree), while the generalized classifier (dark blue bar) results in the best overall and best generalizing classification accuracy.

The optimization of "P300" stimulation parameters is usually based on data from normal subjects obtained in Condition-1-like circumstances (i.e., the subject is allowed to gaze at the target). Our results suggest that such optimization is determined more by the VEP than by P300 (Gonsalvez and Polich 2002). Thus, the lack of early VEP components over visual/occipital cortex, with polarity reversal over central and frontal locations, in Condition 2 (see Section 2.3.3.4) suggests that optimization based on data from normal subjects (Krusienski et al. 2006, 2008; Sellers et al. 2006a; Takano et al. 2009) may not generalize well to subjects in whom gaze control is impaired.

Two aspects of the study methodology may have exaggerated the actual difference in accuracy between the two conditions. That is, the improvement produced by gazing at the target rather than at a central fixation point may not be as great as the present data imply. First, Condition 2, the "center" condition, is a more demanding task than is Condition 1, the "letter" condition. In Condition 1, the subject has only to look at the target and pay attention to it, while in Condition 2 s/he has to look at the fixation

cross and pay attention to the target. Tasks that require greater amounts of attentional resources have been shown to elicit smaller and delayed P300 responses than tasks that require lesser attentional resources (Kok 2001; Polich 1987). This is consistent with our results shown in Section 2.3.3.4. This could account for much of the difference in accuracy between the conditions summarized in Fig. 2.14. Furthermore, it is possible that with continued practice, the subjects might improve their performance on the more difficult task of Condition 2, and thereby reduce the difference in accuracy between the two conditions.

Second, given the inverse relationship between visual acuity and distance from the point of gaze (e.g., Westheimer 1965), under Condition 2, 32 of the 36 possible targets (see Figure 2) were at a disadvantage because some of their non-target competitors (i.e., some of the possible mistakes) were closer to the point of gaze. This finding suggests that, if the impact of having non-targets closer to the fixation point than the target were eliminated (e.g., by having all possible targets in a circle centered on the fixation point), Condition 2 accuracy would improve, and the superiority of Condition 1 would be less marked.

To verify that these aspects did not affect our main result, i.e., that the performance of the "P300" matrix speller in normal subjects not only depends on the P300 evoked potential, but also on other EEG features such as the visual evoked potential (VEP) that strongly depend on eye-gaze direction, we conducted the following analysis. We hypothesized that the classification accuracy in Condition 1, the "letter" condition, that is unaffected by both before-mentioned aspects, would significantly decrease if the visually evoked potential (VEP) were not used. Thus, we compared the classification accuracy within Condition 1, the "letter" condition, when we used either all data (i.e., 0-800 ms after stimulus presentation) or data that excludes VEP components (i.e., 300-800 ms). ERPs that depend on eye gaze such as VEPs are known to occur 150-350 ms post stimulus, while P300 ERPs are known to occur 300-600 ms post stimulus. The results shown in Fig. 2.20 demonstrate that 14/17 subjects performed significantly worse when the ERPs used for classification were restricted to 300 to 800 ms compared to when they were not (29.6%, $p<0.05$, pairwise t-test). This confirms our hypothesis and proves that our main result is not affected by the two aspects mentioned above. At the same time, it is important to remember that the results of this analysis were done in healthy subjects and may not be identical to those for people with impaired eye-gaze.

Visual crowding (Korte 1923; Strasburger 2005), i.e., the impaired recognition of a suprathreshold target due to the presence of distractor elements in the neighborhood

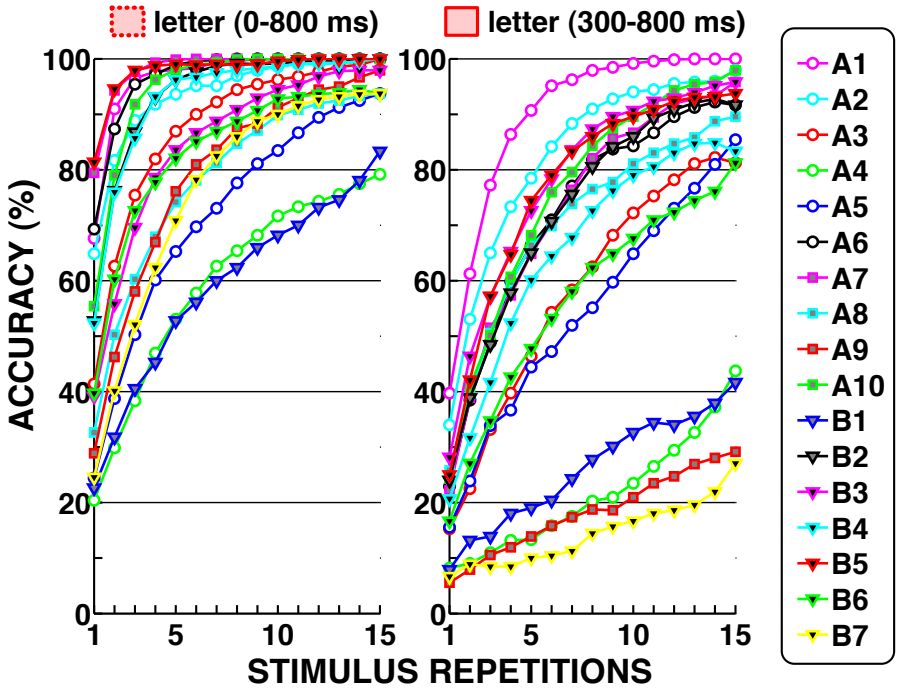

Figure 2.20: **Classification accuracy in the "letter" condition as a function of the number of stimulus repetitions and data period.** The left panel shows results when we used all data (i.e., 0-800 ms post stimulus). The right panel shows results when we used only data after 300 ms (i.e., 300-800 ms post stimulus). See text for details.

of that target, may have also had an adverse effect on the classification accuracy in Condition 2, the "center" condition. Crowding is inevitable in the matrix "P300" speller and can only be avoided by arranging the letters in a circle rather than a matrix.

Finally, while we controlled for eye movements in this study, we did not control for or eliminate very small or very brief eye movements. Such movements, e.g., microsaccades (Cornsweet 1956), contribute to maintaining foveal visibility by continuously stimulating neurons in primary visual areas (Rolfs 2009). While it is known that ALS can impair eye-gaze (Cohen and Caroscio 1983; Palmowski et al. 1995), the effect of ALS on such saccades has not yet been studied. Thus, the difference between the results shown here and the results that can be expected in people with ALS is currently unclear.

Further studies are needed to optimize P300 recording montages and stimulation and analysis parameters and to evaluate the effect of online feedback and extended training in this user population.

2.3.5 Conclusions

In summary, this study shows in normal subjects that the classification accuracy of the "P300" matrix speller BCI is substantially improved when the subject gazes directly at the target. Thus, the study disproves the widespread assumption that the performance of the "P300" speller does not depend on fixating the target. Further research is needed to determine whether this effect is similarly prominent in the potential user population (e.g., people severely disabled by ALS), and whether their performance can be improved by modifications in montage selection, algorithms, or other aspects of BCI operation.

2.3.6 Recommendations

The results of this study show that the traditional design of the matrix speller not only relies on the P300 evoked potential, which does not depend on eye gaze, but also on other features such as visual evoked potentials, which strongly depend on foveation and thus the ability to control eye gaze direction. In addition to the dependence on eye gaze, the spelling rate supported by the matrix speller BCI is still an order of magnitude lower than what conventional assistive devices can provide (Majaranta and Räihä 2002; Schalk 2008). In summary, the limited speed and dependence on gaze of the traditional design of the matrix speller BCI limits the practical value of this BCI approach to individuals in the target population.

Recent studies have attempted to address these two issues. To improve spelling performance, studies have optimized stimulus presentation and algorithms to detect the intended letter. For example, recent studies employed faster stimulation (McFarland et al. 2010a), more robust coding (Hill et al. 2009; Townsend et al. 2010), or probabilistic measures of the letter frequency (Martens et al. 2010). However, these approaches have only modestly increased or in some case even decreased spelling performance. It is likely that the limited gain of these approaches is due to physiological constraints of the brain. For example, limited speed of cortical processing will define the maximal stimulation frequency.

To remove or mitigate the dependence of the matrix speller on eye-gaze, recent studies used oddball paradigms with auditory (Klobassa et al. 2009; Kübler et al. 2009; Schreuder et al. 2010), tactile (Brouwer and van Erp 2010), or simplified visual stimuli (Acqualagna et al. 2010; Treder et al. 2011; Treder and Blankertz 2010; Treder et al. 2010). While the results of these studies are encouraging, further improvements to accuracy and speed in this gaze-independent approach are needed.

3 Brain Signals for Diagnosis

3.1 Summary of Contributions and Approach

This chapter discusses methodologies that overcome the dependence on experts and post-hoc analysis in the application of **Brain Signals for Diagnosis**. At present, the clinical application of brain signals to passively map eloquent cortex has been impeded by the dependence on experts and post-hoc analysis.

The main contribution presented in this chapter is the development of a diagnostic tool that does not depend on experts or post-hoc analysis to passively map eloquent cortex. This encompasses the development of techniques, protocols and methods for chronic real-time recording, modeling and detection of ECoG signals, as well as the development of an intuitive interface that presents the results to the clinical investigator for the purpose of clinical validation. The associated work is described in section 3.2 for the modeling and detection of ECoG signals and in section 3.3 for the clinical validation. The results show that this diagnostic tool does not need experts or post-hoc analysis to provide maps of eloquent cortex that are in general alignment with those obtained from the current gold standard (i.e., ECS). The work accomplished in this chapter should allow clinical investigators to use brain signals for clinical mapping of eloquent cortex.

The work in this chapter was highly multidisciplinary and depended on the integration of methodologies from different areas of engineering and science, such as computer science, signal processing, machine learning, electrical engineering, experimental psychology, neurosurgery and electrophysiology. For example, I used machine learning and computer science methodologies to develop and implement the generative model that enabled the detection of ECoG signals in real-time.

3.2 Detection Instead of Classification

3.2.1 Introduction

Clinical applications that use electrophysiological activity depend on signal processing techniques to identify relevant brain signals and to translate them into diagnostic outputs that provide value to the clinical investigator or the patient.

Brain signals are usually deemed relevant if they are modulated by a particular diagnostic condition. For example, for the diagnosis and localization of epileptic seizures, those brain signals are relevant that selectively change when seizures occur. Seizures themselves can be indicated by overt or covert behavioral patterns, e.g., overt convulsions or covert lapses in attention. The identified relevant brain signals are then translated into a cortical map that delineates the epileptic foci and is informative to the clinical investigator.

Another diagnostic example is the delineation of eloquent cortex prior to resection of the epileptic foci. In this case, brain signals are relevant if they selectively change with specific covert or overt behavior, for example, receptive and expressive language processing or motor movement and sensation. As in the previous example, the identified relevant brain signals are then translated into a cortical map that delineates eloquent cortex and is informative for the clinical investigator.

These two examples show that it is important to identify those brain signals that are modulated by diagnostic conditions. This is challenging, because brain signals are non-stationary due to two main reasons. First, brain signals are not only modulated by diagnostic conditions, but also by other unrelated cognitive processes. Second, the modulation by the diagnostic condition depends on a multitude of latent factors, e.g., the subject's cognitive state and behavioral strategy. The general lack of signal features that are invariant to those factors makes the signal identification problem difficult to solve.

Traditional approaches that identify relevant brain signals rely on discriminative supervised learning. To overcome the issues associated with non-stationary signals, discriminative supervised learning typically depends on a top-down approach in which an expert defines a diagnostic condition and determines the best set of parameters that identifies it. This top-down approach reduces the signal identification problem from a multivariate to a univariate problem. This reduction effectively limits the signal identification capacity to only those diagnostic conditions that are described by the set of parameters. Despite this effort, such an approach inevitably fails if non-stationary effects

markedly affect the brain signals (see Fig. 3.2). Nevertheless, discriminative supervised learning is the most commonly employed approach to the signal identification problem (Meyer-Baese 2003).

Generative unsupervised learning of multivariate statistics presents an alternative approach to the signal identification problem. This bottom-up approach determines a generative model that describes the multivariate data. The generative model is then used to detect the diagnostic condition rather then to classify it. This bottom-up approach effectively detects any signal modulation and therefore is a powerful technique to solve the signal identification problem. Many different generative models and unsupervised learning procedures have been proposed. The following sections expand on the selection of the appropriate generative unsupervised learning approach, which mainly relates to the selection of an appropriate representation, learning, and recognition approach.

3.2.2 Methods

3.2.2.1 Feature Extraction

The extraction of features from non-stationary brain signals entails a series of procedures that preprocess the signals and extract those features that are most reflective of the modulation by the diagnostic condition.

Signal Preprocessing. Raw electrophysiological brain signals are often not reflective of the modulation by the diagnostic condition. This is mainly due to the lack of an absolute reference point and high correlation with processes that are irrelevant to the diagnostic condition. Both issues can be addressed by spatial filters as described in (McFarland et al., 1997). The absolute reference point can be established by re-referencing each electrode to a common potential derived from all electrodes. This is done by using a common average reference (CAR) spatial filter as illustrated in Fig. 3.1(a) whereby as seen in Eq. (3.1) the potential of each electrode c at each time point t is re-referenced using the average over all electrodes N_c.

$$X'_{t,c} = X_{t,c} - \frac{1}{N_c} \sum_{i=1}^{N_c} X_{t,i} \tag{3.1}$$

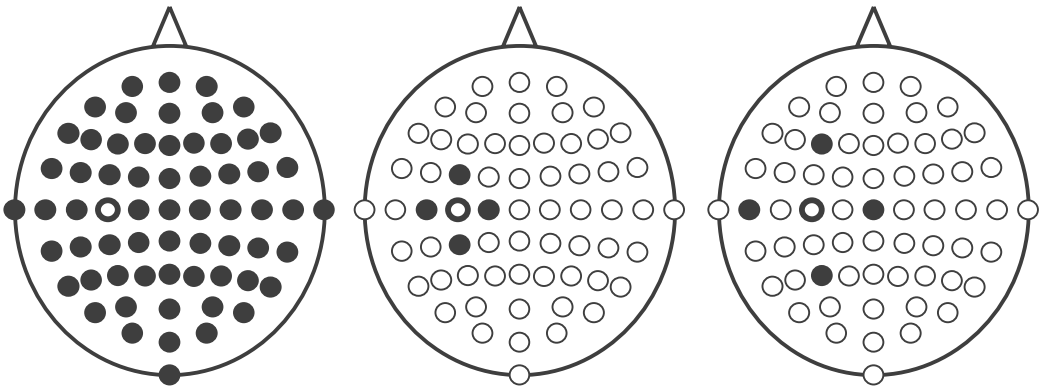

(a) common reference average

(b) small Laplacian

(c) large Laplacian

Figure 3.1: **Spatial filters.** This figure shows three different spatial filters over the electrode C_3.

The correlation with processes that are irrelevant to the diagnostic condition is addressed by using a small or a large Laplacian spatial filter as illustrated in Fig. 3.1(b) and 3.1(c) respectively. This filter assumes that relevant modulations of the electrophysiological signals are spatially focused, while other irrelevant modulations are spatially widespread. A Laplacian filter then removes the averaged spatially widespread irrelevant modulation from the electrophysiological signals. As seen in Eq. (3.2) the weighted sum of the four nearest and next nearest electrodes are subtracted for the small and large Laplacian respectively. The weight $w_{c,i}$ in Eq. (3.3) is derived from the distance $d_{c,i}$ between the electrode of interest c and its neighbor i.

$$X'_{t,c} = X_{t,c} - \sum_{i \in S_c} w_{c,i} X_{t,i} \tag{3.2}$$

$$w_{c,i} = \frac{\frac{1}{d_{c,i}}}{\sum_{i \in S_c} \frac{1}{d_{c,i}}} \tag{3.3}$$

Feature Extraction Electrophysiological brain signals are most markedly modulated by diagnostic conditions in their spectral amplitude (Miller et al. 2007b). Damped harmonic oscillators that inhibit or innervate function serve as a model for this modulation. The damped nature of these oscillators results in the non-stationary characteristics of electrophysiological brain signals. Such signals not only are modulated in their spectral amplitude by the diagnostic condition, they also change their phase unrelated to these conditions. Consequently, techniques that extract the spectral amplitude of these signals need to be invariant to phase changes. While in such a scenario, traditional linear spectral transformations, such as the fast Fourier transform (FFT) result in cancelation effects, but autoregressive spectral estimation methods are invariant to phase changes.

An autoregressive model is a linear model that predicts the data using a limited number of autoregressive coefficients (Kay, 1988; Marple, 1987; Priestley, 1981; Stoica and Moses, 1997). This time domain prediction can be transformed into the frequency domain, which makes autoregressive models well suited for the robust extraction of spectral components from electrophysiological brain signals. One such autoregressive spectral estimation model is the Burg Maximum Entropy Method (Burg 1967, 1968) that is described in the following paragraphs.

An autoregressive model of order p is described by its autoregressive coefficients $a_1 \dots a_p$. The relationship between the autoregressive coefficients and the stationary stochastic signal X_t is given by the following difference equation (3.4). However, since the solution of this equation is of high computational complexity, it is more practical to solve the equivalent in terms of the autocorrelation sequence in Eq. (3.5).

$$X_t + a_1 X_{t-1} + \ldots + a_p X_{t-p} = \epsilon_t \tag{3.4}$$

$$R_X(\tau) = E\left[X(t)X(t-\tau)\right] = -\sum_{k=1}^{p} a_k E\left[X(t-k)X(t-\tau)\right] \tag{3.5}$$

Hence the autocorrelation sequence can be described using the autoregressive coefficients in Eq. (3.6) for any lag τ.

$$R_X(\tau) = \begin{cases} -\sum_{k=1}^{P} a_k R_X(\tau - k) & \tau > 0 \\ -\sum_{k=1}^{P} a_k R_X(\tau - k) + \sigma_\varepsilon^2 & \tau = 0 \\ R_X(-\tau) & \tau < 0 \end{cases} \tag{3.6}$$

In the case of an autoregressive model of the order p the autoregressive sequence can be described in Eq. (3.7) in matrix form or in Eq. (3.8) in vector form. Adding the mean-square error σ_ε^2 from Eq. (3.6) for $\tau = 0$ the matrix R_X is transformed into a persymmetric Toplitz matrix in Eq. (3.10). To solve Eq. (3.8), this matrix has to be inverted, which can be performed in $O(n^2)$ using the Levinson-Durbin recursion algorithm.

$$\begin{bmatrix} R_X(0) & R_X(1) & \ldots & R_X(p-1) \\ R_X(1) & R_X(0) & \ldots & R_X(p-2) \\ \vdots & \vdots & & \vdots \\ R_X(p-1) & R_X(p-2) & \ldots & R_X(0) \end{bmatrix} \begin{bmatrix} a_1 \\ a_2 \\ \vdots \\ a_p \end{bmatrix} = - \begin{bmatrix} R_X(1) \\ R_X(2) \\ \vdots \\ R_X(p) \end{bmatrix} \tag{3.7}$$

$$\mathbf{R_X} \cdot \mathbf{a} = \mathbf{r} \tag{3.8}$$

$$\sigma_\varepsilon^2 = R_X(0) + \sum_{k=1}^{P} a_k R_X(-k) \tag{3.9}$$

$$\begin{bmatrix} R_X(0) & R_X(1) & \dots & R_X(p) \\ R_X(1) & R_X(0) & \dots & R_X(p-1) \\ \vdots & \vdots & & \vdots \\ R_X(p) & R_X(p-2) & \dots & R_X(0) \end{bmatrix} \begin{bmatrix} 1 \\ a_1 \\ \vdots \\ a_p \end{bmatrix} = - \begin{bmatrix} \sigma_\varepsilon^2 \\ 0 \\ \vdots \\ 0 \end{bmatrix} \tag{3.10}$$

In order to achieve a more stable solution for the autoregressive coefficients that incorporate forward and backward prediction, the Burg algorithm was proposed (Burg 1967, 1968). Thus, rather than using the Levinson-Durbin algorithm to invert the persymmetric Toplitz matrix, Burgs Maximum Entropy Method minimizes the forward and backward prediction based on the reflection coefficients K_k with the constraint that the autoregression coefficients satisfy the Levinson-Durbin recursion.

This forward and backward prediction $\hat{X}_t$ and $\hat{X}_{t-p}$ respectively are defined in Eq. (3.11) and Eq. (3.12). The corresponding forward and backward prediction error are defined in Eq. (3.13) and (3.14). The total error that is to be minimized is comprised of the forward and backward prediction error and defined in Eq. (3.15).

$$\hat{X}_t = -\sum_{k=1}^{P} a_p(k) X_{t-k} \tag{3.11}$$

$$\hat{X}_{t-p} = -\sum_{k=1}^{P} a_p^*(k) X_{t-p+k} \tag{3.12}$$

$$e_p^f(t) = X_t - \hat{X}_t \tag{3.13}$$

$$e_p^b(t) = X_{t-p} - \hat{X}_{t-p} \tag{3.14}$$

$$E_p = \sum_{j=p}^{N-1} \left[\left| e_p^f(j) \right|^2 + \left| e_p^b(j) \right|^2 \right] \tag{3.15}$$

For minimization of Eq. (3.15), the Levinson-Durbin recursion is used resulting in the recursive expression for $e_p^f(t)$ in Eq. (3.17) and $e_p^b(t)$ in Eq. (3.18) whereby the initialization is performed according Eq. (3.16). Substituting from Eq. (3.17) and Eq. (3.18) into the minimization function in Eq. (3.15) and minimizing the resulting equation in respect to the reflect coefficient (K_k) the result in Eq. (3.19) is obtained from which after each iteration one autoregressive coefficient in Eq. (3.20) can be obtained. Eq. (3.21) demonstrates that the algorithm always produces p coefficients in p steps while the remaining error converges in each step.

$$e_0^f(t) = e_0^b(t) = X_t \tag{3.16}$$

$$e_k^f(t) = e_{k-1}^f(t) + K_k e_{k-1}^b(t-1), \qquad k = 1, 2 \ldots, p \tag{3.17}$$

$$e_k^b(t) = K_k^* e_{k-1}^f(t) + e_{k-1}^b(t-1), \qquad k = 1, 2 \ldots, p \tag{3.18}$$

$$\hat{K}_k = \frac{-\sum_{j=k}^{N-1} e_{k-1}^f(j) e_{k-1}^b(j-1)}{\frac{1}{2}\sum_{j=k}^{N-1}\left[\left|e_{k-1}^f(j)\right|^2 + \left|e_{k-1}^b(j)\right|^2\right]}, \qquad k = 1, 2 \ldots, p \tag{3.19}$$

$$a_k(k) = K_k \tag{3.20}$$

$$E_k = E_{k-1}\left[1 - |K_k|^2\right] \tag{3.21}$$

Finally, the time series defined by the autoregressive coefficients are transformed in Eq. (3.22) into the frequency domain to yield the amplitude spectrum $P(f)$.

$$P(f) = \frac{a_0}{\left[1 - \sum_{k=1}^{K} a_k e^{-j2\pi k \frac{f}{f_s}}\right]^2} \tag{3.22}$$

3.2.2.2 Representation

Generative approaches can represent data in parametric or non-parametric models. Parametric models assume a structure of the data, whereas non-parametric approaches determine the underlying structure from the data itself. For example, multivariate kernel density estimation is a non-parametric approach to estimating the probability density function of the data. In this approach each data point defines the parameters of one kernel (e.g., Gaussian distribution), and the combination of all kernels defines the probability density function of the data itself. In contrast, Gaussian mixture models (GMMs) are a parametric approach to estimating the probability density function as the joint probability density function of a mixture of Gaussians.

The choice between parametric and non-parametric representations mainly relates to computational complexity, the ability to adapt the model, the capacity to include contextual information, and the robustness to noise, all of which are essential for signal identification from multivariate non-stationary brain signals. For example, high computational complexity, sensitivity to noise and the inability to include contextual information make non-parametric representations such as multivariate kernel density estimation ill-suited for our applications. In contrast, parametric representations that overcome these limitations, such as Gaussian mixture models and hidden Markov models (HMMs), are better suited for the multivariate signal identification of non-stationary brain signals.

Gaussian Mixture Models (GMMs) Gaussian mixture models estimate the probability density function of the underlying data using the joint probability density function of a mixture of Gaussians. This approach has two particular advantages in the context of the signal identification problem. The first advantages is the ability to robustly identify non-stationary signals (Fig. 3.2). This allows detecting unseen diagnostic conditions as long as the diagnostic condition modulates the features. The second advantage is the capacity to model complex multivariate distributions (Fig. 3.3). This allows modeling the interaction between multiple brain processes that result in complex probability density functions.

Model Definition Any Gaussian distribution c can be described by is center μ_c and its covariance matrix Σ_c. As a distance metric the Mahalanobis distance, as defined in Eq. (3.23), assigns every point X_t in a Gaussian distribution (Σ_c, μ_c) a distance that is in units of estimated variance between the point X_t and the center μ_c.

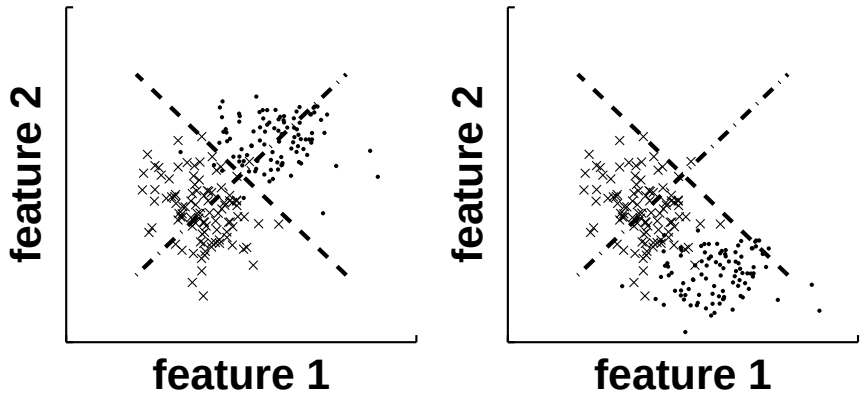

(a) linear regression **working** (b) linear regression **fails**

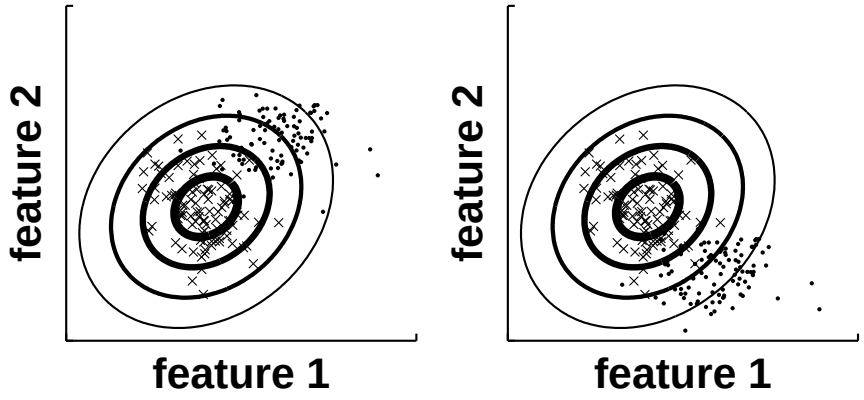

(c) GMM **working** (d) GMM **working**

Figure 3.2: **Linear regression vs. Gaussian Mixture Model (GMM).** Linear regression between the data points in condition A (crosses) and B (dots) in (a) fails as soon as one condition (e.g., B) is non-stationary as seen in (b). In contrast, a GMM trained on the condition A in (c) can be used to discriminate condition A from condition B (Fig. (d)).

$$m(X_t|c) = (X_t - \mu_c)^T \Sigma_c^{-1} (X_t - \mu_c) \tag{3.23}$$

Using this distance metric and introducing the weight ω_c as the proportion of data points assigned to this Gaussian distribution, the probability density function $\eta(X_t|c)$ can be defined in Eq. (3.24). The definition of the negative log likelihood is described in Eq. (3.25).

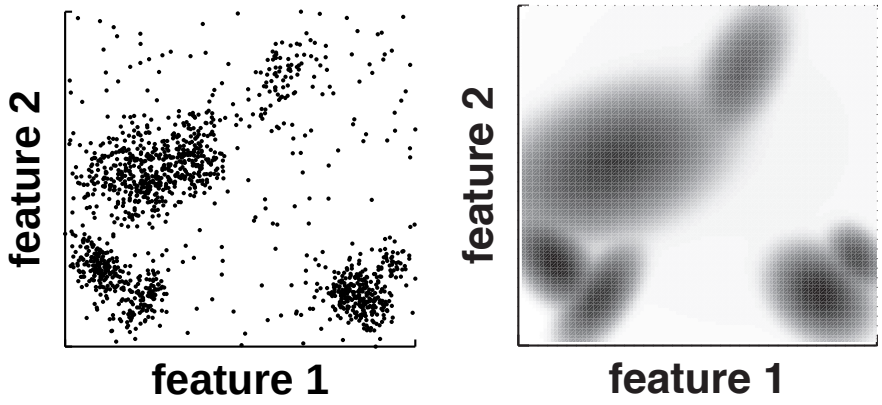

(a) Gaussian distributed data points.

(b) Probability density estimated by SIGFRIED.

Figure 3.3: **Gaussian Mixture Model (GMM).** This figure shows a complex feature distribution (a) for which the probability density is estimated by a Gaussian Mixture Model (b).

$$\eta(X_t|c) = \frac{\omega_c}{(2\pi)^{\frac{D}{2}} \, |\Sigma_c|^{\frac{1}{2}}} e^{-\frac{m(X_t|c)}{2}} \tag{3.24}$$

$$\begin{aligned} LL(X_t|c) &= -log\left[\eta(X_t|c)\right] \\ &= -log(\omega_c) + \frac{D}{2}\log(2\pi) + \frac{1}{2}\log(|\Sigma_c|) + \frac{m(X_t|c)}{2} \end{aligned} \tag{3.25}$$

The maximized likelihood L can be described as the accumulated negative log likelihood L_i in Eq. (3.26) over all Gaussians in Eq. (3.27).

$$L_i = \sum_{t=1}^{N_i} LL(X_t|c_i) \tag{3.26}$$

$$L = \sum_{i=1}^{C} L_i \tag{3.27}$$

For each Gaussian distribution, the number of free parameters N_p can be described as in Eq. (3.28) as the sum of parameters from the covariance matrix Σ_c, the Gaussian center μ_c, and its weight ω_c.

$$\begin{aligned} N_p &= \left[N_{p_{covariance}} + N_{p_{center}} + N_{p_{weight}}\right] \cdot N_c \\ &= \left[\frac{D(D+1)}{2} + D + 1\right] \cdot N_c \end{aligned} \tag{3.28}$$

3.2.2.3 Learning

Parametric representations such as Gaussian mixture models depend on learning algorithms to identify the model parameters. This parameter identification problem is often ill-posed and difficult to solve, because it requires overcoming local minima and verifying the correctness of the model. For example, GMMs use the expectation-maximization (EM) algorithm (Dempster et al., 1977) to learn the model parameters, i.e., the parameters of the Gaussian distributions. Starting from random model parameters, this algorithm alternates between assigning the data to the Gaussian distributions (i.e., expectation-step) and estimating new parameters (i.e., maximization-step) for the Gaussian distributions until a stable solution is reached. However, this stable solution may be a local minimum or not even a correct model.

Model selection is an approach to overcome local minima and to select the correct model. The classification expectation maximization (CEM) algorithm (Celeux and Govaert 1992) is an learning algorithm that extends the EM algorithm by implementing random perturbations, to avoid local minima, and model selection, to find a correct model.

Information Criterion Model selection mainly relates to finding the balance between the goodness of fit and the simplicity of the model as well as to the selection of the correct model. This requires the definition of an information criterion as a measure of the relative goodness of fit of a statistical model that determines the model selection. For Gaussian mixture models (GMM), the number of mixtures to describe the data has to be selected. Therefore an information criterion takes in account the model fit as well as a penalty for model order to avoid overfitting. Most information criteria are in the form of Eq. (3.29).

$$\text{information criteria} = \text{measure of fit} + \text{complexity penalty} \tag{3.29}$$

A number of these information criteria have been described in the literature, e.g., the Akaike Information Criteria (AIC) (Akaike 1973), Vapnik's Structural Risk Minimization

(SRM) (Vapnik and Chervonenkis 1974), Schwarz's Bayesian Information Criteria (BIC) (Schwarz 1978), Rissanen's Minimum Description Length (MDL) and Shortest Data Description (SSD) (Rissanen 1978) and Bozdogan's Corrected Akaike Information Criterion (CAICF) and Consistent Akaike Information Criterion (CAIC) (Bozdogan 1974) (see Torr (1997) for a comprehensive review).

For GMMs, the measure of fit is the maximized likelihood, and each of these information criterions propose a different measure for the complexity penalty:

Bayesian Information Criteria (BIC) As the amount of data goes to infinity, the Bayesian Information Criteria (BIC) promises to select the model that the data was generated from (Schwarz 1978). The complexity penalty is chosen conservatively, accounting for the number of samples N and the number of free parameters N_p. Therefore, the BIC in (3.30) tends to select the best structure instead of the best predictor.

$$\begin{aligned} K_{BIC} &= -2 \cdot \text{maximized likelihood} + \text{bayesian compl. penalty} \\ K_{BIC} &= -2 \cdot L + 2N_p \log N \end{aligned} \tag{3.30}$$

Akaike Information Criteria (AIC) As the amount of data goes to infinity, the Akaike Information Criteria (AIC) promises to select the model that will have the best likelihood for future data (Akaike 1973). Therefore the number of observations N is not accounted for in Eq. (3.31). AIC does not produce an asymptotically consistent estimate of the order of the model and tends to overfit.

$$\begin{aligned} K_{AIC} &= -2 \cdot \text{maximized likelihood} + \text{akaike compl. penalty} \\ K_{AIC} &= -2 \cdot L + 2N_p \end{aligned} \tag{3.31}$$

Mixture of AIC and BIC As there is no evidence that indicates which information criterion best suits the modeling of electrophysiological signals, we chose to introduce another parameter that defines a linear combination of AIC and BIC. Eq. (3.32) defines the information criterion K as a linear combination of AIC and BIC with the linear constant k. For $0 \leq k \leq 1$ the information criterion K selects on the continuum between pure AIC and BIC. Thus k modulates the impact of the number of samples N to the information criteria.

$$K = (1-k) \cdot K_{AIC} + k \cdot K_{BIC}, \qquad 0 \leq k \leq 1 \tag{3.32}$$

Model Selection Maximizing the information criterion in an iterative procedure typically yields the correct model. In our procedure, we test the hypothesis that increasing or decreasing the model order (i.e., the number of Gaussians) benefits the information criterion:

Hypothesis to Decrease Model Order: Deleting Gaussian d with the lowest contribution to the model improves information criterion of whole model.

Hypothesis Test to Decrease Model Order: The improvement in information criteria ΔK is defined in Eq. (3.35) for reducing the number of Gaussians from C to $C-1$.

The contribution of each Gaussian i to the model is defined in Eq. (3.33) as the difference in the total negative log likelihood as the data points are assigned from the best fitting Gaussian i to the second best fitting Gaussian j. The Gaussian d as defined in Eq. (3.34) with the minimal contribution LL_d to the model is selected as candidate to be deleted.

If $\Delta K > LL_D$ the hypothesis is true and the Gaussian D is deleted.

$$\Delta LL_i = \sum_{t=1}^{N_i} LL(X_t|c_j) - LL(X_t|c_i) \tag{3.33}$$

$$\Delta LL_d = \min\left[\Delta LL_i\right], \qquad i = 1 \ldots C \tag{3.34}$$

$$\Delta K = K(C) - K(C-1) \tag{3.35}$$

Hypothesis to Increase Model Order: Splitting one Gaussian i into two Gaussians improves the information criterion of data points assigned to Gaussian i and the information criterion of the whole model.

Hypothesis Test to Increase Model Order: For each Gaussian i this hypothesis is tested by splitting the Gaussian i into two Gaussians. The CEM algorithm is executed for all data points that are assigned to the Gaussian i for one (unsplit) Gaussian and for two (split) Gaussians. If the resulting information criterion $K_{i_{split}} < K_{i_{unsplit}}$, the hypothesis is true for the Gaussian i and the Gaussian remains split.
In this case, the maximization and expectation step of the CEM algorithm is executed on

the whole data set with now $C+1$ Gaussians. If the information criterion $K_{C+1} < K_C$, the hypothesis for the whole model is true.

CEM Algorithm The Classification Expectation Maximization (CEM) algorithm as described in (Celeux and Govaert, 1992) and (Biernacki et al., 2003) is based on the EM-Algorithm that was originally described in (Dempster et al., 1977).

Initialization: The initialization uses a user-defined number of initial Gaussians and randomly assigns each data point to one Gaussian.

Maximization: The maximization (i.e., M) step calculates for each Gaussian c its weight w_c in Eq. (3.36), mean $\overline{X_c}$ in Eq. (3.37) and covariance matrix Σ_c in Eq. (3.38). To calculate the Mahalanobis distance $m(X_t|c)$ in Eq. (3.41), the inverse of the covariance matrix Σ_c^{-1} is calculated using the Cholesky decomposition in Eq. (3.39), which provides a lower triangular matrix L_c that provides the inverse of the covariance matrix Σ_c^{-1} in Eq. (3.40). If the determinant of each covariance matrix $|\Sigma_c|$ is very small, the covariance matrix tends to be singular. In these cases, this Gaussian c is deleted.

$$w_c = \frac{N_c}{N} \tag{3.36}$$

$$\overline{X_c} = \frac{1}{N_c} \sum_{t=1}^{N_c} X_t \tag{3.37}$$

$$\Sigma_c = \frac{1}{N_c - 1} \sum_{t=1}^{N_c} (X_t - \overline{X_c})(X_t - \overline{X_c})^T \tag{3.38}$$

$$\Sigma_c = L_c L_c^T \tag{3.39}$$

$$\Sigma_c^{-1} = (L_c L_c^T)^{-1} = (L_c^T)^{-1} L_c^{-1} = (L_c^{-1})^T L_c^{-1} \tag{3.40}$$

Expectation: For each data point X_t, the Expectation (i.e., E) step calculates the distance $m(X_t|c)$ in Eq. (3.41) to each Gaussian c and its likelihood $\eta(X_t|c)$ in Eq. (3.42) that it belongs to each c.

$$m(X_t|c) = (X_t - \overline{X_c})\Sigma_c^{-1}(X_t - \overline{X_c})^T \tag{3.41}$$

$$\eta(X_t|c) = \frac{w_c}{(2\pi)^{\frac{D}{2}}\sqrt{|\Sigma_c|}} e^{-\frac{m(X_t|c)}{2}} \tag{3.42}$$

Classification: For each data point X_t, the Gaussians c_1 and c_2 with the lowest and second lowest negative log likelihood $-\log[\eta(X_t|c)]$ are determined. Furthermore, each data point X_t is assigned to the best fitting Gaussian c_1.

Deletion: For the Gaussian c with the lowest contribution to the model in Eq. (3.43), the selection criterion for model decrease is applied and the Gaussian is deleted if that suites the information criteria.

$$\Delta - \log[\eta(X|c)] = \sum_{t=1}^{N_c} \{-\log[\eta(X_t, c_2)]\} - \{-\log[\eta(X_t, c)]\} \tag{3.43}$$

Split: The split step applies the information criterion for model increase to each Gaussian c.

Termination: The program is not terminating as long it is within a maximum number of iterations and any data point was reassigned or any Gaussian was split during the last iteration.

3.2.2.4 Recognition

Signal recognition techniques apply the learned model to brain signals and detect relevant modulations. This entails experimental paradigms that trigger behavior, scoring algorithms that translate signal modulations into statistically relevant measures, and interfaces that provide value to the investigator. The following paragraphs expand the issues that are associated with these techniques.

Experimental Paradigms Experimental paradigms aim to selectively elicit covert and overt behavior that modulates those brain signals that are relevant for the diagnostic condition. For example, experimental paradigms for mapping eloquent cortex selectively elicit expressive or receptive sensorimotor and language behavior. However, as behavioral compliance cannot always be obtained, experimental paradigms need to validate compliance and thus the data, using control conditions, e.g., behavioral observations for expressive and control questions for receptive behavior.

Another issue are non-stationary changes in the signals that are not relevant to the diagnostic condition. For example, mapping of eloquent cortex in people with intractable epilepsy may be affected selectively in one diagnostic condition by brief electrographic seizures, i.e., brief seizures that are only reflected in the brain signals but not in the behavior. To mitigate this effect, interleaving and re-referencing the behavioral task with a baseline condition distributes such rare events equally across all diagnostic conditions.

Another issue are systematic errors in the modulation of brain signals. Such errors result from the anticipation and transition during a deterministic sequence of behavioral tasks. Counterbalancing the sequence of tasks avoids such systematic errors.

Scoring Algorithms Scoring algorithms translate signal modulations into statistically relevant measures. The signal detection algorithm results in a likelihood measure for each time point. This likelihood is then translated into a measure that represents statistical significance. This is accomplished by correlating the likelihood measure with behavior (e.g., sensorimotor activity and rest).

Intuitive Interfaces Intuitive interfaces present the detected signal modulations to the investigator. This form of presentation depends on the particular clinical application and can either be abstract or anatomically correct. For example, for verification of identified eloquent cortex through a gold standard procedure (e.g., electrical cortical stimulation (ECS)), a 2-dimensional form of presentation (Fig. 3.4A) that mimics the electrode grid is most intuitive to the neurologist. In contrast, a 3-dimensional anatomical correct presentation (Fig. 3.4B) is most intuitive for the neurosurgeon to plan cortical resection.

3.2.3 Conclusions

In conclusion, in this section we presented signal detection as a practical approach for diagnostic applications. We showed that while the signal detection problem can be approached by generative unsupervised learning, it requires careful consideration of the appropriate representation, learning and recognition method.

3.2.4 Recommendations

This section developed a framework for signal detection using generative models. The following section (3.3) will validate my implementation of this framework in a multi-center clinical study.

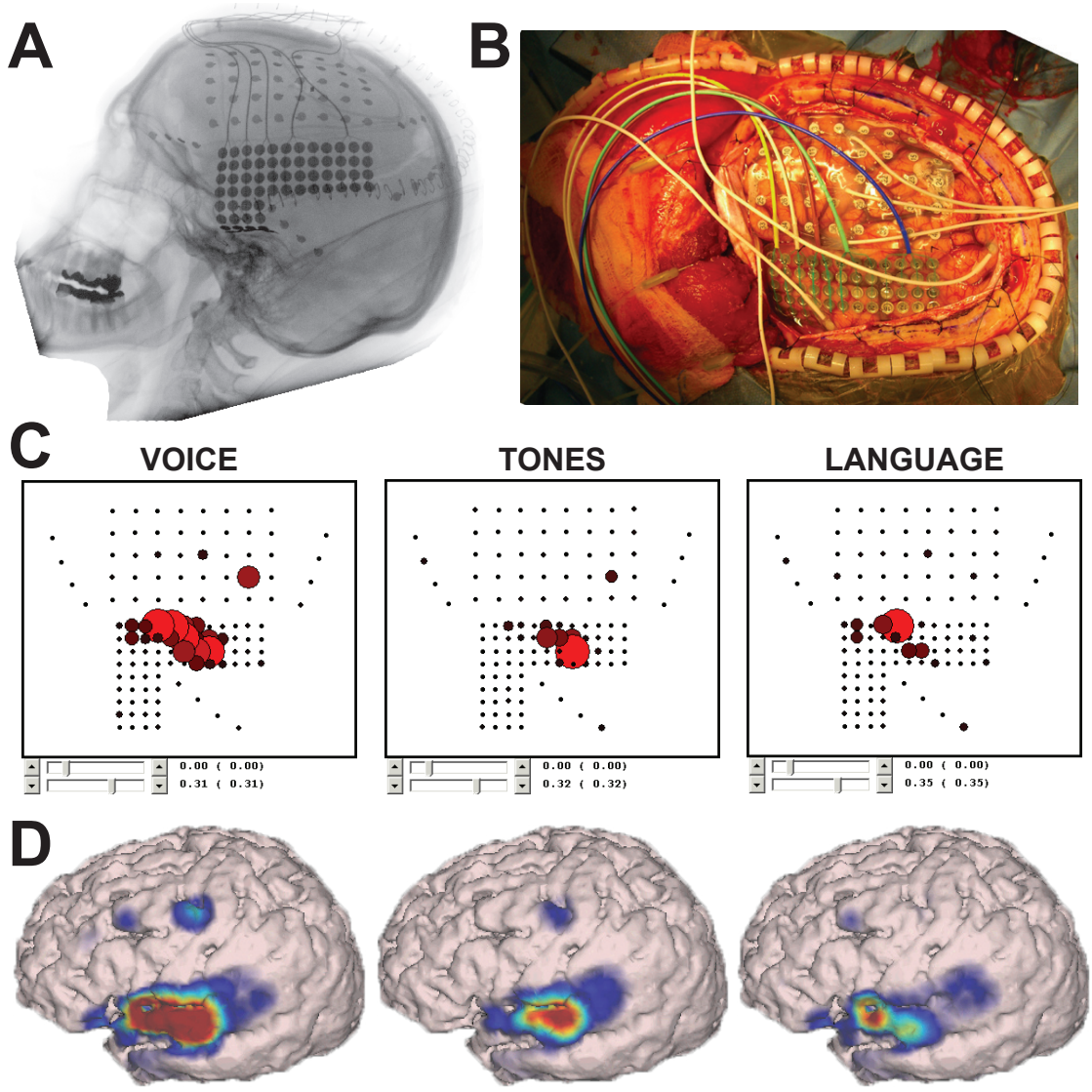

Figure 3.4: **Intuitive interface for mapping eloquent cortex.** For the purpose of mapping eloquent cortex and for localizing the epileptic foci, this patient with intractable epilepsy had 120 electrocorticographic electrodes implanted over left frontal, parietal and temporal cortex. A lateral x-ray (A) and an operative photograph (B) depict the configuration of two grids (one 40-contact frontal grid, one 68-contact temporal grid) and three 4-contact strips. From the recorded seizures, a neurologist localized the epileptic foci and determined that surgical resection of the left temporal lobe while sparing eloquent language cortex was necessary. The passive mapping procedure developed in this dissertation (SIGFRIED) identified eloquent language cortex by contrasting task-related changes during listening to voices and tones (C and D). The results were presented in two intuitive interfaces, a 2-dimensional interface that mimics the electrode grid and was most intuitive for the neurologist, and a 3-dimensional anatomical correct interface that was most intuitive for the neurosurgeon to plan cortical resection.

3.3 A Practical Procedure for Real-Time Functional Mapping of Eloquent Cortex

3.3.1 Introduction

Resective brain surgery is often performed in people with intractable epilepsy, congenital structural lesions, vascular anomalies, and neoplasms. Surgical planning of the resection procedure depends substantially on the delineation of abnormal tissue, e.g., epileptic foci or tumor tissue, and on the creation of a functional map of eloquent cortex in the area close to that abnormal tissue. Traditionally, different methodologies have been used to produce this functional map: electrical cortical stimulation (ECS) (Hara et al., 1991; Ojemann, 1991; Uematsu et al., 1992), functional magnetic resonance imaging (fMRI) (Chakraborty and McEvoy, 2008), positron emission tomography (PET) (Bittar et al., 1999; Meyer et al., 2003), magnetoencephalography (MEG) (Ganslandt et al., 1999), or evoked potentials (EP) (Dinner et al., 1986). Each of these methods has problems that include morbidity, time consumption, expense, or practicality. Since ECS has three quarters of a century of historical and clinical relevance (Foerster, 1931), and perhaps also due to its relative procedural simplicity and low cost, ECS has become the gold standard in mapping eloquent cortex. It has gained broad acceptance despite limited data to support efficacy (Hamberger, 2007) and despite of several substantial issues. For example, ECS is time consuming because it requires a comprehensive search, i.e., stimulation of each grid contact, while simultaneously determining the appropriate stimulation amplitude. ECS can also produce after-discharges that may trigger seizures or even status epilepticus. This can result in substantial delays, aborted procedures, and patient morbidity. The results derived using ECS may also not be correct because: 1) stimulation may produce inhibitory responses that cannot readily be observed; 2) propagation of stimulation current is affected by the anatomy and potential after-discharges, and thus variable; 3) there may be substantial procedural variability; and 4) stimulation-based mapping is based on a lesional and not a physiological model. Finally, ECS depends on patient compliance and thus cannot easily be used in some patient populations (such as pediatric patients). The characteristics of ECS are summarized in Table 3.1, and are reviewed in (Devinsky et al., 1993) and (Ojemann et al., 1989). The problems described above increase the risk to the patient and the time and cost associated with surgical planning.

Table 3.1: **Comparison of the properties of ECS mapping and ECoG-based mapping.**

	Electrical Cortical Stimulation	ECoG-Based Passive Mapping
time consuming	Yes	No
risk of seizure induction	Yes	No
difficulty in observing inhib. resp.	Yes	No
necessity for anti-epileptic drugs	Yes	No
variable prop. of stim. current	Yes	No
procedural variability	Yes	No
non-physiological model	Yes	No
patient compliance necessary	Yes	currently yes
proven by clinical studies	Yes	not yet

Patients undergoing invasive brain surgery would benefit greatly from a mapping methodology that does not have the problems associated with existing techniques, i.e., a method that is safe, can be rapidly applied, is comparatively inexpensive, procedurally simple, and also congruent to existing techniques (in particular to electrical stimulation). Task-related changes detected in electrocorticographic (ECoG) recordings appear to have attractive properties (see Table 3.1) and thus could provide the basis for a technique with those desirable characteristics. This approach seems attractive in particular because existing surgical protocols typically already include the placement of subdural electrodes, and because a number of recent studies showed that ECoG activity recorded from these electrodes reflect task-related changes (Aoki et al., 1999, 2001; Crone et al., 2001, 1998a,b; Fries, 2005; Graimann et al., 2002; Lachaux et al., 2003; Leuthardt et al., 2007; Miller et al., 2007b; Sinai et al., 2005; Varela et al., 2001). These studies showed that ECoG amplitudes in particular frequency bands carry substantial information about movement or language tasks. Specifically, amplitudes typically decrease in the mu (8-12 Hz) and beta (18-25 Hz) bands, whereas amplitudes usually increase in the gamma (>40 Hz) band (see Fig. 3.5). Furthermore, recent studies demonstrated that such ECoG changes, in particular those in the gamma band, were in general agreement with those derived using fMRI (Lachaux et al., 2007a) and with results determined using ECS (Leuthardt et al., 2007; Miller et al., 2007b; Sinai et al., 2005). However, these traditional ECoG-based analyses usually need to be optimized for each individual. Typically they are generated by signal processing experts after comprehensive post-hoc analyses. While a few recent studies have provided encouraging evidence that ECoG-based analyses could become more accessible to clinicians (Lachaux et al., 2007b,c; Miller et al., 2007a), a widely available and robust procedure that can be utilized by non-experts is needed.

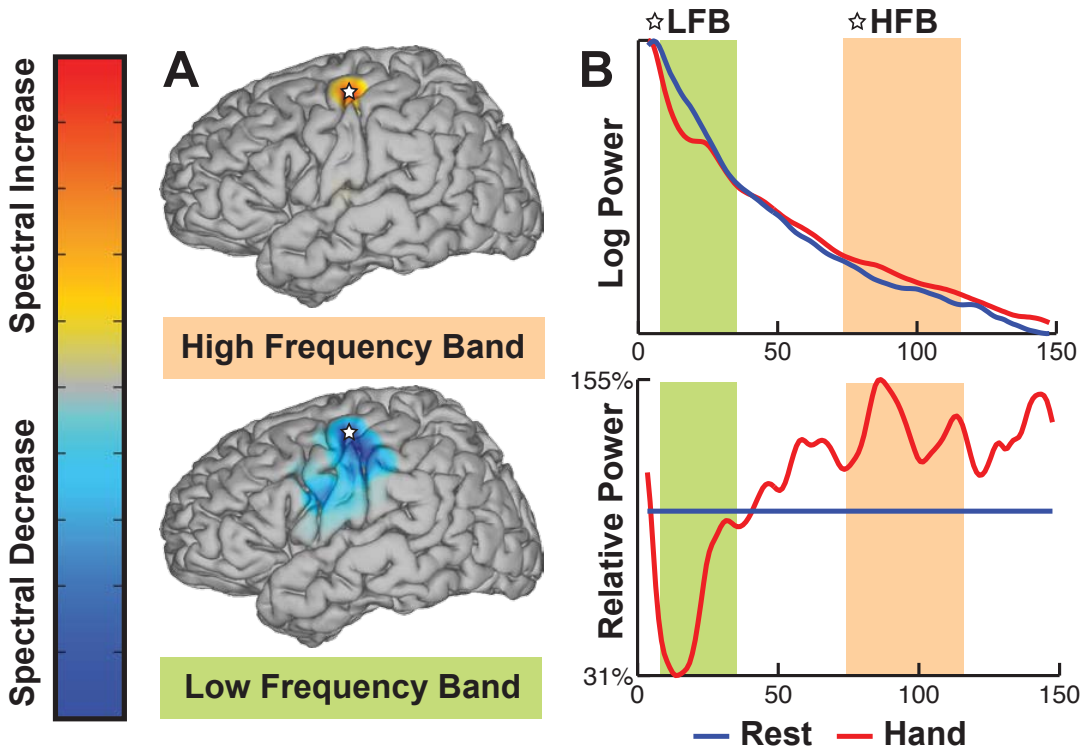

Figure 3.5: **Example for ECoG signal changes between the tasks of repetitively opening and closing of the hand and resting.** (A) Signals in the mu/beta band (5-30 Hz) decrease with the task and are spatially less specific (lower topography), whereas signals in the gamma band (70-116 Hz) increase with the task and are spatially more specific (upper topography). (B) The power spectrum on a logarithmic scale for the electrode marked with a star in the topographies illustrates the spectral decrease in the mu/beta band (marked by the green bar) and spectral increase in the gamma band (orange bar).

We demonstrate here a comprehensive evaluation of a robust, practical, and readily available procedure for presurgical functional mapping of eloquent cortex using subdural electrodes. This procedure is based on our BCI2000 and SIGFRIED (SIGnal modeling For Real-time Identification and Event Detection) technologies. BCI2000 is a general-purpose software platform for real-time biosignal acquisition, processing, and feedback (Mellinger and Schalk, 2007; Schalk et al., 2004) (http://www.bci2000.org). In collaboration with other institutions, most notably the University of Tübingen in Germany, we have been developing BCI2000 for more then ten years. BCI2000 is currently in use by more than 1000 laboratories world-wide for a variety of studies. It supports more than 35 different signal acquisition devices and can thus be readily integrated in different

research or clinical environments. SIGFRIED (Schalk et al., 2008a,b) is a signal processing procedure that I implemented within BCI2000 as part of this dissertation to detect and visualize task-related changes in real time without prior parameterization (e.g., of frequency bands, visualization parameters, etc.) by an expert.

In this thesis, I demonstrate the use of the SIGFRIED/BCI2000 system for delineating cortical areas related to tongue and hand motor function in ten patients from four institutions. The results show that this method can provide a functional map within only a few minutes and that this map is in strong congruence to that derived by ECS mapping. Furthermore, they demonstrate that this technique provides robust and practical mapping capabilities in different clinical environments.

3.3.2 Methods

3.3.2.1 Human Subjects

A total of 10 patients (Table 3.2) at Albany Medical Center (Albany, NY) [AMC1-5], Barnes-Jewish Hospital (St. Louis, MO) [BJH1], Middleton Memorial Veterans Hospital (Madison, WI) [VAH1-2] and University Medical Center Utrecht (Utrecht, The Netherlands) [UMC1-2] were implanted with subdural platinum electrodes arrays (4 mm diameter, 2.3 mm exposed, 1 cm inter-electrode spacing, Ad-Tech, Racine, WI) for a period of 5-12 days prior to resection of a seizure focus. In each patient, the seizure focus was identified by neurologists using visual inspection, and eloquent cortex was identified over a period of 1.5-7.5 hours using electrical cortical stimulation (ECS). For the majority of patients, this stimulation was not completed, thereby leaving 12% to 74% of the covered cortex without stimulation results. Grid locations were classified as hand or tongue function if stimulation (typically 1 to 4 mA) elicited or inhibited motor activity or sensation. Some of the contacts were not stimulated for different reasons: (1) they had no relevance to the surgical procedure, i.e., they were sufficiently distant to any planned resection; (2) the minimum stimulation current (e.g., 4 mA) could not be reached without inducing pain; (3) stimulation induced a seizure before any response was detected; (4) time constraints; (5) stimulation induced global after-discharges. The locations of the seizure foci and eloquent cortex were subsequently used for planning of surgical resection. Location and duration of the implantation were solely determined by clinical criteria and only patients with some peri-rolandic coverage were included in the study. All patients gave informed consent through a protocol reviewed and approved by each of the participating institution's review board.

3.3.2.2 Data Collection

During the monitoring period, we recorded ECoG signals at the bedside from 32-128 contacts of the implanted grids using different biosignal acquisition devices (Table 3.3). Scalp or grid electrodes were used for reference and ground. Data collection and stimulus presentation was accomplished using BCI2000 (Schalk et al., 2004) software, a general-purpose system for real-time biosignal acquisition, processing and feedback. Real-time signal processing and visualization was performed using the SIGFRIED method (Schalk et al., 2008a,b) implemented within BCI2000.

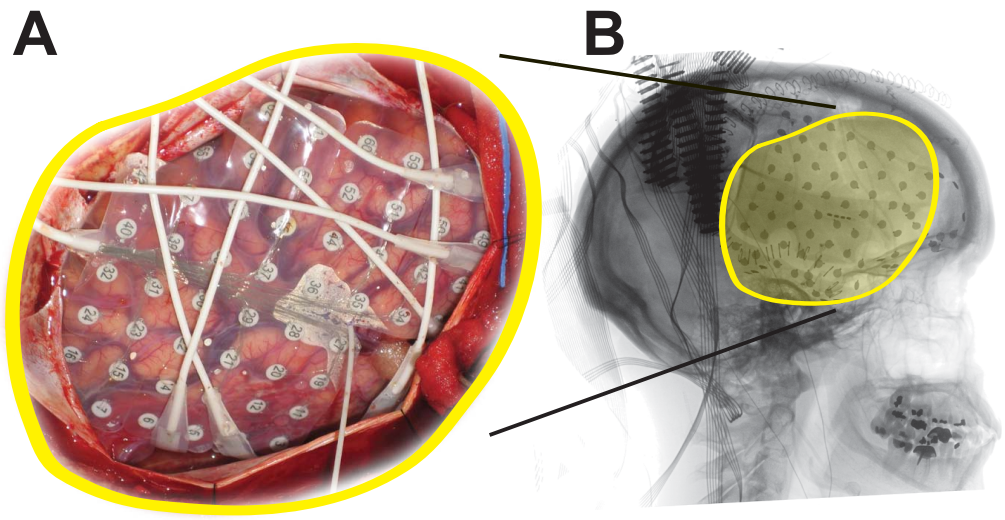

Figure 3.6: **Example of an implanted subdural grid in patient AMC3.** (A) Subdural grid placed over fronto-parietal areas. (B) Lateral radiograph indicating the position of the grid.

Table 3.2: **Patient characteristics.**

Subject	Age	Handedness	Gender	Hemispheric dominance for language (IAP)	Full scale IQ	Surgery hemisphere	Simulation duration	Fraction of electrodes stimulated
AMC1	19	right	male	N/A[a]	N/A[b]	left	5 hours	100% (48/48)
AMC2	61	right	female	left	95	left	5 hours	71% (52/77)
AMC3	32	right	female	left	99	right	4 hours	40% (24/48)
AMC4	29	right	male	left	94	right	3 hours	100% (84/84)
AMC5	50	right	male	bilateral	109	right	2 hours	43% (36/83)
VAH1	62	right	male	left	N/A[c]	right	1.5 hours	70% (45/64)
VAH2	36	right	male	left	N/A[d]	right	2.5 hours	26% (26/128)
UMC1	28	right	male	left	92	left	4.5 hours	93% (112/120)
UMC2	27	right	female	left	69	left	7.5 hours	69% (72/112)
BJH1	44	left	female	bilateral	95	left	1.5 hours	88% (56/64)

Note:
[a] IAP was not administered.
[b] IQ was not tested; patient completed 12 years of education.
[c] IQ was not tested; information about education not available.
[d] IQ was not tested; patient completed 13 years of education.

3.3.2.3 Experimental Protocol

We first recorded 6 minutes of baseline data during which the subject was asked to remain relaxed and to avoid any movements. Then, each subject performed alternating sequences of repetitive movements of the tongue, i.e., protrusion and retracting of the tongue, movements of the hand, i.e., opening and closing of the hand contralateral to the side of the grid placement, and resting. The subject was visually cued by the words "tongue" or "hand," which were presented on a computer screen (a blank screen indicated the resting period). Each task was performed for a duration of 3 seconds (15 seconds for subject UMC1) at a self-paced rate of about two repetitions per second, followed by a resting period of the same duration (Fig. 3.7) before the next task. One run consisted of 15 repetitions of this sequence over the course of 180 seconds. We typically recorded one initial run to familiarize the subject with the task. All analyses in this thesis are for one run following the initial training run. The visual display to the investigator during online operation of this run was provided as described below.

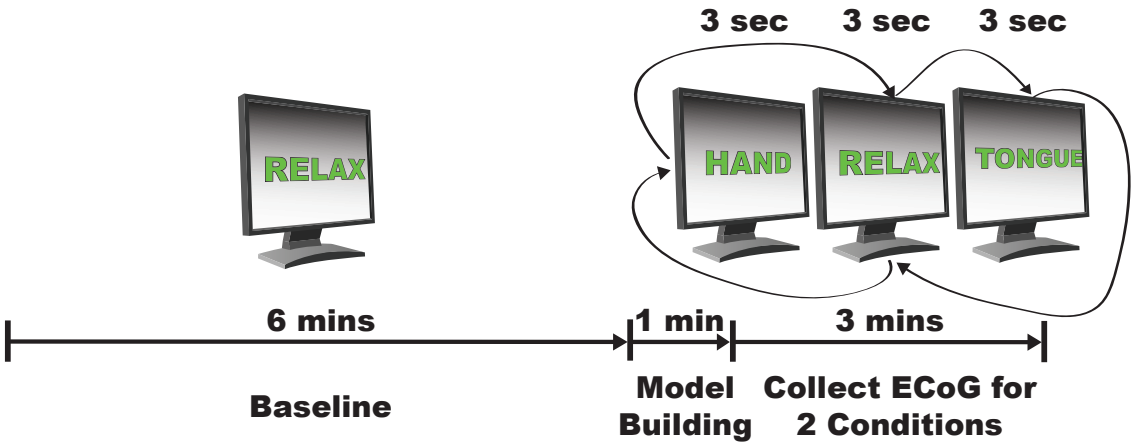

Figure 3.7: **SIGFRIED-based mapping procedure:** After an initial 6 min baseline period, an automated routine generates a statistical signal model for that baseline period for each electrode (this automated procedure takes less than one min). The subject then alternated between hand and tongue movement tasks interspersed with rest periods.

Table 3.3: **Signal Recording Properties**

Subject	Channels	Sampling	Filter	Update Rate
AMC1	32	256 Hz	0.1 Hz	32 Hz
AMC2	32	256 Hz	0.1 Hz	32 Hz
AMC3	32	1200 Hz	0.1 Hz	30 Hz
AMC4	32	1200 Hz	0.1 Hz	30 Hz
AMC5	64	1200 Hz	0.01 Hz	15 Hz
VAH1	32	1061 Hz	3-512 Hz	35 Hz
VAH2	64	1061 Hz	3-512 Hz	35 Hz
UMC1	128	512 Hz	0.15-134.4 Hz	16 Hz
UMC1	128	512 Hz	0.15-134.4 Hz	16 Hz
BJH1	64	1200 Hz	0.1 Hz	30 Hz

3.3.2.4 Signal Analysis

To provide a basis for real-time feedback, we first used the SIGFRIED procedure (Schalk et al., 2008a,b) to establish a statistical model of the recorded baseline data. While the subject executed the task, we then used this procedure to identify in real-time those grid contacts that showed activity changes that were statistically different from the baseline model. In short, we used the following signal preprocessing, feature extraction and feature selection configurations: first, the signal from each grid contact was re-referenced using a common average reference (CAR) filter (McFarland et al., 1997). Then, for each grid contact and 500 ms time period, the time series ECoG signal was converted into the frequency domain using an autoregressive model (Burg, 1968, 1972; Childers, 1978) with a model order of 1/10th of the sampling rate. Frequencies between 70-100 Hz (ten bins at 4 Hz bandwidth) were submitted to SIGFRIED. During online processing, SIGFRIED then utilized the established baseline model to calculate for each grid contact the likelihood that the signal at that grid contact was statistically different from the modeled baseline signals. This likelihood was calculated every 28.27 to 66.66 ms (see Table 3.2).

Fig. 3.8 illustrates time courses of the negative log-transformed likelihood values for two locations recorded from subject VAH2. The upper trace corresponds to the location marked with a star in Fig. 3.11. The bottom trace corresponds to the location marked with a rectangle. The times of cue presentation for hand movements are marked with yellow bars and for tongue movements with red bars. Interleaved rest periods are shown in white. The SIGFRIED trace in the upper figure detects hand movements but not tongue movements, whereas the bottom trace detects tongue but not hand movements.

Finally, for each grid contact and task, the distribution of the negative log-transformed

likelihood values was further re-referenced to those values calculated during the resting period between the tasks by calculating the value of r^2, i.e., the proportion of values that was accounted for by the task. This resulted in a value between 0 (not different) and 1 (very different) for each grid contact and task.

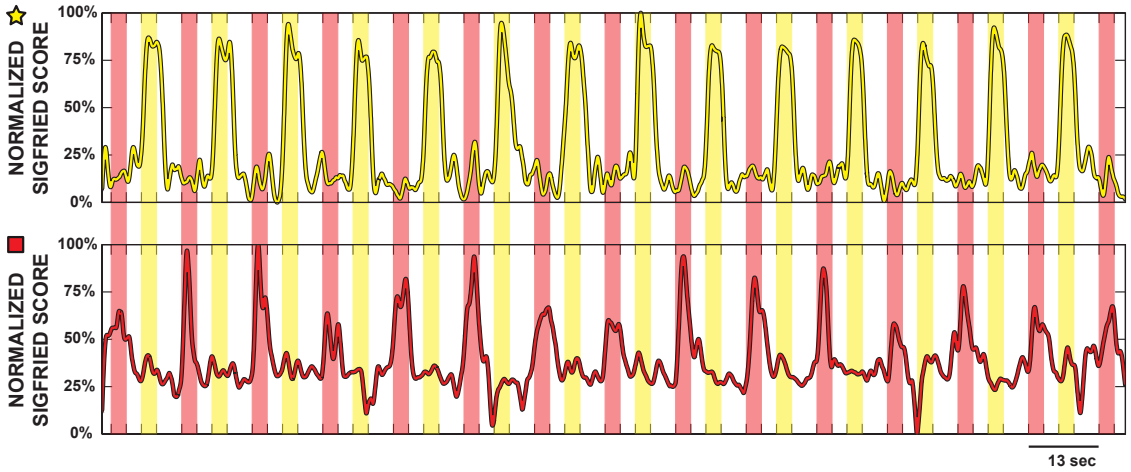

Figure 3.8: **Output of the SIGFRIED procedure for two locations recorded from subject VAH2.** Locations for hand (top) and tongue (bottom) electrode are each marked in Fig. 3.11 by a star and rectangle, respectively.

3.3.2.5 Interface to the Investigator

The results from the signal analyses described above were presented to the investigator in real time using a topographic interface (Fig. 3.9). The interface contained, for each task (i.e., hand or tongue), a display of the r^2 values at each location. Each display contained one circle at each electrode's location. The size of each circle and its tint was proportional to the r^2 value. Thus, a large red circle represented a large statistical difference between the corresponding task and rest, while a small black circle indicated a small statistical difference. The display corresponding to each task was autoscaled to the minimum and maximum r^2 value. Thus, no parameter (e.g., frequency range, display or detection parameters, etc.) needed to be changed by the investigator prior to or during system operation.

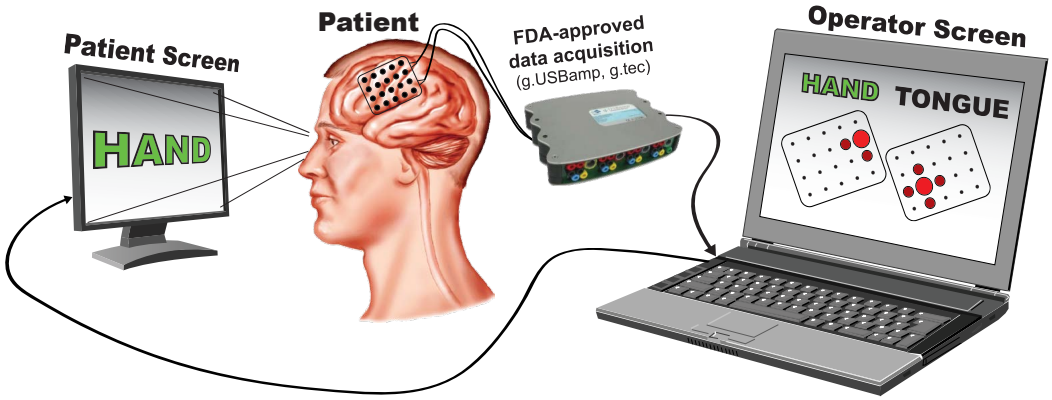

Figure 3.9: **Equipment setup and interface to the investigator.** The subject is presented with visual cues shown on a computer monitor while electrocorticographic signals are recorded. Both the patient screen and the data acquisition device are interfaced with a laptop computer running BCI2000. BCI2000 acquires signals from the device, submits these signals in real time to the SIGFRIED method, and presents the results visually in a topographical display to the investigator.

3.3.3 Results

3.3.3.1 Qualitative Results

The following paragraphs present the results derived using the SIGFRIED mapping procedure, and qualitatively and quantitatively compare the results to those obtained with ECS mapping.

The main results are shown for all subjects in Fig. 3.10 and 3.11. In each figure, the lateral radiographs (all subjects except UMC1 and UMC2) or computer tomography (CT) images (UMC1 and UMC2) on the left show grid contacts marked by colored circles. Contacts that were stimulated and identified as eloquent cortex associated with hand function are shown in yellow, those associated with tongue function are shown in red, and those associated with neither hand nor tongue function are shown in white. Semi-transparent white circles indicate locations that were not stimulated.

The four detailed lateral radiographs/CT images on the right show the results of the SIGFRIED mapping procedure derived after 30, 60, 120 and 180 seconds. Similarly to the ECS results shown on the very left, yellow circles indicate the results for the hand task, and red circles indicate the results for the tongue task. Locations that were excluded (e.g., due to broken connectors) or not recorded (e.g., due to limitation in the number of channels) are left blank. The final maximum r^2 (i.e., the value of r^2 of the largest circle in each figure) after 180 seconds is noted on the right for hand (range 0.05 to 0.61) and tongue (range 0.10 to 0.51).

3.3.3.2 Quantitative Results

The results in Fig. 3.10 and 3.11 show substantial agreement to those derived using electrical stimulation. In addition, we assessed these results using two quantitative comparisons. For both comparisons of tongue and hand, the r^2 values at each location were classified as eloquent or non-eloquent with a threshold that was derived using Minimum Bayesian Error (Berger, 1985).

The first comparison in Table 3.4 provides a quantitative analysis for the 18 to 77 contacts that were both stimulated by ECS and mapped with SIGFRIED. This comparison was done independently for hand and tongue and resulted in a correct or incorrect match between ECS and SIGFRIED at each location. The incorrect results were further classified into false positives, i.e., contacts identified by SIGFRIED but not by ECS, and false negatives, i.e., contacts identified by ECS but not by SIGFRIED. Table 3.4 shows that there were more false positives than false negatives. For three subjects (AMC1, VAH1 and VAH2), no false negatives for hand and tongue were identified. We hypothesized that most of the incorrect results would have been correct if they had been derived for a next neighbor. Table 3.5 shows the results of the corresponding analysis. While this analysis effectively corresponds to a reduction in the resolution of the mapping, this procedure resulted in no false negatives, and only in 0.46% and 1.10% false positives for hand and tongue maps, respectively.

Table 3.4: **Quantitative results.** Highest squared correlation (r^2) between the task and the SIGFRIED output and Minimum Bayesian Error between the results of the electrical cortical stimulation and the SIGFRIED mapping.

	HAND			TONGUE		
subject	r^2	false positive	false negative	r^2	false positive	false negative
AMC1	0.40	0.00%	0.00%	0.51	12.50%	0.00%
AMC2	0.21	4.17%	4.17%	0.49	12.50%	12.50%
AMC3	N/A[a]	N/A[a]	N/A[a]	0.37	16.67%	11.11%
AMC4	0.38	0.00%	0.00%	0.46	4.00%	12.00%
AMC5	0.15	0.00%	0.00%	0.10	0.00%	3.70%
VAH1	0.07	10.35%	0.00%	0.14	10.35%	0.00%
VAH2	0.61	3.57%	0.00%	0.37	3.57%	0.00%
UMC1	0.18	3.33%	1.67%	0.11	10.00%	1.67%
UMC2	0.25	3.75%	2.50%	0.48	10.00%	1.25%
BJH1	0.30	3.57%	1.79%	0.31	10.71%	0.00%
average	0.26	3.19%	1.12%	0.33	9.03%	4.22%

Note:
[a] The electrical cortical stimulation resulted in no hand hits for subject AMC3.

Table 3.5: **Quantitative results in a next-neighbor comparison.** Highest squared correlation (r^2) between the task and the SIGFRIED output and Minimum Bayesian Error between the results of the electrical cortical stimulation and the SIGFRIED mapping in a next-neighbor comparison.

	HAND			TONGUE		
subject	r^2	false positive	false negative	r^2	false positive	false negative
AMC1	0.40	0.00%	0.00%	0.51	0.00%	0.00%
AMC2	0.21	4.17%	0.00%	0.49	4.17%	0.00%
AMC3	N/A[a]	N/A[a]	N/A[a]	0.37	5.56%	0.00%
AMC4	0.38	0.00%	0.00%	0.46	0.00%	0.00%
AMC5	0.15	0.00%	0.00%	0.10	0.00%	0.00%
VAH1	0.07	0.00%	0.00%	0.14	0.00%	0.00%
VAH2	0.61	0.00%	0.00%	0.37	0.00%	0.00%
UMC1	0.18	0.00%	0.00%	0.11	0.00%	0.00%
UMC2	0.25	0.00%	0.00%	0.48	1.25%	0.00%
BJH1	0.30	0.00%	0.00%	0.31	0.00%	0.00%
average	0.26	0.46%	0.00%	0.33	1.10%	0.00%

Note:
[a] The electrical cortical stimulation resulted in no hand hits for subject AMC3.

3.3.4 Discussion

We provide the first comprehensive demonstration of a functional mapping procedure that is rapid, practical, robust, and accurate in localizing primary motor cortex. In our evaluation of ten patients from four institutions, we found that the SIGFRIED procedure identifies at least the same contacts or their immediate neighbors compared to ECS mapping.

These results may have important implications for functional localization prior to invasive brain surgery. Our method can be used with little training and can be readily implemented in the typical clinical environment. In fact, our system is currently in evaluation by a number of epilepsy centers in the US and Europe. Thus, we believe that the SIGFRIED/BCI2000 system has the potential for widespread adoption in a large number of centers world-wide. At the same time, this new mapping platform is opening up several important research questions: e.g., which tasks are best suited to elicit appropriate responses for different classes of anatomical areas? What are the situations or populations (e.g., children) for which this method provides the maximum benefit? What is the efficacy of the SIGFRIED method for other brain functions, in particular for mapping expressive and receptive language? (Ongoing work in our laboratory is providing encouraging evidence in this regard.) It is at present also unclear how this method will be integrated in the clinical workflow. Despite the strong congruence of the SIGFRIED-based results to ECS-based results, it is likely premature to replace ECS mapping with SIGFRIED-based mapping. Rather, it seems to be more appropriate to optimize ECS mapping based on the results of prior SIGFRIED mapping.

Like the recent study by Miller et al. (Miller et al., 2007b), our study demonstrates considerable variance in the somatotopy across subjects and coherence with the ECS mapping results. Both location and area identified as eloquent cortex vary among subjects. While for Miller et al. it was not clear whether this was due to subject variability or expert variability in performing the ECS, our study shows that a next-neighbor analysis achieves an almost perfect coherence with the ECS mapping results. This suggests that most of the variance is due to expert variability.

Crone et al. (Crone et al., 1998a) reported that not all subjects displayed changes in the gamma band. This is in contrast to the results of this study that showed adequate task-related changes of gamma amplitudes (which were the basis for the SIGFRIED calculations) in all ten subjects. It is possible that this is due to a difference in hardware, processing, or motor tasks. For example, our own experience, and also results from a previous study (Aoki et al., 1999), suggest that more complex tasks (such as the Rubic's

cube manipulation task) increase the amplitude of the gamma changes.

The SIGFRIED results were generally in substantial agreement to those derived using electrical stimulation, but there were some differences. These differences could be attributed to several factors that include expert variability in ECS mapping or ECS's variable current spread, low statistical significance, or the characteristics of the subject's task. Cortex at remote locations may be activated due to current spread, and thus result in a site that is registered by ECS and not by SIGFRIED. Conversely, SIGFRIED may falsely register sites with low statistical significance. For example, consider the map for hand function in subject AMC3 (shown in Fig. 3.10). This subject's grid did not have hand coverage, i.e., ECS mapping did not detect hand function in any electrode. The SIGFRIED map highlights several sites, although the maximum r^2 value (0.05) was very low. Thus, the magnitude of the maximum r^2 value gives an index of confidence in a particular map. Future versions of the software could even calculate such a confidence index (i.e., a p-value) explicitly. The factor that may have the largest influence on the differences between the ECS and the SIGFRIED maps may be the nature of the subject's task. In one extreme, this task would be very simple, and only require very limited areas of cortex for its execution. In this case, SIGFRIED would only register very few electrodes or none at all. In the other extreme, the subject's task would be difficult and require engagement of different cortical facilities. Thus, the use of this task would result in activation of more widespread areas of cortex, and consequently, SIGFRIED would detect changes in more electrodes. As described above, recent experiments suggest that the use of more complex visuomotor tasks results in even more robust maps. In sum, the optimal tasks for mapping motor and other cortices using the SIGFRIED method are currently unknown. However, the rapidity of our method facilitates the use of several tasks that engage the desired cortical area in different ways.

The SIGFRIED mapping overcomes many problems associated with ECS. It is also based on a different principle. While ECS is based on a lesional model (Engel, 1993), SIGFRIED is based on task-related changes in ECoG signals. The clinical impact of this difference is currently unclear. It is thought that the lesional model utilized with ECS closely resembles the effect of surgical resection, in that it allows the identification of those areas that are critical for a particular function. In contrast, SIGFRIED detects those areas that change their activity with a particular task. It may not detect areas that do not change their activity but are critical for a particular function, or may detect areas that change their activity but are not critical. At the same time, ECS clearly has problems of accuracy itself, e.g., because there is no defined standard for ECS mapping,

because there are practical (in particular time) constraints for using ECS, and because the resolution of ECS is limited due to current spread and the need for bipolar stimulation. In summary, at this early stage of clinical validation, replacing ECS with the SIGFRIED/BCI2000 system is not warranted. Nevertheless, despite its potential limitations, there may already be distinct advantages over ECS mapping.

The ECS protocol labels each contact with the eloquent function that is elicited or inhibited as the contact is stimulated. Finding eloquent function at a low threshold terminates the protocol for this contact, assuming that each type eloquent function is spatially contiguous as it is suggested by the motor homunculus model (Penfield and Rasmussen, 1950). Recent fMRI (Meier et al., 2008) and ECS (Hamberger, 2007) studies, however, show a more complex and spatially noncontiguous somatotopy. The SIGFRIED mapping could establish a comparable somatotopy by exploring different tasks, for example a dedicated motor/sensory evaluation for each finger. This could allow more detailed surgical planning and thus benefit the outcome of the resection procedure. However, the lack of a verifiable gold standard makes it difficult to assess the quality of such a more detailed somatotopy. Only surgical outcome can provide a detailed assessment on whether a more detailed somatotopy may be beneficial.

Studies have shown task-related changes associated with ipsilateral movements in the low frequency band (Chollet et al., 1991; Colebatch et al., 1991; Grafton et al., 1992; Kawashima et al., 1994, 1993; Kim et al., 1993; Wisneski et al., 2008; Yoshii et al., 1989). The implications of resecting cortical areas associated with these ipsilateral movements have not been defined, mainly because ECS is not able to elicit ipsilateral limb movement within the conventional stimulation thresholds (Foerster, 1936; Penfield and Boldrey, 1937). The SIGFRIED mapping could facilitate such studies by exploring ipsilateral tasks.

An initial application of the SIGFRIED/BCI2000 system is shown here, but there are several ways in which this system can be further improved. As a first example of the potential for improvement, we observed a noticeable delay between stimulus onset and the patient's response even when there was good compliance of the subject. Crone et al. also reported such delays, and estimated them to be in the 300-400 ms range for simple visually cued hand movements and tongue protrusions (Crone et al., 1998a). Our results show similar delays (see Fig. 3.8). Because the total duration of each stimulus was only 3 sec (15 sec for subject UMC1), a significant fraction of the signals were thus effectively assigned to the incorrect task category. In more recent experiments, we have begun to alert the subject to the change in condition by presenting an auditory stimulus,

and we suspend data analysis for 1 sec. In the end, it may be possible to partially or even completely eliminate this need for patient compliance, which is currently an issue for all mapping techniques. For example, for motor tasks it would be relatively straightforward to utilize motion sensors, such as a data glove, motion capture device, or EMG electrodes, and to simply correlate SIGFRIED values with the detected motion rather than with the stimulus. For sensory input, it would be possible to use programmable tactile stimulators and earphones. Thus, such approaches may fully remove the requirement for patient compliance and facilitate mapping in pediatric environments where patient compliance is either impossible (e.g., with infants) or hard to obtain (e.g., with young children). As another example for potential further improvements, it may be possible to use the SIGFRIED mapping intraoperatively. This possibility could replace the two surgeries that are currently necessary with one surgery that encompasses grid placement, mapping of eloquent cortex, and resection. In particular in patients that do not require longer monitoring periods (e.g., tumor patients), this would significantly decrease risks to the patient and costs of the hospitalization.

3.3.5 Conclusions

In conclusion, in this section we presented the SIGFRIED/BCI2000 system as a practical functional mapping procedure. This system is readily available at no cost for research and educational purposes at www.bci2000.org, and there is substantial documentation on its theory (Mellinger and Schalk, 2007; Schalk et al., 2008a,b, 2004) and use (doc.bci2000.org). BCI2000 currently supports signal acquisition from 35 different devices, and more are continually added. This should facilitate the integration in existing clinical environments.

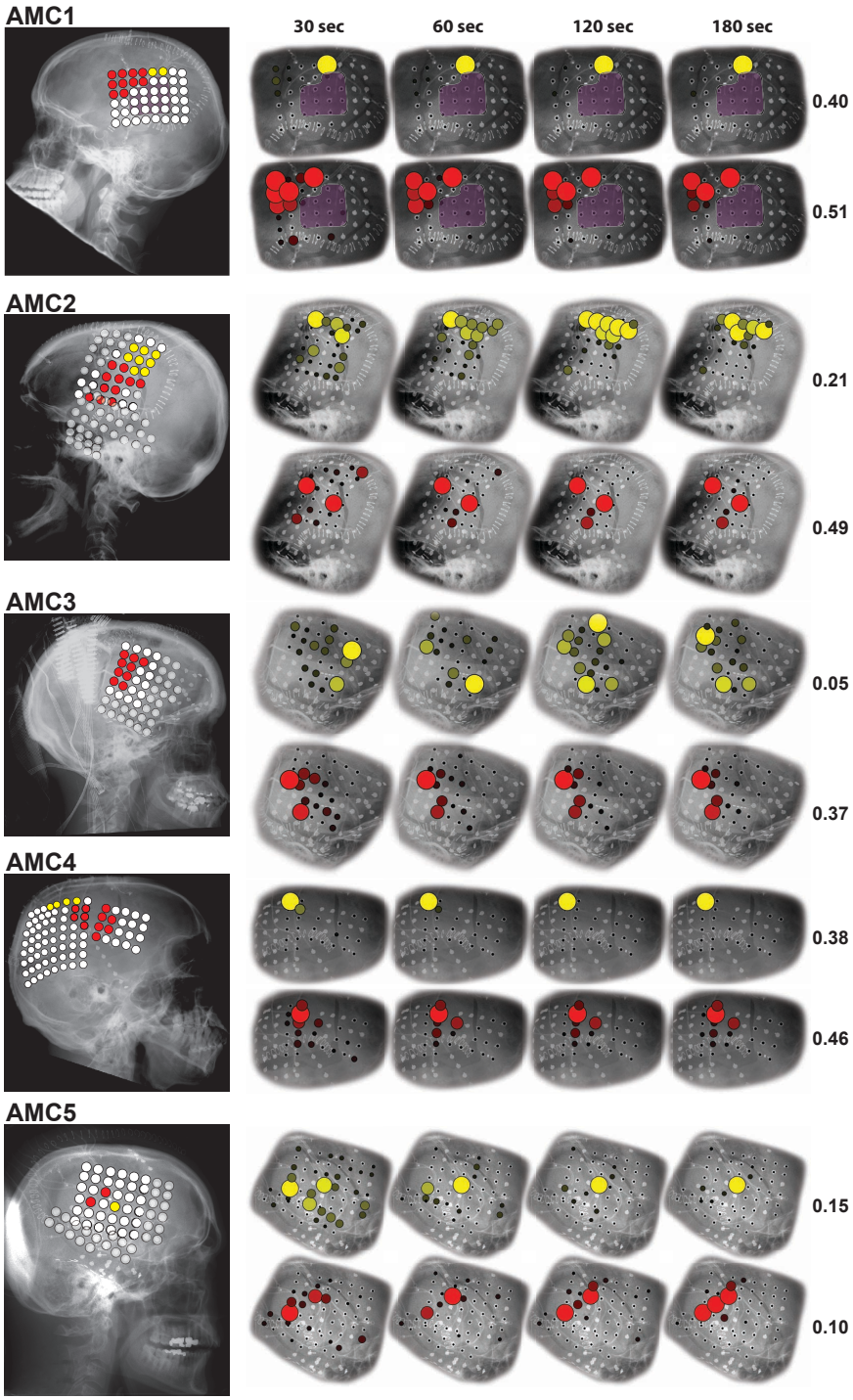

Figure 3.10: **Results of electrical cortical stimulation (left) and the passive functional mapping using SIGFRIED (right) for subjects AMC1 to AMC5.** Lateral radiographs (left) show the results of the electrical cortical stimulation for hand (yellow) and tongue (red) and no response to hand or tongue (white). Transparent circles indicate no stimulation. Detailed lateral radiographs (right) show the result of the passive functional mapping using SIGFRIED after 30, 60, 120 and 180 seconds for hand (yellow) and tongue (red). The number indicates the final maximum r^2 between the stimulus and the SIGFRIED response (0 to 1).

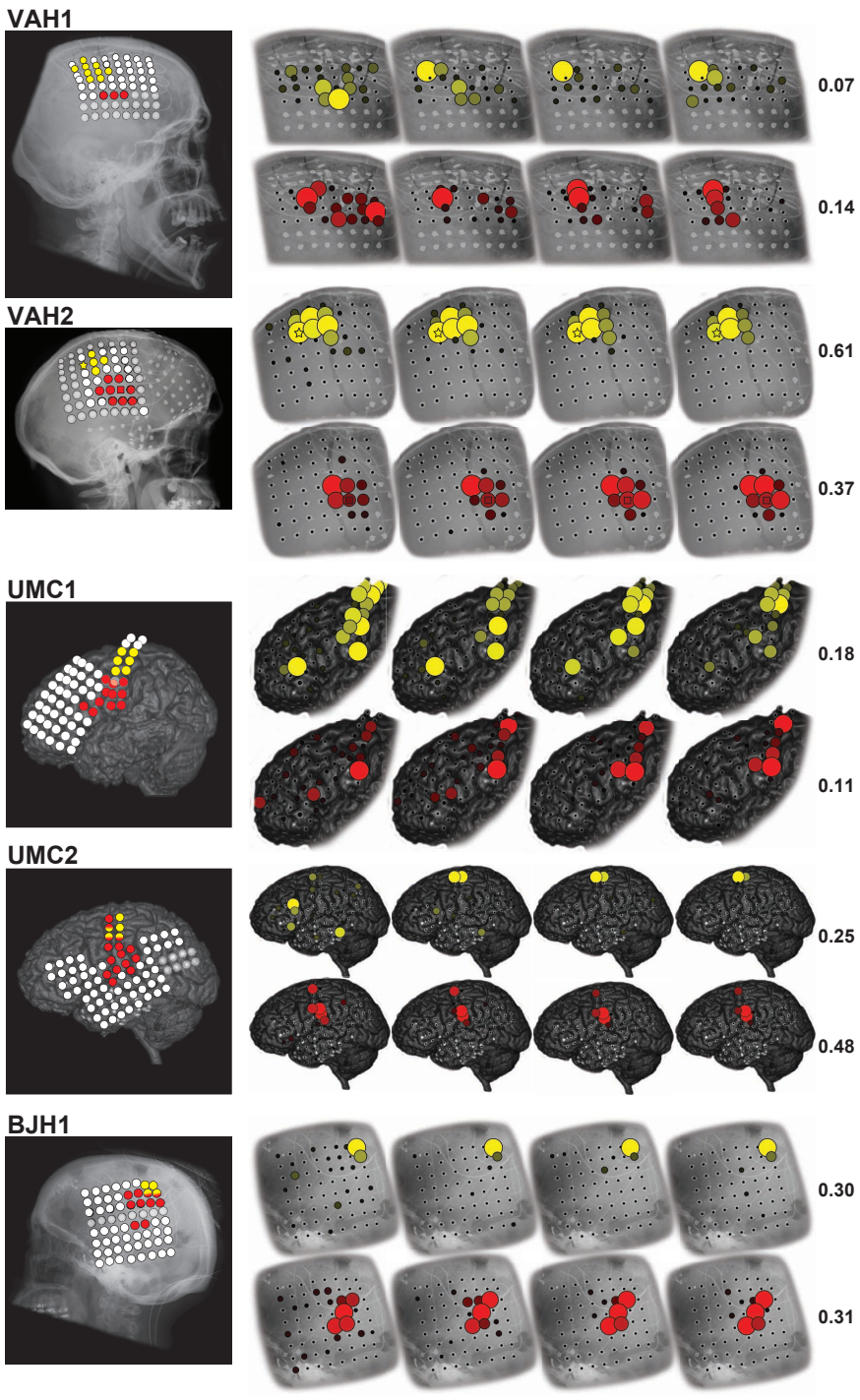

Figure 3.11: **Results of electrical cortical stimulation (left) and the passive functional mapping using SIGFRIED (right) for subjects VAH1, VAH2, UMC1, UMC2 and BJH1.** Lateral radiographs or computer tomographic renderings (left) show the results of the electrical cortical stimulation for hand (yellow) and tongue (red) and no response to hand or tongue (white). Transparent circles indicate no stimulation. Detailed lateral radiographs (right) show the result of the passive functional mapping using SIGFRIED after 30, 60, 120 and 180 seconds for hand (yellow) and tongue (red). The number indicates the final maximum r^2 between the stimulus and the SIGFRIED response (0 to 1). The real-time SIGFRIED traces in Fig.3.8 are for the locations marked by a yellow star and red rectangle in subject VAH2, respectively.

4 Conclusion and Future Work

4.1 Conclusion

In this dissertation, we set out to identify and overcome some important deficiencies that currently limit the utility of emerging clinical applications for communication and diagnosis. Specifically, we identified low communication performance and the dependency on experts and post-hoc analysis for diagnosis of eloquent cortex as two important deficiencies. To overcome these, we hypothesized that ECoG signals could support higher communication performance in the BCI context and that generative models could eliminate the need for experts and post-hoc analysis in clinical diagnosis.

To test our hypotheses, we conducted two studies. The first study used ECoG signals and external stimuli to provide BCI communication. In this study, we showed that our BCI system could provide a sustained communication rate of 17 characters per minute (69 bits/min), which is 3-4 times higher than what had previously been reported.

The second study was the development and validation of a diagnostic tool that used ECoG and generative models to passively map eloquent cortex. In this study, we showed that this system did not need experts or post-hoc analysis to provide maps of eloquent cortex that were in general alignment with those obtained from the current gold standard.

While the results of these two studies unequivocally support our hypotheses, they also raised questions. For example, the results suggest that ERPs over visual areas (VEPs) contribute significantly to the performance of the BCI communication system. This is of critical relevance to clinical application of this BCI method, because the target population may be impaired in their ability to fixate on the target and thus to generate

VEPs. This raised the question whether the performance of the matrix speller BCI depends on fixating the target. In response to this issue, we conducted a follow-up study that disproved the widespread assumption that the performance of the matrix speller BCI does not depend on fixating the target. While this finding effectively limits the utility of increased spelling performance to people that that are able to fixate on the target, our study created an awareness on this dependency and sparked scientific interest to develop exogenous BCI systems that do not depend on eye-gaze. As a result, recent studies proposed exogenous BCI systems that use auditory (Klobassa et al. 2009; Kübler et al. 2009; Schreuder et al. 2010), tactile (Brouwer and van Erp 2010), or simplified visual stimuli (Acqualagna et al. 2010; Treder et al. 2011; Treder and Blankertz 2010; Treder et al. 2010).

4.2 Future Work

Other questions go beyond the scope of this dissertation and require future work. For example, this dissertation has shown that, despite the 3 to 4 fold improvement in communication performance, it remains unclear whether clinical BCI systems will ever be a viable alternative to other established (i.e., muscle-based) and emerging (e.g., bionic) assistive communication devices that tend to provide a better communication performance (e.g., MyTobii P10 eye-tracker system, 10 words per minute at close to 100% accuracy). This is because the communication performance of BCIs is limited to the speed in which the user can re-locate his attention and/or sensory input towards the next intended target, and the number of targets the user can simultaneously pursue. While there is evidence that in endogenous BCIs users may pursue multiple target simultaneously (McFarland et al. 2010b; Taylor et al. 2002), exogenous BCIs are limited through their sensory input (e.g., visual, auditory, tactile) to one simultaneous target. With this restriction, the paradigm presented in this dissertation should be limited to a communication performance that is only modestly higher than the 22 characters per minute we report here. If clinical BCI systems are to become widely used, they need to either improve on their performance or complement established and emerging assistive devices. Hybrid BCIs, i.e., the combination of a BCI with other BCIs or existing assistive systems, follow a current trend that addresses this issue (Allison et al. 2010; Millán et al. 2010; Pfurtscheller et al. 2010; Zander et al. 2010). Future work could investigate how the BCI presented in this dissertation could benefit from such hybridization.

More questions also arise from our results on passive mapping of eloquent cortex.

While the developed diagnostic tool overcomes the most critical deficiencies of passive mapping, it does not yet fully encompass all components that are necessary to translate this technique into clinical practice. To facilitate this translation, future work needs to expand on clinical validation and address regulatory certification as well as clinical integration and dissemination.

Another question is whether the developed diagnostic tool fully exploits the potential that passive mapping of eloquent cortex using ECoG offers. For example, the presented technique has not yet exploited the potential to map detailed aspects of behavior at very high spatial resolution and without the patient's compliance. In future work, a combination of higher resolution ECoG grids (e.g., Fig. 4.1) and more advanced tasks that engage the subject in more detailed aspects of behavior could improve the delineation of eloquent cortex. Further, the integration of behavioral sensors could remove the requirement for patient compliance and facilitate mapping in pediatric environments where patient compliance is either impossible (e.g., with infants) or hard to obtain (e.g., with young children). Finally, translating the procedure into the operating room could spare the patient a second surgery and reduce morbidity. While some of these aspects have already been investigated by us (Ritaccio et al. 2010; Roland et al. 2010) or others (Cervenka et al. 2011), a system that fully exploits the potential of passive mapping of eloquent cortex has not yet been demonstrated.

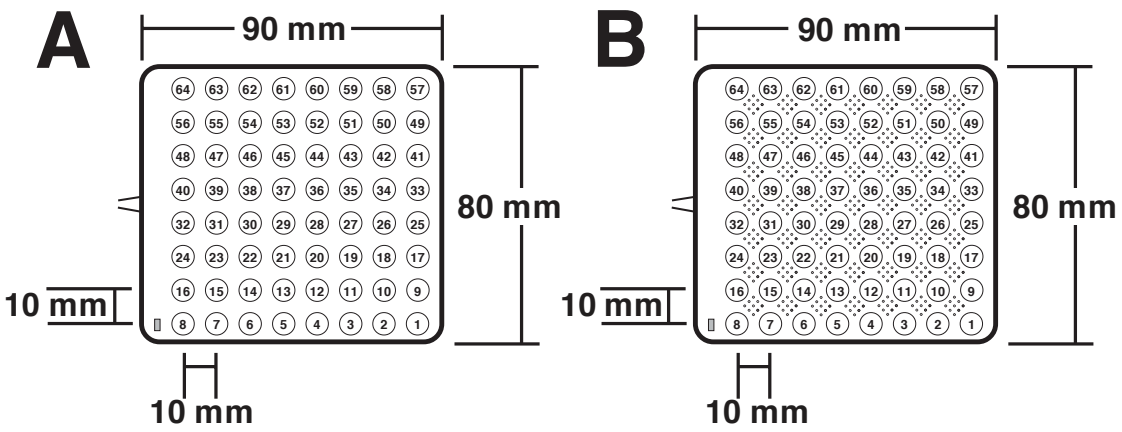

Figure 4.1: **High spatial resolution ECoG grid.** This figure shows how the currently used 1 cm spaced ECoG grid (A) can be translated into an ECoG grid that provides high spatial resolution while remaining its compatibility with ECS (B). This is accomplished by retaining the 2.3 mm exposed contacts of (A) in (B) that still can be used for ECoG while adding additional 1 mm spaced microelectrodes that provide high spatial resolution.

A List of Publications

The publications created during the course of this thesis are grouped by topic and roughly sorted by importance.

A.1 Technology

- P. Brunner, L. Bianchi, C. Guger, F. Cincotti, G. Schalk, Current trends in hardware and software for brain-computer interfaces (BCIs), *Journal of Neural Engineering*, 8(2):025001, 2011.
  (ISI impact factor 3.837)

- A. Ritaccio, M. Beauchamp, C. Bosman, P. Brunner, E. Chang, N. Crone, A. Gunduz, D. Gupta, R. Knight, E. Leuthardt, B. Litt, D. Moran, J. Ojemann, J. Parvizi, N. Ramsey, J. Rieger, J. Viventi, B. Voytek, J. Williams, G. Schalk, Proceedings of the Third International Workshop on Advances in Electrocorticography, *Epilepsy Behav*, 25(4): 605-13, 2012.
  (ISI impact factor 2.335)

- A. Ritaccio, D. Boatman-Reich, P. Brunner, M. C. Cervenka, A. J. Cole, N. Crone, R. Duckrow, A. Korzeniewska, B. Litt, K. J. Miller, D. W. Moran, J. Parvizi, J. Viventi, J. Williams, G. Schalk, Proceedings of the Second International Workshop on Advances in Electrocorticography, *Epilepsy Behav*, 22(4): 641-50, 2011.
  (ISI impact factor 2.335)

- A.L. Ritaccio, P. Brunner, M.C. Cervenka, N. Crone, C. Guger, E. Leuthardt, R. Oostenveld, W. Stacey, G. Schalk, Proceedings of the First International Workshop on Advances in Electrocorticography, *Epilepsy and Behavior*, 19(3):204-215, 2010.
  (ISI impact factor 2.335)

- S.C. Schachter, J. Guttag, S. Schiff, D.L. Schomer, and Summit Contributors (incl. P. Brunner). Advances in the Application of Technology to Epilepsy: The CIMIT/NIO., *Epilepsy and Behavior*, 16(1):3-46, 2009.
  (ISI impact factor 2.335)

A.2 Methods

- G. Schalk, E.C. Leuthardt, P. Brunner, J.G. Ojemann, L.A. Gerhardt, J.R. Wolpaw, Real-time detection of event-related brain activity. *NeuroImage*, 43(2):245-249, 2008.
  (ISI impact factor 5.895)

- G. Schalk, P. Brunner, L.A. Gerhardt, H. Bischof, J.R. Wolpaw, Brain-Computer Interfaces (BCI's): Detection instead of classification. *Journal of Neuroscience Methods*, 167:51-62, 2008.
  (ISI impact factor 1.980)

A.3 Brain Signals for Communication

- P. Brunner, A.L. Ritaccio, J.F. Emrich, H. Bischof, G. Schalk, Rapid Communication With a P300 Matrix Speller Using Electrocorticographic Signals (ECoG), *Frontiers in Neuroscience*, 5:5, 2011.
  (ISI impact factor 3.588)

- P. Brunner, G. Schalk, Toward Gaze-Independent Matrix Speller Brain-Computer Interfaces, *Clinical Neurophysiology*, 124(5):831-3, 2013.
  (ISI impact factor 3.406)

- P. Brunner, G. Schalk, Toward a Gaze-Independent Matrix Speller Brain-Computer Interface, *Clinical Neurophysiology*, 122(6):1063-1064, 2011.
  (ISI impact factor 3.406)

- P. Brunner, S. Joshi, S. Briskin, J.R. Wolpaw, H. Bischof, G. Schalk, Does the P300 Speller Depend on Eye Gaze?, *Journal of Neural Engineering*, 7(5):056013, 2010.
  (ISI impact factor 3.837)

- J. Kubanek, P. Brunner, A. Gunduz, D. Poeppel, G. Schalk, The tracking of speech envelope in the human cortex, *PLoS One*, 8(1):e53398, 2013.
  (ISI impact factor 4.09)

- A. Gunduz, P. Brunner, A. Daitch, E. C. Leuthardt, A. L. Ritaccio, B. Pesaran, G. Schalk, Decoding Covert Spatial Attention Using Electrocorticographic (ECoG) Signals in Humans, *NeuroImage*, 60(4): 2285-93, 2012.
  (ISI impact factor 5.895)

- C. Potes, A. Gunduz, P. Brunner, G. Schalk, Dynamics of Electrocorticographic (ECoG) Activity in Human Temporal and Frontal Cortical Areas During Music Listening, *NeuroImage*, 61(4):841-8, 2012.
  (ISI impact factor 5.895)

- Z. Wang, A. Gunduz, P. Brunner, A. L. Ritaccio, Q. Ji, G. Schalk, Decoding Onset and Direction of Movements Using Electrocorticographic (ECoG) Signals in Humans, *Frontiers in Neuroengineering*, 5:15, 2012.

- J. Hill, P. Brunner, T. Vaughan, Brain-Computer Interaction. Proceedings to the 6th Intl. Conference on Augmented Cognition. In: Foundations of Augmented Cognition. Neuroergonomics and Operational Neuroscience. *Springer Lecture Notes in Computer Science*, 2011.

- A. Gunduz, P. Brunner, A. Daitch, E.C. Leuthardt, A.L. Ritaccio, B. Pesaran, G. Schalk, Neural Correlates of Orienting Attention in Electrocorticographic (ECoG) Signals in Humans, *Frontiers in Human Neuroscience*, 5:89, 2011.
  (ISI impact factor 2.339)

- D.S. Klobassa, T.M. Vaughan, P. Brunner, N.E. Schwartz, J.R. Wolpaw, C. Neuper, E.W. Sellers, Toward A High-Throughput Auditory P300-based Brain-Computer Interface. *Clinical Neurophysiology*, 120(7):1252-1261, 2009.
  (ISI impact factor 3.406)

- E.V. Friedrich, D.J. McFarland, C. Neuper, T.M. Vaughan, P. Brunner, J.R. Wolpaw, A scanning protocol for a sensorimotor rhythm-based brain-computer interface. *Biological Psychology*, 80(2):169-175, 2009.
  (ISI impact factor 3.225)

A.4 Brain Signals for Diagnosis

- P. Brunner, A.L. Ritaccio, T.M. Lynch, J.F. Emrich, J.A. Wilson, J.C. Williams, E.J. Aarnoutse, N.F. Ramsey, E.C. Leuthardt, H. Bischof, G. Schalk, A Practical Procedure for Real-Time Functional Mapping of Eloquent Cortex Using Electrocorticographic Signals in Humans. *Epilepsy and Behavior*, 15(3):278-286, 2009.
  (ISI impact factor 2.335)

- P. Brunner, G. Schalk, Brain-Computer Interaction. Proceedings to the 5th Intl. Conference on Augmented Cognition. In: Foundations of Augmented Cognition. Neuroergonomics and Operational Neuroscience. *Springer Lecture Notes in Computer Science*, 5638:719-723, 2009.

- N.J. Hill, D. Gupta, P. Brunner, A. Gunduz, M.A. Adamo, A.L. Ritaccio, G. Schalk, Recording Human Electrocorticographic (ECoG) Signals for Neuroscientific Research and Real-time Functional Cortical Mapping, Journal of Visualized Experiments, *Journal of Visualized Experiments*, e39930, 2012.

- J. Roland, J. Johnston, P. Brunner, G. Schalk, E.C. Leuthardt, Passive Real-Time Identification of Speech and Motor Cortex during an Awake Craniotomy, *Epilepsy and Behavior*, 18(1-2):123-128, 2010.
  (ISI impact factor 2.335)

- X. Pei, E.C. Leuthardt, P. Brunner, J.R. Wolpaw, G. Schalk, Spatiotemporal Dynamics of ECoG Activity Related to Language Processing, *NeuroImage*, 54(4):2960-2972, 2011.
  (ISI impact factor 5.895)

B

Acronyms and Symbols

List of Acronyms

AIC	Akaike Information Criteria
ALS	Amyotrophic Lateral Sclerosis
AugCog	Augmented Cognition
BCI	Brain-Computer Interface
BIC	Bayesian Information Criteria
CAIC	Consistent Akaike Information Criterion
CAICF	Corrected Akaike Information Criterion
CAR	Common Average Reference
CE	European Commission
CEM	Classification-Expectation-Maximization
CNS	Central Nervous System
CSTP	Common Spatio-Temporal Patterns
ECoG	Electrocorticography
ECS	Electrical Cortical Stimulation
eECoG	Epidural Electrocorticography
EEG	Electroencephalography
EM	Expectation-Maximization
EP	Evoked Potential
ERD	Event-RelatedÊDesynchronization
ERP	Event-Related Potentials
ERS	Event-Related Synchronization

FDA	Food and Drug Administration
FFT	Fast Fourier Transform
fMRI	Functional Magnetic Resonance Imaging
fNIR	Functional Near-Infrared Imaging
GMM	Gaussian Mixture Model
HFB	High Frequency Band
HMM	Hidden Markov Model
IAP	Intracarotid Amobarbital Procedure
ICA	Independent Component Analysis
IQ	Intelligence Quotient
LDA	Linear Discriminant Analysis
LFB	Low Frequency Band
LFP	Local Field Potential
MDL	Minimum Description Length
MEG	Magnetoencephalography
MHLW	Ministry of Health, Labor, and Welfare
NIH	National Institutes of Health
PCA	Principal Component Analysis
PET	Positron Emission Tomography
PNS	Peripheral Nervous System
SIGFRIED	SIGnal modeling For Real-time Identification and Event Detection
SMR	Sensory Motor Rhythm
SRM	Structural Risk Minimization
SSD	Shortest Data Description
SSEP	Steady-State Evoked Potential
SSVEP	Steady State Visually Evoked Potentials
STG	Superior Temporal Gyrus
SUA	Single Unit Activity
VEP	Visual Evoked Potential
WAIS	Wechsler Adult Intelligence Scale

List of Symbols

$X_{t,c}$	signal from channel c at time point t
N_c	number of channels
w_c	weight of channel c
R_X	autocorrelation of signal X
a_k	k-th autocorrelation coefficient
σ_ε^2	mean-square error
τ	lag
K_k	k-th reflection coefficient
$\hat{X}_t$	forward prediction
$\hat{X}_{t-p}$	backward prediction
$P(f)$	amplitude spectrum
f_s	sampling frequency
m	Mahalanobis distance
Σ_c	covariance matrix
$\eta(X_t\|c)$	probability density function
LL	negative log likelihood
L	maximized likelihood
N	number of free parameters
D	dimensionality
ΔK	improvement in information criteria

Bibliography

Acqualagna, L., Treder, M. S., Schreuder, M., and Blankertz, B. (2010). A novel brain-computer interface based on the rapid serial visual presentation paradigm. *Conf Proc IEEE Eng Med Biol Soc*, 1:2686–2689. (cited on pages 79 and 120)

Akaike, H. (1973). Information theory and an extension of the maximum likelihood principle. In Petrov, B. N. and Csaki, F., editors, *2nd International Symposium on Information Theory, Budapest*, pages 267–281. (cited on pages 92 and 93)

Allison, B., Graimann, B., and Graser, A. (2007). Why use a BCI if you are healthy? In *ACE Workshop - Brainplay'07: Brain-Computer Interfaces and Games, Salzburg, Austria*. (cited on page 25)

Allison, B. Z., Brunner, C., Kaiser, V., Müller-Putz, G. R., Neuper, C., and Pfurtscheller, G. (2010). Toward a hybrid brain-computer interface based on imagined movement and visual attention. *J Neural Eng*, 7(2):26007–26007. (cited on pages 27 and 120)

Allison, B. Z. and Pineda, J. A. (2003). ERPs evoked by different matrix sizes: implications for a brain computer interface (BCI) system. *IEEE Trans Neural Syst Rehabil Eng*, 11(2):110–113. (cited on page 59)

Ang, K., Guan, C., Chua, K., Ang, B., Kuah, C., Wnag, C., Phua, K., Chin, Z., and Zhang, H. (2010). Clinical study of neurorehabilitation in stroke using EEG-based motor imagery brain-computer interface with robotic feedback. In *32nd Annual International Conference of the IEEE Engineering in Medicine and Biology Society (EMBC), Buenos Aires, Argentina*, pages 5549–5552. (cited on page 29)

Angelakis, E., Stathopoulou, S., Frymiare, J. L., Green, D. L., Lubar, J. F., and Kounios, J. (2007). EEG neurofeedback: a brief overview and an example of peak alpha frequency training for cognitive enhancement in the elderly. *Clin Neuropsychol*, 21(1):110–129. (cited on page 29)

Aoki, F., Fetz, E. E., Shupe, L., Lettich, E., and Ojemann, G. A. (1999). Increased gamma-range activity in human sensorimotor cortex during performance of visuomotor tasks. *J Clin Neurophysiol*, 110(3):524–537. (cited on pages 5, 35, 100, and 112)

Aoki, F., Fetz, E. E., Shupe, L., Lettich, E., and Ojemann, G. A. (2001). Changes in power and coherence of brain activity in human sensorimotor cortex during performance of visuomotor tasks. *Biosystems*, 63(1-3):89–99. (cited on pages 5, 35, and 100)

Baernreuther, B., Zander, T., Reissland, J., Kothe, C., Jatzev, S., Gaertner, M., and Makeig, S. (2010). Access to covert aspects of user intentions: Detecting bluffing in a game context with a passive BCI. In *Fourth International BCI Meeting, Asilomar, CA, June*. (cited on pages 25 and 29)

Bahramisharif, A., van Gerven, M., Heskes, T., and Jensen, O. (2010). Covert attention allows for continuous control of brain-computer interfaces. *Eur J Neurosci*, 31(8):1501–1508. (cited on pages 25 and 29)

Ball, T., Kern, M., Mutschler, I., Aertsen, A., and Schulze-Bonhage, A. (2009). Signal quality of simultaneously recorded invasive and non-invasive EEG. *NeuroImage*, 46(3):708–716. (cited on pages 4, 12, 14, and 43)

Belliveau, J. W., Kennedy, D. N., McKinstry, R. C., Buchbinder, B. R., Weisskoff, R. M., Cohen, M. S., Vevea, J. M., Brady, T. J., and Rosen, B. R. (1991). Functional mapping of the human visual cortex by magnetic resonance imaging. *Science*, 254(5032):716–719. (cited on pages 8 and 34)

Berger, H. (1929). Ueber das Electroenkephalogramm des Menschen. *Arch Psychiat Nervenkr*, 87:527–570. (cited on pages 6, 9, and 24)

Berger, J. (1985). *Statistical Decision Theory and Bayesian Analysis*. Springer-Verlag. (cited on page 110)

Berger, T. W., Chapin, J., Gerhardt, G. A., and McFarland, D. J. (2007). International Assessment of Research and Development in Brain-Computer Interfaces. WTEC Panel Report. *Storming Media*. (cited on pages 24 and 29)

Berger, T. W. and Glanzman, D. L. (2005). *Toward Replacement Parts for the Brain: Implantable Biomimetic Electronics as Neural Prostheses*. The MIT Press. (cited on page 27)

Beyer, T., Townsend, D. W., Brun, T., Kinahan, P. E., Charron, M., Roddy, R., Jerin, J., Young, J., Byars, L., and Nutt, R. (2000). A combined pet/ct scanner for clinical oncology. *J Nucl Med*, 41(8):1369–1379. (cited on page 34)

Bianchi, L., Babiloni, F., Cincotti, F., Salinari, S., and Marciani, M. G. (2003). Introducing BF++: A C++ framework for cognitive bio-feedback systems design. *Meth Inform Med*, 42(1):102–110. (cited on page 30)

Bianchi, L., Quitadamo, L. R., Abbafati, M., Marciani, M. G., and Saggio, G. (2009). Introducing NPXLab 2010: A tool for the analysis and optimization of P300 based brain-computer interfaces. In *2009 2nd International Symposium on Applied Sciences in Biomedical and Communication Technologies*, pages 1–4, Bratislava, Slovakia. (cited on page 29)

Biernacki, C., Celeux, G., and Govaert, G. (2003). Choosing starting values for the EM algorithm for getting the highest likelihood in multivariate gaussian mixture models. *Computational Statistics and Data Analysis*, 41:561–575. (cited on page 95)

Bin, G., Gao, X., Wang, Y., Hong, B., and Gao, S. (2009). VEP-based brain-computer interfaces: time, frequency, and code modulations [Research Frontier]. *Computational Intelligence Magazine, IEEE*, 4(4):22–26. (cited on pages 3, 24, 54, and 55)

Birbaumer, N. and Cohen, L. G. (2007). Brain-computer interfaces: communication and restoration of movement in paralysis. *J Physiol*, 579(Pt 3):621–636. (cited on pages 55 and 60)

Birbaumer, N., Ghanayim, N., Hinterberger, T., Iversen, I., Kotchoubey, B., Kubler, A., Perelmouter, J., Taub, E., and Flor, H. (1999). A spelling device for the paralysed. *Nature*, 398(6725):297–298. (cited on page 24)

Bittar, R. G., Olivier, A., Sadikot, A. F., Andermann, F., Comeau, R. M., Cyr, M., Peters, T. M., and Reutens, D. C. (1999). Localization of somatosensory function by using positron emission tomography scanning: a comparison with intraoperative cortical stimulation. *J Neurosurg*, 90(3):478–483. (cited on pages 4, 32, 34, and 99)

Blankertz, B., Tangermann, M., Vidaurre, C., Fazli, S., Sannelli, C., Haufe, S., Maeder, C., Ramsey, L., Sturm, I., Curio, G., and Müller, K. R. (2010). The Berlin Brain-Computer Interface: Non-Medical Uses of BCI Technology. *Front Neurosci*, 4:198–198. (cited on page 25)

Bozdogan, H. (1974). Model selection and akaike's information criterion. *Psychometrika*, 52:345–370. (cited on page 93)

Brouwer, A. M. and van Erp, J. B. (2010). A tactile P300 brain-computer interface. *Front Neurosci*, 4:19–19. (cited on pages 79 and 120)

Brunner, P., Joshi, S., Briskin, S., Wolpaw, J. R., Bischof, H., and Schalk, G. (2010a). Does the P300 speller depend on eye gaze? In *Presentation at the TOBI Workshop, Graz*. (cited on page 54)

Brunner, P., Joshi, S., Briskin, S., Wolpaw, J. R., Bischof, H., and Schalk, G. (2010b). Does the 'P300' speller depend on eye gaze? *J Neural Eng*, 7(5):056013. (cited on pages 54 and 57)

Brunner, P., Ritaccio, A. L., Lynch, T. M., Emrich, J. F., Wilson, J. A., Williams, J. C., Aarnoutse, E. J., Ramsey, N. F., Leuthardt, E. C., Bischof, H., and Schalk, G. (2009). A practical procedure for real-time functional mapping of eloquent cortex using electrocorticographic signals in humans. *Epilepsy Behav*, 15(3):278–286. (cited on pages 4 and 43)

Buch, E., Weber, C., Cohen, L. G., Braun, C., Dimyan, M. A., Ard, T., Mellinger, J., Caria, A., Soekadar, S., Fourkas, A., and Birbaumer, N. (2008). Think to move: a neuromagnetic brain-computer interface (BCI) system for chronic stroke. *Stroke*, 39(3):910–917. (cited on page 29)

Burg, J. P. (1967). Maximum entropy spectral analysis. In *Proceedings 37th Meeting of Society of Exploration Geophysicists, Oklahoma City, OK*. (cited on pages 85 and 87)

Burg, J. P. (1968). A new analysis technique for time series data. *NATO Advanced Study Institute on Signal Processing: Underwater Acoustics.* . Reprinted in Childers (1978), pp. 42-48. (cited on pages 85, 87, and 106)

Burg, J. P. (1972). The relationship between maximum entropy spectra and maximum likelihood spectra. *Geophysics*, 37:375–376. (cited on page 106)

Carmena, J. M., Lebedev, M. A., Crist, R. E., O'Doherty, J. E., Santucci, D. M., Dimitrov, D. F., Patil, P. G., Henriquez, C. S., and Nicolelis, M. A. (2003). Learning to control a brain-machine interface for reaching and grasping by primates. *PLoS Biol*, 1(2). (cited on page 29)

Celeux, G. and Govaert, G. (1992). A classification EM algorithm for clustering and two stochastic versions. *Computational Statistics and Data Analysis*, 14:279–416. (cited on pages 92 and 95)

Cervenka, M. C., Boatman-Reich, D. F., Ward, J., Franaszczuk, P. J., and Crone, N. E. (2011). Language mapping in multilingual patients: electrocorticography and cortical stimulation during naming. *Front Hum Neurosci*, 5:13–13. (cited on page 121)

Chakraborty, A. and McEvoy, A. W. (2008). Presurgical functional mapping with functional MRI. *Curr Opin Neurol*, 21(4):446–451. (cited on pages 4, 32, 34, and 99)

Cham, J. G., Branchaud, E. A., Nenadic, Z., Greger, B., Andersen, R. A., and Burdick, J. W. (2005). Semi-chronic motorized microdrive and control algorithm for autonomously isolating and maintaining optimal extracellular action potentials. *J Neurophysiol*, 93(1):570–579. (cited on page 14)

Chance, B., Anday, E., Nioka, S., Zhou, S., Hong, L., Worden, K., Li, C., Murray, T., Ovetsky, Y., Pidikiti, D., and Thomas, R. (1998). A novel method for fast imaging of brain function, non-invasively, with light. *Opt Express*, 2(10):411–423. (cited on page 9)

Chao, Z. C., Nagasaka, Y., and Fujii, N. (2010). Long-term asynchronous decoding of arm motion using electrocorticographic signals in monkeys. *Front Neuroengineering*, 3:1–12. (cited on pages 14 and 57)

Childers, D., editor (1978). *Modern Spectrum Analysis*. IEEE Press. (cited on pages 106 and 134)

Chollet, F., DiPiero, V., Wise, R. J., Brooks, D. J., Dolan, R. J., and Frackowiak, R. S. (1991). The functional anatomy of motor recovery after stroke in humans: a study with positron emission tomography. *Ann Neurol*, 29(1):63–71. (cited on page 114)

Cincotti, F., Bianchi, L., Birch, G., Guger, C., Mellinger, J., Scherer, R., Schmidt, R. N., Yáñez Suárez, O., and Schalk, G. (2006). BCI meeting 2005–workshop on technology: hardware and software. *IEEE Trans Neural Syst Rehabil Eng*, 14(2):128–131. (cited on pages 24 and 27)

Cincotti, F., Mattia, D., Aloise, F., Bufalari, S., Schalk, G., Oriolo, G., Cherubini, A., Marciani, M. G., and Babiloni, F. (2008). Non-invasive brain-computer interface system: towards its application as assistive technology. *Brain Res Bull*, 75(6):796–803. (cited on pages 25 and 26)

Citi, L., Poli, R., Cinel, C., and Sepulveda, F. (2008). P300-based BCI mouse with genetically-optimized analogue control. *IEEE Trans Neural Syst Rehabil Eng*, 16(1):51–61. (cited on page 59)

Cohen, B. and Caroscio, J. (1983). Eye movements in amyotrophic lateral sclerosis. *J Neural Transm Suppl*, 19:305–315. (cited on pages 55, 60, and 78)

Cohen, D. (1968). Magnetoencephalography: evidence of magnetic fields produced by alpha-rhythm currents. *Science*, 161(843):784–786. (cited on pages 8 and 35)

Colebatch, J. G., Adams, L., Murphy, K., Martin, A. J., Lammertsma, A. A., Tochon-Danguy, H. J., Clark, J. C., Friston, K. J., and Guz, A. (1991). Regional cerebral blood flow during volitional breathing in man. *J Physiol*, 443:91–103. (cited on page 114)

Cornsweet, T. N. (1956). Determination of the stimuli for involuntary drifts and saccadic eye movements. *J Opt Soc Am*, 46(11):987–993. (cited on page 78)

Costa, E. J. and Cabral, E. F. (2000). EEG-based discrimination between imagination of left and right hand movements using adaptive gaussian representation. *Med Eng Phys*, 22(5):345–8. (cited on pages 5 and 16)

Coyle, S. M., Ward, T. E., and Markham, C. M. (2007). Brain-computer interface using a simplified functional near-infrared spectroscopy system. *J Neural Eng*, 4(3):219–226. (cited on page 24)

Crone, N. E., Boatman, D., Gordon, B., and Hao, L. (2001). Induced electrocorticographic gamma activity during auditory perception. *J Clin Neurophysiol*, 112(4):565–582. (cited on pages 5, 35, and 100)

Crone, N. E., Miglioretti, D. L., Gordon, B., and Lesser, R. P. (1998a). Functional mapping of human sensorimotor cortex with electrocorticographic spectral analysis. II. Event-related synchronization in the gamma band. *Brain*, 121 (Pt 12):2301–2315. (cited on pages 1, 5, 16, 22, 24, 32, 35, 100, 112, and 114)

Crone, N. E., Miglioretti, D. L., Gordon, B., Sieracki, J. M., Wilson, M. T., Uematsu, S., and Lesser, R. P. (1998b). Functional mapping of human sensorimotor cortex with electrocorticographic spectral analysis. I. Alpha and beta event-related desynchronization. *Brain*, 121 (Pt 12):2271–2299. (cited on pages 5, 35, and 100)

Daly, J. J., Cheng, R., Rogers, J., Litinas, K., Hrovat, K., and Dohring, M. (2009). Feasibility of a new application of noninvasive brain computer interface (BCI): a case study of training for recovery of volitional motor control after stroke. *J Neurol Phys Ther*, 33(4):203–211. (cited on page 29)

Daly, J. J. and Wolpaw, J. R. (2008). Brain-computer interfaces in neurological rehabilitation. *Lancet Neurol*, 7(11):1032–1043. (cited on page 29)

Daniel, P. M. and Whitteridge, D. (1961). The representation of the visual field on the cerebral cortex in monkeys. *J Physiol*, 159:203–221. (cited on page 56)

Davson, H. (1976). Review lecture. The blood-brain barrier. *J Physiol*, 255(1):1–28. (cited on pages 12 and 57)

De Keyser, M., Vissenberg, I., and Neetens, A. (1990). Are visually evoked potentials (VEP) useful for determination of visual acuity?: A clinical trial. *Neuro-Ophthalmology*, 10(3):153–163. (cited on pages 56, 60, and 74)

deCharms, R. C., Maeda, F., Glover, G. H., Ludlow, D., Pauly, J. M., Soneji, D., Gabrieli, J. D., and Mackey, S. C. (2005). Control over brain activation and pain learned by using real-time functional MRI. *Proc Natl Acad Sci U S A*, 102(51):18626–18631. (cited on page 29)

Dempster, A., Laird, N., and Rubin, D. (1977). Maximum likelihood from incomplete data via the EM algorithm. *Journal of Royal Statistical Society B*, 39:1–38. (cited on pages 92 and 95)

Devinsky, O., Beric, A., and Dogali, M. (1993). *Electrical and Magnetic Stimulation of the Brain and Spinal Cord*. Raven Press. (cited on pages 34 and 99)

Di Russo, F., Martínez, A., Sereno, M. I., Pitzalis, S., and Hillyard, S. A. (2002). Cortical sources of the early components of the visual evoked potential. *Hum Brain Mapp*, 15(2):95–111. (cited on pages 56 and 75)

Dinner, D. S., Lüders, H., Lesser, R. P., and Morris, H. H. (1986). Invasive methods of somatosensory evoked potential monitoring. *J Clin Neurophysiol*, 3(2):113–130. (cited on pages 4, 32, and 99)

Donchin, E. and Arbel, Y. (2009). P300 Based Brain Computer Interfaces: A Progress Report. In *FAC '09: Proceedings of the 5th International Conference on Foundations of Augmented Cognition. Neuroergonomics and Operational Neuroscience*, pages 724–731, Berlin, Heidelberg. Springer-Verlag. (cited on pages 3, 43, and 59)

Donchin, E., Spencer, K. M., and Wijesinghe, R. (2000). The mental prosthesis: assessing the speed of a P300-based brain-computer interface. *IEEE Trans Rehabil Eng*, 8(2):174–179. (cited on page 60)

Dorneich, M. C., Whitlow, S. D., Santosh, M., May Ververs, P., and B, S. J. (2009). Augmented cognition transition. Technical report, Honeywell Aerospace Advanced Technology. (cited on pages 25 and 29)

Edlinger, G., Holzner, C., Groenegress, C., Guger, C., and Slater, M. (2009). Goal-Oriented Control with Brain-Computer Interface. In *FAC '09: Proceedings of the 5th International Conference on Foundations of Augmented Cognition. Neuroergonomics and Operational Neuroscience*, pages 732–740, Berlin, Heidelberg. Springer-Verlag. (cited on page 59)

Engel, J., editor (1993). *Surgical Treatment of the Epilepsies*. Lippincott Williams & Wilkins, second edition. (cited on page 113)

Engel, S. A., Glover, G. H., and Wandell, B. A. (1997). Retinotopic organization in human visual cortex and the spatial precision of functional MRI. *Cereb Cortex*, 7(2):181–192. (cited on pages 56 and 57)

Engel, S. A., Rumelhart, D. E., Wandell, B. A., Lee, A. T., Glover, G. H., Chichilnisky, E. J., and Shadlen, M. N. (1994). fMRI of human visual cortex. *Nature*, 369(6481):525–525. (cited on pages 56 and 57)

Fairclough, S. H. (2008). BCI and Physiological Computings: Differences, Similarities & Intuitive Control. In *Workshop on BCI and Computer Games, CHI(08), Florence, Italy*. (cited on page 25)

Farwell, L. A. and Donchin, E. (1988). Talking off the top of your head: toward a mental prosthesis utilizing event-related brain potentials. *Electroencephalogr Clin Neurophysiol*, 70(6):510–523. (cited on pages 3, 22, 24, 43, 47, and 59)

Fee, M. S. and Leonardo, A. (2001). Miniature motorized microdrive and commutator system for chronic neural recording in small animals. *J Neurosci Methods*, 112(2):83–94. (cited on page 14)

Felton, E. A., Wilson, J. A., Williams, J. C., and Garell, P. C. (2007). Electrocorticographically controlled brain-computer interfaces using motor and sensory imagery in patients with temporary subdural electrode implants. report of four cases. *J Neurosurg*, 106(3):495–500. (cited on pages 4 and 43)

Fetz, E. E. (1969). Operant conditioning of cortical unit activity. *Science*, 163(870):955–958. (cited on pages 14 and 29)

Foerster, O. (1931). The cerebral cortex in man. *Lancet*, 221:309–312. (cited on pages 4, 32, 33, 34, and 99)

Foerster, O. (1936). The motor cortex in man in the light of Hughlings Jackson's Doctrines. *Brain*, 59:135–59. (cited on page 114)

Fountas, K. N. and Smith, J. R. (2007). Subdural electrode-associated complications: a 20-year experience. *Stereotact Funct Neurosurg*, 85(6):264–272. (cited on pages 12 and 57)

Friedman, N. and Russell, S. (1997). Image segmentation in video sequences: A probabilistic approach. In *IEEE Proceedings, of the Thirteenth Conference on Uncertainty in Artificial Intelligence(UAI), Aug. 1-3*. (cited on pages 5 and 16)

Fries, P. (2005). A mechanism for cognitive dynamics: neuronal communication through neuronal coherence. *Trends Cogn Sci*, 9(10):474–480. (cited on pages 5, 35, and 100)

Furdea, A., Halder, S., Krusienski, D. J., Bross, D., Nijboer, F., Birbaumer, N., and Kübler, A. (2009). An auditory oddball (P300) spelling system for brain-computer interfaces. *Psychophysiology*, 46(3):617–625. (cited on page 74)

Ganslandt, O., Fahlbusch, R., Nimsky, C., Kober, H., Möller, M., Steinmeier, R., Romstöck, J., and Vieth, J. (1999). Functional neuronavigation with magnetoencephalography: outcome in 50 patients with lesions around the motor cortex. *J Neurosurg*, 91(1):73–79. (cited on pages 4, 32, 35, and 99)

Gao, X., Xu, D., Cheng, M., and Gao, S. (2003). A BCI-based environmental controller for the motion-disabled. *IEEE Trans Neural Syst Rehabil Eng*, 11(2):137–140. (cited on pages 24 and 54)

Gardner, A. B., Krieger, A. M., Vachtsevanos, G., and Litt, B. (2006). One-class novelty detection for seizure analysis from intracranial EEG. *J. Mach. Learn. Res.*, 7:1025–1044. (cited on pages 5 and 16)

Gargiulo, G., Calvo, R. A., Bifulco, P., Cesarelli, M., Jin, C., Mohamed, A., and van Schaik, A. (2010). A new EEG recording system for passive dry electrodes. *Clin Neurophysiol*, 121(5):686–693. (cited on page 28)

Georgopoulos, A. P., Karageorgiou, E., Leuthold, A. C., Lewis, S. M., Lynch, J. K., Alonso, A. A., Aslam, Z., Carpenter, A. F., Georgopoulos, A., Hemmy, L. S., Koutlas, I. G., Langheim, F. J., McCarten, J. R., McPherson, S. E., Pardo, J. V., Pardo, P. J., Parry, G. J., Rottunda, S. J., Segal, B. M., Sponheim, S. R., Stanwyck, J. J., Stephane, M., and Westermeyer, J. J. (2007). Synchronous neural interactions assessed by magnetoencephalography: a functional biomarker for brain disorders. *J Neural Eng*, 4(4):349–355. (cited on page 29)

Gibbs, F., Lennox, W., and Gibbs, E. (1936). The electro-encephalogram in diagnosis and in localization of epileptic seizures. *Arch Neurol Psychiatry*, 36:1225–1235. (cited on pages 1 and 32)

Gonsalvez, C. L. and Polich, J. (2002). P300 amplitude is determined by target-to-target interval. *Psychophysiology*, 39(3):388–396. (cited on page 76)

Grafton, S. T., Mazziotta, J. C., Presty, S., Friston, K. J., Frackowiak, R. S., and Phelps, M. E. (1992). Functional anatomy of human procedural learning determined with regional cerebral blood flow and PET. *J Neurosci*, 12(7):2542–2548. (cited on page 114)

Graimann, B., Huggins, J. E., Levine, S. P., and Pfurtscheller, G. (2002). Visualization of significant ERD/ERS patterns in multichannel EEG and ECoG data. *J Clin Neurophysiol*, 113(1):43–47. (cited on pages 5, 35, and 100)

Guger, C., Daban, S., Sellers, E., Holzner, C., Krausz, G., Carabalona, R., Gramatica, F., and Edlinger, G. (2009). How many people are able to control a P300-based brain-computer interface (BCI)? *Neurosci Lett*, 462(1):94–98. (cited on pages 25, 26, 43, 54, 59, and 74)

Guger, C., Schlogl, A., Neuper, C., Walterspacher, D., Strein, T., and Pfurtscheller, G. (2001). Rapid prototyping of an EEG-based brain-computer interface (BCI). *IEEE Trans Neur Syst Rehabil Eng*, 9(1):49–58. (cited on page 24)

Guger, C., Schlögl, A., Walterspacher, D., and Pfurtscheller, G. (1999). Design of an EEG-based brain-computer interface (BCI) from standard components running in real-time under Windows. *Biomed Tech (Berl)*, 44(1-2):12–16. (cited on page 24)

Hamberger, M. J. (2007). Cortical language mapping in epilepsy: a critical review. *Neuropsychol Rev*, 17(4):477–489. (cited on pages 34, 99, and 114)

Hamer, H. M., Morris, H. H., Mascha, E. J., Karafa, M. T., Bingaman, W. E., Bej, M. D., Burgess, R. C., Dinner, D. S., Foldvary, N. R., Hahn, J. F., Kotagal, P., Najm, I., Wyllie, E., and Lüders, H. O. (2002). Complications of invasive video-EEG monitoring with subdural grid electrodes. *Neurology*, 58(1):97–103. (cited on pages 12 and 57)

Hara, K., Uematsu, S., Lesser, R., Gordon, B., Hart, J., and Vining, E. (1991). Representation of primary motor cortex in humans: studied with chronic subdural grid. *Epilepsia*, 32(suppl):23–24. (cited on pages 4 and 99)

Harris, K. D., Henze, D. A., Csicsvari, J., Hirase, H., and Buzsáki, G. (2000). Accuracy of tetrode spike separation as determined by simultaneous intracellular and extracellular measurements. *Journal of Neurophysiology*, 84:401–414. (cited on pages 5 and 16)

Harville, M., Gordon, G., and Woodfill, J. (2001). Foreground segmentation using adaptive mixture models in color and depth. In *IEEE Proceedings, IEEE Workshop on, 8 July 2001*, pages 3–4. (cited on pages 5 and 16)

Haselager, P., Vlek, R., Hill, J., and Nijboer, F. (2009). A note on ethical aspects of BCI. *Neural Netw*, 22(9):1352–1357. (cited on page 31)

Higson, G. R. (2002). *Medical Device Safety: The Regulation of Medical Devices for Public Health and Safety*. Taylor & Francis, London, UK, 1 edition. (cited on pages 27 and 57)

Hill, J., Farquhar, J., Martens, S. M. M., Biessmann, F., and Schölkopf, B. (2009). Effects of stimulus type and of error-correcting code design on bci speller performance. In Koller, D.,

Schuurmans, D., Bengio, Y., and Bottou, L., editors, *Twenty-Second Annual Conference on Neural Information Processing Systems*, pages 665–672, Red Hook, NY, USA. Curran. (cited on page 79)

Hill, N. J., Lal, T. N., Schröder, M., Hinterberger, T., Wilhelm, B., Nijboer, F., Mochty, U., Widman, G., Elger, C., Schölkopf, B., Kübler, A., and Birbaumer, N. (2006). Classifying EEG and ECoG signals without subject training for fast BCI implementation: comparison of nonparalyzed and completely paralyzed subjects. *IEEE Trans Neural Syst Rehabil Eng*, 14(2):183–186. (cited on page 57)

Hochberg, L. R., Serruya, M. D., Friehs, G. M., Mukand, J. A., Saleh, M., Caplan, A. H., Branner, A., Chen, D., Penn, R. D., and Donoghue, J. P. (2006). Neuronal ensemble control of prosthetic devices by a human with tetraplegia. *Nature*, 442(7099):164–171. (cited on page 14)

Hubel, D. H. and Wiesel, T. N. (1959). Receptive fields of single neurones in the cat's striate cortex. *J Physiol*, 148:574–591. (cited on pages 56 and 75)

Hubel, D. H. and Wiesel, T. N. (1962). Receptive fields, binocular interaction and functional architecture in the cat's visual cortex. *J. Physiol.*, 160:106–154. (cited on pages 56 and 75)

Jackson, N., Sridharan, A., Anand, S., Baker, M., Okandan, M., and Muthuswamy, J. (2010). Long-term neural recordings using MEMS based movable microelectrodes in the brain. *Front Neuroengineering*, 3:10–10. (cited on page 14)

Jasper, H. H. (1958). The ten-twenty electrode system of the International Federation. *Electroencephalography and Clinical Neurophysiology*, (10):371–375. (cited on page 32)

Jennrich, R. I. (1977). *Stepwise regression*, pages 58–75. John Wiley and Sons, New York. (cited on pages 48 and 64)

Kawashima, R., Roland, P. E., and O'Sullivan, B. T. (1994). Activity in the human primary motor cortex related to ipsilateral hand movements. *Brain Res*, 663(2):251–256. (cited on page 114)

Kawashima, R., Yamada, K., Kinomura, S., Yamaguchi, T., Matsui, H., Yoshioka, S., and Fukuda, H. (1993). Regional cerebral blood flow changes of cortical motor areas and prefrontal areas in humans related to ipsilateral and contralateral hand movement. *Brain Res*, 623(1):33–40. (cited on page 114)

Kay, S. (1988). *Modern Spectral Estimation*. Prentice-Hall, Upper Saddle River, NJ. (cited on page 85)

Kennedy, P. R. (1989). The cone electrode: a long-term electrode that records from neurites grown onto its recording surface. *J Neurosci Methods*, 29(3):181–193. (cited on page 13)

Kim, S. G., Ashe, J., Georgopoulos, A. P., Merkle, H., Ellermann, J. M., Menon, R. S., Ogawa, S., and Ugurbil, K. (1993). Functional imaging of human motor cortex at high magnetic field. *J Neurophysiol*, 69(1):297–302. (cited on page 114)

Klobassa, D. S., Vaughan, T. M., Brunner, P., Schwartz, N. E., Wolpaw, J. R., Neuper, C., and Sellers, E. W. (2009). Toward a high-throughput auditory P300-based brain-computer interface. *Clin Neurophysiol*, 120(7):1252–1261. (cited on pages 74, 79, and 120)

Kok, A. (2001). On the utility of P3 amplitude as a measure of processing capacity. *Psychophysiology*, 38(3):557–577. (cited on page 77)

Korte, W. (1923). Über die Gestaltauffassung im indirekten Sehen. *Zeitschrift für Psychologie*, 93:17–82. (cited on pages 60 and 77)

Kotchetkov, I. S., Hwang, B. Y., Appelboom, G., Kellner, C. P., and Connolly, E. S. (2010). Brain-computer interfaces: military, neurosurgical, and ethical perspective. *Neurosurg Focus*, 28(5). (cited on page 25)

Krüger, J., Caruana, F., Volta, R. D., and Rizzolatti, G. (2010). Seven years of recording from monkey cortex with a chronically implanted multiple microelectrode. *Front Neuroengineering*, 3:6–6. (cited on page 14)

Krusienski, D. J., Sellers, E. W., Cabestaing, F., Bayoudh, S., McFarland, D. J., Vaughan, T. M., and Wolpaw, J. R. (2006). A comparison of classification techniques for the P300 Speller. *J Neural Eng*, 3(4):299–305. (cited on pages 46, 48, 59, 63, 64, 66, 71, and 76)

Krusienski, D. J., Sellers, E. W., McFarland, D. J., Vaughan, T. M., and Wolpaw, J. R. (2008). Toward enhanced P300 speller performance. *J Neurosci Methods*, 167(1):15–21. (cited on pages 59, 63, 66, 71, 74, and 76)

Kübler, A. and Birbaumer, N. (2008). Brain-computer interfaces and communication in paralysis: extinction of goal directed thinking in completely paralysed patients? *Clin Neurophysiol*, 119(11):2658–2666. (cited on page 57)

Kübler, A., Furdea, A., Halder, S., Hammer, E. M., Nijboer, F., and Kotchoubey, B. (2009). A brain-computer interface controlled auditory event-related potential (P300) spelling system for locked-in patients. *Ann N Y Acad Sci*, 1157:90–100. (cited on pages 79 and 120)

Kübler, A., Mushahwar, V. K., Hochberg, L. R., and Donoghue, J. P. (2006). BCI Meeting 2005–workshop on clinical issues and applications. *IEEE Trans Neural Syst Rehabil Eng*, 14(2):131–134. (cited on pages 27 and 31)

Kübler, A., Nijboer, F., Mellinger, J., Vaughan, T. M., Pawelzik, H., Schalk, G., McFarland, D. J., Birbaumer, N., and Wolpaw, J. R. (2005). Patients with ALS can use sensorimotor rhythms to operate a brain-computer interface. *Neurology*, 64(10):1775–1777. (cited on pages 25 and 26)

Kuo, B., Yan, J., and Landgrebe, D. (2003). Gaussian mixture classifier with regularized covariance estimator for hyperspectral data classification. In *Proceedings IGARSS '03, of the Geoscience and Remote Sensing Symposium*, volume 1, pages 276–278. (cited on pages 5 and 16)

Lachaux, J. P., Fonlupt, Pt, P., Kahane, P., Minotti, L., Hoffmann, D., Bertrand, O., and Baciu, M. (2007a). Relationship between task-related gamma oscillations and bold signal: new insights from combined fMRI and intracranial EEG. *Hum Brain Mapp*, 28(12):1368–1375. (cited on pages 5, 36, and 100)

Lachaux, J. P., Jerbi, K., Bertrand, O., Minotti, L., Hoffmann, D., Schoendorff, B., and Kahane, P. (2007b). A blueprint for real-time functional mapping via human intracranial recordings. *PLoS ONE*, 2(10). (cited on pages 5, 36, and 100)

Lachaux, J. P., Jerbi, K., Bertrand, O., Minotti, L., Hoffmann, D., Schoendorff, B., and Kahane, P. (2007c). BrainTV: a novel approach for online mapping of human brain functions. *Biol Res*, 40(4):401–413. (cited on pages 5, 36, and 100)

Lachaux, J. P., Rudrauf, D., and Kahane, P. (2003). Intracranial EEG and human brain mapping. *J Physiol Paris*, 97(4-6):613–628. (cited on pages 5, 35, and 100)

Leach, J. B., Achyuta, A. K., and Murthy, S. K. (2010). Bridging the divide between neuroprosthetic design, tissue engineering and neurobiology. *Front Neuroengineering*, 2:18–18. (cited on page 14)

Lee, D. (2005). Effective gaussian mixture learning for video background subtraction. *IEEE Trans. Pattern Anal. Mach. Intell.*, 27(5):827–832. (cited on pages 5 and 16)

Legatt, A. D., Arezzo, J., and Vaughan, H. G. (1980). Averaged multiple unit activity as an estimate of phasic changes in local neuronal activity: effects of volume-conducted potentials. *J Neurosci Methods*, 2(2):203–217. (cited on page 13)

Lenhardt, A., Kaper, M., and Ritter, H. J. (2008). An adaptive P300-based online brain-computer interface. *IEEE Trans Neural Syst Rehabil Eng*, 16(2):121–130. (cited on pages 43, 54, and 59)

Lesser, R. P., Crone, N. E., and Webber, W. R. (2010). Subdural electrodes. *Clin Neurophysiol*, 121(9):1376–1392. (cited on page 25)

Leuthardt, E. C., Miller, K., Anderson, N. R., Schalk, G., Dowling, J., Miller, J., Moran, D. W., and Ojemann, J. G. (2007). Electrocorticographic frequency alteration mapping: a clinical technique for mapping the motor cortex. *Neurosurgery*, 60(4 Suppl 2):260–270. (cited on pages 5, 35, 36, and 100)

Leuthardt, E. C., Miller, K. J., Schalk, G., Rao, R. P., and Ojemann, J. G. (2006). Electrocorticography-based brain computer interface–the Seattle experience. *IEEE Trans Neural Syst Rehabil Eng*, 14(2):194–198. (cited on pages 4 and 43)

Leuthardt, E. C., Schalk, G., Wolpaw, J. R., Ojemann, J. G., and Moran, D. W. (2004). A brain-computer interface using electrocorticographic signals in humans. *J Neural Eng*, 1(2):63–71. (cited on pages 4, 29, and 43)

Liyuan, L., Huang, W., Gu, I. Y.-H., and Tian, Q. (2004). Statistical modeling of complex backgrounds for foreground object detection. In *IEEE Transactions, Image Processing*, volume 13, pages 1459–1472. (cited on pages 5 and 16)

Majaranta, P. and Räihä, K. J. (2002). Twenty years of eye typing: systems and design issues. In *ETRA '02: Proceedings of the 2002 symposium on eye tracking research & applications*, pages 15–22, New York, NY, USA. ACM. (cited on pages 27, 54, 55, and 79)

Mak, J. N. and Wolpaw, J. R. (2009). Clinical applications of brain-computer interfaces: Current state and future prospects. *IEEE Rev Biomed Eng*, 2:187–199. (cited on pages 25 and 26)

Makeig, S., Westerfield, M., Jung, T. P., Enghoff, S., Townsend, J., Courchesne, E., and Sejnowski, T. J. (2002). Dynamic brain sources of visual evoked responses. *Science*, 295(5555):690–694. (cited on page 56)

Marin, C. and Fernández, E. (2010). Biocompatibility of intracortical microelectrodes: current status and future prospects. *Front Neuroengineering*, 3:8–8. (cited on page 14)

Marple, L. (1987). *Digital Spectral Analysis with Applications*. Prentice-Hall, Upper Saddle River, NJ. (cited on page 85)

Martens, S. M., Hill, N. J., Farquhar, J., and Schölkopf, B. (2009). Overlap and refractory effects in a brain-computer interface speller based on the visual P300 event-related potential. *J Neural Eng*, 6(2):026003–026003. (cited on pages 55, 56, and 75)

Martens, S. M., Mooij, J. M., Hill, N. J., Farquhar, J., and Schölkopf, B. (2010). A Graphical Model Framework for Decoding in the Visual ERP-Based BCI Speller. *Neural Comput*. (cited on page 79)

Mason, S. G. and Birch, G. E. (2003). A general framework for brain-computer interface design. *IEEE Trans Neur Syst Rehabil Eng*, 11(1):70–85. (cited on pages 2, 22, 24, and 29)

Matthews, R., McDonald, N. J., Hervieux, P., Turner, P. J., and Steindorf, M. A. (2007). A Wearable Physiological Sensor Suite for Unobtrusive Monitoring of Physiological and Cognitive State. In *Engineering in Medicine and Biology Society, 2007. EMBS 2007. 29th Annual International Conference of the IEEE*, pages 5276–5281. (cited on page 28)

Maynard, E. M., Nordhausen, C. T., and Normann, R. A. (1997). The Utah intracortical Electrode Array: a recording structure for potential brain-computer interfaces. *Electroencephalogr Clin Neurophysiol*, 102(3):228–239. (cited on page 25)

McFarland, D. J., McCane, L. M., David, S. V., and Wolpaw, J. R. (1997). Spatial filter selection for EEG-based communication. *Electroenceph Clin Neurophysiol*, 103(3):386–394. (cited on pages 84 and 106)

McFarland, D. J., Sarnacki, W. A., Townsend, G., Vaughan, T. M., and Wolpaw, J. R. (2010a). The P300-based brain–computer interface (BCI): Effects of stimulus rate. *Clin Neurophysiol*, in press. (cited on page 79)

McFarland, D. J., Sarnacki, W. A., and Wolpaw, J. R. (2003). Brain-Computer Interface (BCI) Operation: Optimizing Information Transfer Rates. *Biol Psychol*, 63(3):237–251. (cited on pages 3 and 54)

McFarland, D. J., Sarnacki, W. A., and Wolpaw, J. R. (2010b). Electroencephalographic (EEG) control of three-dimensional movement. *J Neural Eng*, 7(3):036007–036007. (cited on pages 24 and 120)

Meier, J. D., Aflalo, T. N., Kastner, S., and Graziano, M. S. (2008). Complex organization of human primary motor cortex: a high-resolution fMRI study. *J Neurophysiol*, 100(4):1800–1812. (cited on page 114)

Mellinger, J. and Schalk, G. (2007). BCI2000: A general-purpose software platform for BCI. In Dornhege, G., del R. Millan, J., Hinterberger, T., McFarland, D., and Müller, K., editors, *Toward Brain-Computer Interfacing*, pages 359–367, Cambridge, MA, USA. MIT Press. (cited on pages 24, 26, 44, 61, 101, and 115)

Meyer, P. T., Sturz, L., Sabri, O., Schreckenberger, M., Spetzger, U., Setani, K. S., Kaiser, H. J., and Buell, U. (2003). Preoperative motor system brain mapping using positron emission tomography and statistical parametric mapping: hints on cortical reorganisation. *J Neurol Neurosurg Psychiatry*, 74(4):471–478. (cited on pages 4, 32, 34, and 99)

Meyer-Baese, A. (2003). *Pattern recognition for medical imaging*. Elsevier Academic Press, Orlando, FL, USA. (cited on page 83)

Middendorf, M., McMillan, G., Calhoun, G., and Jones, K. S. (2000). Brain-computer interfaces based on the steady-state visual-evoked response. *IEEE Trans Rehabil Eng*, 8(2):211–214. (cited on pages 3 and 55)

Millán, J. D., Rupp, R., Müller-Putz, G. R., Murray-Smith, R., Giugliemma, C., Tangermann, M., Vidaurre, C., Cincotti, F., Kübler, A., Leeb, R., Neuper, C., Müller, K. R., and Mattia, D. (2010). Combining brain-computer interfaces and assistive technologies: State-of-the-art and challenges. *Front Neurosci*, 4(161). (cited on pages 27 and 120)

Miller, K. J., denNijs, M., Shenoy, P., Miller, J. W., Rao, R. P., and Ojemann, J. G. (2007a). Real-time functional brain mapping using electrocorticography. *Neuroimage*, 37(2):504–507. (cited on pages 5, 36, and 100)

Miller, K. J., Leuthardt, E. C., Schalk, G., Rao, R. P., Anderson, N. R., Moran, D. W., Miller, J. W., and Ojemann, J. G. (2007b). Spectral changes in cortical surface potentials during motor movement. *J Neurosci*, 27(9):2424–2432. (cited on pages 4, 5, 35, 36, 43, 85, 100, and 112)

Miller, K. J., Schalk, G., Fetz, E. E., den Nijs, M., Ojemann, J. G., and Rao, R. P. (2010). Cortical activity during motor execution, motor imagery, and imagery-based online feedback. *Proc Natl Acad Sci U S A*, 107(9):4430–4435. (cited on pages 4, 26, 29, and 43)

Miller, K. J., Shenoy, P., den Nijs, M., Sorensen, L. B., Rao, R. N., and Ojemann, J. G. (2008). Beyond the gamma band: the role of high-frequency features in movement classification. *IEEE Trans Biomed Eng*, 55(5):1634–1637. (cited on pages 4, 26, and 43)

Monastra, V. J., Lynn, S., Linden, M., Lubar, J. F., Gruzelier, J., and LaVaque, T. J. (2005). Electroencephalographic biofeedback in the treatment of attention-deficit/hyperactivity disorder. *Appl Psychophysiol Biofeedback*, 30(2):95–114. (cited on page 29)

Monderer, R. S., Harrison, D. M., and Haut, S. R. (2002). Neurofeedback and epilepsy. *Epilepsy Behav*, 3(3):214–218. (cited on page 29)

Mugler, E., Bensch, M., Halder, S., Rosenstiel, W., Bogdan, M., Birbaumer, N., and Kübler, A. (2008). Control of an Internet Browser Using the P300 Event Related Potential. *International Journal of Bioelectromagnetism*, 10(1):56–63. (cited on page 59)

Müller, K. R., Tangermann, M., Dornhege, G., Krauledat, M., Curio, G., and Blankertz, B. (2008). Machine learning for real-time single-trial EEG-analysis: from brain-computer interfacing to mental state monitoring. *J Neurosci Methods*, 167(1):82–90. (cited on pages 3, 24, and 54)

Niedermeyer, E. and Lopes da Silva, F., editors (1993). *Electroencephalography. Basic Principles, Clinical Applications, and Related fields*. Williams & Wilkins. (cited on page 26)

Nijboer, F., Sellers, E. W., Mellinger, J., Jordan, M. A., Matuz, T., Furdea, A., Halder, S., Mochty, U., Krusienski, D. J., Vaughan, T. M., Wolpaw, J. R., Birbaumer, N., and Kübler, A. (2008). A P300-based brain-computer interface for people with amyotrophic lateral sclerosis. *Clin Neurophysiol*, 119(8):1909–1916. (cited on pages 3, 25, 26, 43, 54, 57, 59, and 74)

Ojemann, G., Ojemann, J., Lettich, E., and Berger, M. (1989). Cortical language localization in left, dominant hemisphere. an electrical stimulation mapping investigation in 117 patients. *J Neurosurg*, 71(3):316–326. (cited on pages 1, 34, and 99)

Ojemann, G. A. (1991). Cortical organization of language. *J Neurosci*, 11(8):2281–2287. (cited on pages 4, 33, and 99)

Palmowski, A., Jost, W. H., Prudlo, J., Osterhage, J., Käsmann, B., Schimrigk, K., and Ruprecht, K. W. (1995). Eye movement in amyotrophic lateral sclerosis: a longitudinal study. *Ger J Ophthalmol*, 4(6):355–362. (cited on pages 55, 60, and 78)

Penfield, W. and Boldrey, E. (1937). Somatic motor and sensory representation in the cerebral cortex of man as studied by electrical stimulation. *Brain*, 60:389–443. (cited on pages 12 and 114)

Penfield, W., Erickson, T., and Thomas, C. (1942). Epilepsy and cerebral localization: a study of the mechanism, treatment and prevention of epileptic seizures. *Arch Intern Med*, 70:916–917. (cited on pages 1 and 32)

Penfield, W. and Rasmussen, T., editors (1950). *The Cerebral Cortex of Man*. MacMillan, New York. (cited on page 114)

Pernkopf, F. and Bouchaffra, D. (2005). Genetic-based EM algorithm for learning gaussian mixture models. *IEEE Trans. Pattern Anal. Mach. Intell.*, 27(8):1344–1348. (cited on pages 5 and 16)

Pfurtscheller, G., Allison, B. Z., Brunner, C., Bauernfeind, G., Solis-Escalante, T., Scherer, R., Zander, T. O., Mueller-Putz, G., Neuper, C., and Birbaumer, N. (2010). The Hybrid BCI. *Front Neurosci*, 4:42–42. (cited on pages 27 and 120)

Pfurtscheller, G., Flotzinger, D., and Kalcher, J. (1993). Brain-computer interface – a new communication device for handicapped persons. *J Microcomput Appl*, 16:293–299. (cited on page 24)

Pfurtscheller, G., Neuper, C., Müller, G. R., Obermaier, B., Krausz, G., Schlögl, A., Scherer, R., Graimann, B., Keinrath, C., Skliris, D., Wörtz, M., Supp, G., and Schrank, C. (2003). Graz-BCI: state of the art and clinical applications. *IEEE Trans Neural Syst Rehabil Eng*, 11(2):177–180. (cited on pages 3, 24, and 54)

Pless, R. (2003). Evaluation of local models of dynamic backgrounds. In *IEEE Proceedings, Computer Vision and Pattern Recognition*, volume 2, pages 73–78. (cited on pages 5 and 16)

Polich, J. (1987). Task difficulty, probability, and inter-stimulus interval as determinants of P300 from auditory stimuli. *Electroencephalogr Clin Neurophysiol*, 68(4):311–320. (cited on page 77)

Popescu, F., Fazli, S., Badower, Y., Blankertz, B., and Müller, K. R. (2007). Single trial classification of motor imagination using 6 dry EEG electrodes. *PLoS One*, 2(7). (cited on page 28)

Pradeep, A. K. (2010). *The Buying Brain: Secrets for Selling to the Subconscious Mind*. Wiley, John & Sons, Inc., 1 edition. (cited on pages 25 and 29)

Priestley, M. (1981). *Spectral Analysis and Time Series*. Academic Press, Orlando, Florida. (cited on page 85)

Pylatiuk, C. and Döderlein, L. (2006). "Bionic" arm prostheses. State of the art in research and development. *Orthopade*, 35(11):1169–1170. (cited on page 27)

Quitadamo, L. R., Abbafati, M., Saggio, G., Marciani, M. G., Cardarilli, G. C., and Bianchi, L. (2008). A UML model for the description of different brain-computer interface systems. In *2008 30th Annual International Conference of the IEEE Engineering in Medicine and Biology Society*, pages 1363–1366, Vancouver, BC. (cited on page 30)

Raab, G. G. and Parr, D. H. (2006). From medical invention to clinical practice: the reimbursement challenge facing new device procedures and technology–part 2: coverage. *J Am Coll Radiol*, 3(10):772–777. (cited on pages 27 and 57)

Rebsamen, B., Burdet, E., Guan, C., Zhang, H., Teo, C. L., Zeng, Q., Laugier, C., and Ang Jr., M. H. (2007). Controlling a Wheelchair Indoors Using Thought. *IEEE Intelligent Systems*, 22(2):18–24. (cited on page 59)

Reitan, R. M. (1958). Validity of the trail making test as an indicator of organic brain damage. *Percept Mot Skills*, 8:271–276. (cited on page 44)

Renard, Y., Lotte, F., Gibert, G., Congedo, M., Maby, E., and V, D. (2010). OpenViBE: An Open-Source Software Platform to Design, Test and Use Brain-Computer Interfaces in Real and Virtual Environments. In *Presence Teleoperators & Virtual Environments / Presence Teleoperators and Virtual Environments*, volume 19, pages 35–53. (cited on pages 24, 26, and 30)

Reuderink, B. (2008). Games and Brain-Computer Interfaces: The State of the Art. Technical Report TR-CTIT-08-81, Centre for Telematics and Information Technology, University of Twente, Enschede, The Netherlands. (cited on page 25)

Rissanen, J. (1978). Modelling by the shortest data description. *Automatica*, 14:465–471. (cited on page 93)

Ritaccio, A. L., Brunner, P., Cervenka, M. C., Crone, N., Guger, C., Leuthardt, E. C., Oostenveld, R., Stacey, G., and Schalk, G. (2010). Proceedings of the first international workshop on advances in electrocorticography. *Epilepsy Behav*, 19(3):204–215. (cited on pages 4, 43, and 121)

Roland, J., Brunner, P., Johnston, J., Schalk, G., and Leuthardt, E. C. (2010). Passive real-time identification of speech and motor cortex during an awake craniotomy. *Epilepsy Behav*, 18(1-2):123–128. (cited on page 121)

Rolfs, M. (2009). Microsaccades: small steps on a long way. *Vision Res*, 49(20):2415–2441. (cited on page 78)

Schalk, G. (2008). Brain-computer symbiosis. *J Neural Eng*, 5(1):1–15. (cited on pages 4, 24, 27, 54, and 79)

Schalk, G. (2010). Can Electrocorticography (ECoG) Support Robust and Powerful Brain-Computer Interfaces? *Front Neuroengineering*, 3:1–1. (cited on page 57)

Schalk, G., Brunner, P., Gerhardt, L. A., Bischof, H., and Wolpaw, J. R. (2008a). Brain–computer interfaces (BCIs): Detection instead of classification. *J Neurosci Meth*, 167(1):51–62. (cited on pages 102, 103, 106, and 115)

Schalk, G., Leuthardt, E. C., Brunner, P., Ojemann, J. G., Gerhardt, L. A., and Wolpaw, J. R. (2008b). Real-time detection of event-related brain activity. *Neuroimage*, 43(2):245–249. (cited on pages 102, 103, 106, and 115)

Schalk, G., McFarland, D. J., Hinterberger, T., Birbaumer, N., and Wolpaw, J. R. (2004). BCI2000: a general-purpose brain-computer interface (BCI) system. *IEEE Trans Biomed Eng*, 51(6):1034–1043. (cited on pages 24, 26, 44, 61, 101, 103, and 115)

Schalk, G. and Mellinger, J. (2010). *A Practical Guide to Brain-Computer Interfacing with BCI2000*. Springer, London, UK, 1st edition. (cited on pages 24, 26, 30, 44, and 61)

Schalk, G., Miller, K. J., Anderson, N. R., Wilson, J. A., Smyth, M. D., Ojemann, J. G., Moran, D. W., Wolpaw, J. R., and Leuthardt, E. C. (2008c). Two-dimensional movement control using electrocorticographic signals in humans. *J Neural Eng*, 5(1):75–84. (cited on pages 4 and 43)

Schreuder, M., Blankertz, B., and Tangermann, M. (2010). A new auditory multi-class brain-computer interface paradigm: spatial hearing as an informative cue. *PLoS One*, 5(4). (cited on pages 74, 79, and 120)

Schwartz, A. B., Cui, X. T., Weber, D. J., and Moran, D. W. (2006). Brain-controlled interfaces: movement restoration with neural prosthetics. *Neuron*, 52(1):205–220. (cited on page 24)

Schwarz, G. (1978). Estimating the dimension of a model. *Annals of Statistics*, 6:461–464. (cited on page 93)

Sellers, E. W., Krusienski, D. J., McFarland, D. J., Vaughan, T. M., and Wolpaw, J. R. (2006a). A P300 event-related potential brain-computer interface (BCI): the effects of matrix size and inter stimulus interval on performance. *Biol Psychol*, 73(3):242–252. (cited on pages 43, 54, 59, and 76)

Sellers, E. W., Kübler, A., and Donchin, E. (2006b). Brain-computer interface research at the University of South Florida Cognitive Psychophysiology Laboratory: the P300 Speller. *IEEE Trans Neural Syst Rehabil Eng*, 14(2):221–224. (cited on pages 3, 25, 26, 43, 57, 59, 60, and 74)

Sellers, E. W., Turner, P., Sarnacki, W. A., Mcmanus, T., Vaughan, T. M., and Matthews, R. (2009). A novel dry electrode for brain-computer interface. In *Proceedings of the 13th International Conference on Human-Computer Interaction. Part II: Novel Interaction Methods and Techniques*, pages 623–631, Berlin, Heidelberg. Springer-Verlag. (cited on page 28)

Sellers, E. W., Vaughan, T. M., and Wolpaw, J. R. (2010). A brain-computer interface for long-term independent home use. *Amyotroph Lateral Scler*, 11(5):449–455. (cited on pages 3, 25, 26, 43, 54, and 59)

Serby, H., Yom-Tov, E., and Inbar, G. F. (2005). An improved P300-based brain-computer interface. *IEEE Trans Neural Syst Rehabil Eng*, 13(1):89–98. (cited on pages 43, 54, 59, and 60)

Sharbrough, F., Chatrian, G. E., Lesser, R. P., Luders, H., Nuwer, M., and Picton, T. W. (1991). American Electroencephalographic Society guidelines for standard electrode position nomenclature. *Electroenceph Clin Neurophysiol*, 8:200–202. (cited on pages 25, 56, 63, 66, and 71)

Sherman, J. (1979). Visual evoked potential (VEP): basic concepts and clinical applications. *J Am Optom Assoc*, 50(1):19–30. (cited on pages 56, 60, and 74)

Sinai, A., Bowers, C. W., Crainiceanu, C. M., Boatman, D., Gordon, B., Lesser, R. P., Lenz, F. A., and Crone, N. E. (2005). Electrocorticographic high gamma activity versus electrical cortical stimulation mapping of naming. *Brain*, 128(Pt 7):1556–1570. (cited on pages 5, 35, 36, and 100)

St. John, M., Kobus, D. A., Morrison, J. G., and Schmorrow, D. (2005). Overview of the DARPA Augmented Cognition Technical Integration Experiment. In *Proceedings of the First International Conference on Augmented Cognition*, pages 131–149. Delft University Press. (cited on pages 25 and 29)

Stauffer, C. and Grimson, W. (1999). Adaptive background mixture models for real-time tracking. In *IEEE Proceedings, Computer Vision and Pattern Recognition*, volume 2, pages 246–252. (cited on pages 5 and 16)

Stavisky, S. D., Simeral, J. D., Kim, S. P., Centrella, K. A., Donoghue, J. P., and Hochberg, L. R. (2009). Architecture of the braingate neural interface system in the ongoing pilot clinical trial for individuals with tetraplegia. In *abstracts of the Society for Neuroscience Annual Meeting, Chicago, IL*. (cited on pages 25 and 26)

Sterman, M. B. and Egner, T. (2006). Foundation and practice of neurofeedback for the treatment of epilepsy. *Appl Psychophysiol Biofeedback*, 31(1):21–35. (cited on page 29)

Stoica, P. and Moses, R. L. (1997). *Introduction to Spectral Analysis*. Prentice-Hall, Upper Saddle River, NJ. (cited on page 85)

Strasburger, H. (2005). Unfocused spatial attention underlies the crowding effect in indirect form vision. *J Vis*, 5(11):1024–1037. (cited on pages 60 and 77)

Sullivan, T. J., Deiss, S. R., Jung, T.-P., and Cauwenberghs, G. (2008). A brain-machine interface using dry-contact, low-noise EEG sensors. In *2008 IEEE International Symposium on Circuits and Systems*, pages 1986–1989. (cited on page 28)

Takano, K., Komatsu, T., Hata, N., Nakajima, Y., and Kansaku, K. (2009). Visual stimuli for the P300 brain-computer interface: a comparison of white/gray and green/blue flicker matrices. *Clin Neurophysiol*, 120(8):1562–1566. (cited on pages 59 and 76)

Talairach, J. and Tournoux, P. (1988). *Co-Planar Sterotaxic Atlas of the Human Brain*. Thieme Medical Publishers, Inc., New York. (cited on page 44)

Tassey, G. (1997). *The economics of R&D policy*. Quorum Books, Westport, CT. (cited on page 30)

Tassey, G. (2000). Standardization in technology-based markets. *Research Policy*, 29(4-5):587–602. (cited on page 30)

Taylor, D. M., Tillery, S. I., and Schwartz, A. B. (2002). Direct cortical control of 3D neuroprosthetic devices. *Science*, 296(5574):1829–1832. (cited on pages 24, 29, and 120)

Torr, P. H. S. (1997). An assessment of information criteria for motion model selection. In *Proceedings CVPR '97, of Conference on Computer Vision and Pattern Recognition*, pages 47–52. (cited on page 93)

Torres Valderrama, A., Oostenveld, R., Vansteensel, M. J., Huiskamp, G. M., and Ramsey, N. F. (2010). Gain of the human dura in vivo and its effects on invasive brain signal feature detection. *J Neurosci Methods*, 187(2):270–279. (cited on pages 12 and 57)

Townsend, G., LaPallo, B. K., Boulay, C. B., Krusienski, D. J., Frye, G. E., Hauser, C. K., Schwartz, N. E., Vaughan, T. M., Wolpaw, J. R., and Sellers, E. W. (2010). A novel P300-based brain-computer interface stimulus presentation paradigm: moving beyond rows and columns. *Clin Neurophysiol*, 121(7):1109–1120. (cited on page 79)

Toyama, K., Krumm, J., Brumitt, B., and Meyers, B. (1999). Statistical modeling of complex backgrounds for foreground object detection. In *IEEE Proceedings, of the Seventh IEEE International Conference on Computer Vision*, volume 1, pages 20–27. (cited on pages 5 and 16)

Treder, M. S., Bahramisharif, A., Schmidt, N. M., van Gerven, M. A., and Blankertz, B. (2011). Brain-computer interfacing using modulations of alpha activity induced by covert shifts of attention. *J Neuroeng Rehabil*, 8:24–24. (cited on pages 79 and 120)

Treder, M. S. and Blankertz, B. (2010). (C)overt attention and visual speller design in an ERP-based brain-computer interface. *Behav Brain Funct*, 6(1):28–28. (cited on pages 54, 57, 74, 79, and 120)

Treder, M. S., Schmidt, N. M., and Blankertz, B. (2010). Towards gaze-independent visual brain-computer interfaces. In *Front. Comput. Neurosci. Conference Abstract: Bernstein Conference on Computational Neuroscience*, volume 5, page 5. (cited on pages 79 and 120)

Uematsu, S., Lesser, R., Fisher, R. S., Gordon, B., Hara, K., Krauss, G. L., Vining, E. P., and Webber, R. W. (1992). Motor and sensory cortex in humans: topography studied with chronic subdural stimulation. *Neurosurgery*, 31(1):59–71. (cited on pages 4 and 99)

Van Gompel, J. J., Worrell, G. A., Bell, M. L., Patrick, T. A., Cascino, G. D., Raffel, C., Marsh, W. R., and Meyer, F. B. (2008). Intracranial electroencephalography with subdural grid electrodes: techniques, complications, and outcomes. *Neurosurgery*, 63(3):498–505. (cited on pages 12 and 57)

Vansteensel, M. J., Hermes, D., Aarnoutse, E. J., Bleichner, M. G., Schalk, G., van Rijen, P. C., Leijten, F. S., and Ramsey, N. F. (2010). Brain-computer interfacing based on cognitive control. *Ann Neurol*, 67(6):809–816. (cited on pages 4, 43, and 57)

Vapnik, V. N. and Chervonenkis, A. J. (1974). Ordered risk minimization (I and II). *Automation and Remote Control*, 34:1226–1235 and 1403–1412. (cited on page 93)

Varela, F., Lachaux, J. P., Rodriguez, E., and Martinerie, J. (2001). The brainweb: phase synchronization and large-scale integration. *Nat Rev Neurosci*, 2(4):229–239. (cited on pages 5, 35, and 100)

Vaughan, T. M., McFarland, D. J., Schalk, G., Sarnacki, W. A., Krusienski, D. J., Sellers, E. W., and Wolpaw, J. R. (2006). The Wadsworth BCI Research and Development Program: at home with BCI. *IEEE Trans Neural Syst Rehabil Eng*, 14(2):229–233. (cited on pages 3, 25, 26, 43, 59, and 74)

Velliste, M., Perel, S., Spalding, M. C., Whitford, A. S., and Schwartz, A. B. (2008). Cortical control of a prosthetic arm for self-feeding. *Nature*, 453(7198):1098–1101. (cited on pages 14 and 24)

Vidal, J. J. (1973). Toward direct brain-computer communication. *Annu Rev Biophys Bioeng*, 2:157–180. (cited on pages 1, 16, and 24)

Walker, J. E. and Kozlowski, G. P. (2005). Neurofeedback treatment of epilepsy. *Child Adolesc Psychiatr Clin N Am*, 14(1):163–176. (cited on page 29)

Wechsler, D. (1997). *Weschsler Adult Intelligence Scale-III*. The Psychological Corporation, San Antonio, TX. (cited on page 44)

Westheimer, G. (1965). Visual acuity. *Annu Rev Psychol*, 16:359–380. (cited on pages 60, 74, and 77)

Wilson, J. A., Felton, E. A., Garell, P. C., Schalk, G., and Williams, J. C. (2006). ECoG factors underlying multimodal control of a brain-computer interface. *IEEE Trans Neural Syst Rehabil Eng*, 14(2):246–250. (cited on pages 4 and 43)

Wilson, J. A., Mellinger, J., Schalk, G., and Williams, J. (2010). A procedure for measuring latencies in brain-computer interfaces. *IEEE Trans Biomed Eng*, 57(7):1785–1797. (cited on pages 24 and 26)

Wisneski, K. J., Anderson, N., Schalk, G., Smyth, M., Moran, D., and Leuthardt, E. C. (2008). Unique cortical physiology associated with ipsilateral hand movements and neuroprosthetic implications. *Stroke*, 39(12):3351–3359. (cited on page 114)

Wolpaw, J. R., Birbaumer, N., McFarland, D. J., Pfurtscheller, G., and Vaughan, T. M. (2002). Brain-computer interfaces for communication and control. *Clin Neurophysiol*, 113(6):767–791. (cited on page 24)

Wolpaw, J. R. and McFarland, D. J. (2004). Control of a two-dimensional movement signal by a noninvasive brain-computer interface in humans. *Proc Natl Acad Sci U S A*, 101(51):17849–17854. (cited on pages 24 and 29)

Wolpaw, J. R., McFarland, D. J., Neat, G. W., and Forneris, C. A. (1991). An EEG-based brain-computer interface for cursor control. *Electroenceph Clin Neurophysiol*, 78(3):252–259. (cited on pages 3, 24, and 54)

Wolpaw, J. R. and Winter-Wolpaw, E., editors (2011). *Brain-Computer Interfaces: Principles and Practice*. Oxford University Press, USA, 1 edition. (cited on page 1)

Wong, C. H., Birkett, J., Byth, K., Dexter, M., Somerville, E., Gill, D., Chaseling, R., Fearnside, M., and Bleasel, A. (2009). Risk factors for complications during intracranial electrode recording in presurgical evaluation of drug resistant partial epilepsy. *Acta Neurochir (Wien)*, 151(1):37–50. (cited on pages 12 and 57)

Yoshii, F., Ginsberg, M. D., Kelley, R. E., Chang, J. Y., Barker, W. W., Ingenito, G., Apicella, A. M., Globus, M. Y., Duara, R., and Boothe, T. E. (1989). Asymmetric somatosensory activation with right- vs left-hand stimulation: a positron emission tomographic study. *Brain Res*, 483(2):355–360. (cited on page 114)

Yoshor, D., Bosking, W. H., Ghose, G. M., and Maunsell, J. H. (2007). Receptive fields in human visual cortex mapped with surface electrodes. *Cereb Cortex*, 17(10):2293–2302. (cited on page 56)

Zander, T., Gaertner, M., Kothe, C., and Vilimek, R. (2010). Combining Eye Gaze Input with a Brain-Computer Interface for Touchless Human-Computer Interaction. *International Journal of Human-Computer Interaction*, 27(1):38–51. (cited on pages 27 and 120)

Zander, T. and Jatzev, S. (2009). Detecting affective covert user states with passive brain–computer interfaces. In *Proceedings 3rd International Conference on Affective Computing and Intelligent Interaction (ACII 2009)*, pages 1–9. (cited on pages 25 and 29)

Zeki, S., Watson, J. D., Lueck, C. J., Friston, K. J., Kennard, C., and Frackowiak, R. S. (1991). A direct demonstration of functional specialization in human visual cortex. *J Neurosci*, 11(3):641–649. (cited on page 56)